

MESOZOIC AND CENOZOIC CHRONOSTRATIGRAPHY AND CYCLES OF SEA-LEVEL CHANGE

BILAL U. HAQ,¹ JAN HARDENBOL, AND PETER R. VAIL²

Exxon Production Research Company, P.O. Box 2189, Houston, Texas 77252-2189

In collaboration with

L. E. Stover, J. P. Colin, N. S. Ioannides, R. C. Wright, G. R. Baum, A. M. Gombos, Jr., C. E. Pflum, T. S. Loutit, R. Jan du Chêne, K. K. Romine, J. F. Sarg, H. W. Posamentier, and B. E. Morgan

ABSTRACT: Sequence-stratigraphic concepts are used to identify genetically related strata and their bounding regional unconformities, or their correlative conformities, in seismic, well-log, and outcrop data. Documentation and age dating of these features in marine outcrops in different parts of the world have led to a new generation of Mesozoic and Cenozoic sea-level cycle charts with greater event resolution than that obtainable from seismic data alone. The cycles of sea-level change, interpreted from the rock record, are tied to an integrated chronostratigraphy that combines state-of-the-art geochronologic, magnetostratigraphic and biostratigraphic data. In this article we discuss the reasoning behind integrated chronostratigraphy and list the sources of data used to establish this framework. Once this framework has been constructed, the depositional sequences from sections around the world, interpreted as having been formed in response to sea-level fluctuations, can be tied into the chronostratigraphy.

Four cycle charts summarizing the chronostratigraphy, coastal-onlap patterns, and sea-level curves for the Cenozoic, Cretaceous, Jurassic, and Triassic are presented. A large-scale composite-cycle chart for the Mesozoic and Cenozoic is also included (in pocket). The relative magnitudes of sea-level falls, interpreted from sequence boundaries, are classified as major, medium, and minor, as are the condensed sections associated with the intervals of sediment starvation on the shelf and slope during the phase of maximum shelf flooding during each cycle. Generally, only the sequence boundaries produced by major and some medium-scale sea-level falls can be recognized at the level of seismic stratigraphic resolution; detailed well-log and/or outcrop studies are usually necessary to resolve the minor sequences.

INTRODUCTION

The usefulness of a chronostratigraphic eustatic framework in exploration geology lies in the fact that it provides predrill estimates of geologic parameters from seismic data. This enhances interregional correlations, particularly in frontier areas, leading to more accurate stratigraphic, structural, and facies interpretations. The first such eustatic stratigraphic framework (Vail and others, 1977; Vail and Hardenbol, 1979) was an outcome of developments in seismic stratigraphy that were based on the realization that primary seismic reflections had chronostratigraphic significance. The cycles of sea-level change on the cycle chart (Vail and others, 1977) were derived from seismic data, aided by paleontologic age control from wells. Now, a new generation of cycle charts has been constructed, representing a considerable improvement on the earlier cycle charts constructed from seismic data alone. The new cycle charts were made possible by the recognition of depositional patterns interpreted as having formed during various phases of the sea-level cycle, coupled with an enhanced ability to recognize accurately genetically related sediment packages in outcrops and well logs.

Recent advances in magnetobiostratigraphy, especially for the Late Cretaceous and Cenozoic, have been important for the refinement of the global cycle charts. In numerous sections of marine strata in different parts of the world, magnetic-polarity reversals have been correlated directly to biohorizons (fossil first and last occurrences) that are the most readily available source of age dating. Over the past several years, researchers at Exxon Production Research Company have attempted to develop a sequence-keyed global

stratigraphic framework that is based on up-to-date magneto-, bio-, and sequence chronostratigraphies in sedimentary basins in different parts of the world. Updated and integrated chronostratigraphies were seen as a prerequisite to the construction of cycle charts. Existing time scales for the Mesozoic and Cenozoic were disparate and were based on differing criteria and approaches. We felt that an internally consistent approach was needed and that existing time scales could be improved. This led to an integrated chronostratigraphic framework to which the sea-level changes of the Mesozoic and Cenozoic have been tied. An early summary of this work (Haq and others, 1987) disseminated the results expediently so that the testing of the model of sea-level change and constructive feedback could ensue. In the present paper we include details of the approach used to construct the chronostratigraphic framework that could not be included in the summary, and we discuss the results of this effort. The cycle charts presented here include some modifications and corrections to our earlier versions presented with the summary. One important modification is the inclusion of the prominent 2.4-Ma event in the latest Pliocene, which was inadvertently left off the Cenozoic cycle chart (Haq and others, 1987, fig. 2).

The ultimate objective of stratigraphy is to identify and arrange successions of events that aid in increasingly precise correlations. From a practical standpoint, the best stratigraphic correlations are those that have a high degree of reproducibility within increasingly narrower temporal limits. Toward this end, it is important to identify and employ multiple stratigraphic criteria concurrently to maximize precision. As additional, independent, correlative systems are found and used parallel to the existing systems, a greater degree of consistency and confidence in the results is to be expected. An excellent example of a new system that has only recently become available is Sr-isotopic stratigraphy, based on the relatively slow but significant vari-

¹Present addresses: Marine Geology/Geophysics Program, National Science Foundation, 1800 G Street, NW, Washington D.C., 20550.

²Department of Geology, Rice University, Houston, Texas 77251.

ations in the ratios of ^{87}Sr to ^{86}Sr of sea water with time, which holds much promise for the future as an age-dating tool (Burke and others, 1982, DePaolo and Ingram, 1985).

Our chronostratigraphic framework has been aided significantly by the recently developed sequence-stratigraphic models that assist in the recognition of depositional sequences in outcrops and well logs. This not only helps in the precise dating of the sea-level events, but also in the more accurate integration of standard chronostratigraphic units (stages).

THE CALIBRATION OF GEOLOGIC TIME

Because units of time are not unique in themselves, we perceive the passing of time by association with unique events. The transition of geologic time is similarly conceptualized by either the sequence of geologic events that are distinctive in themselves, or by cyclic events that are distinguished from each other by association with other unique events.

The only strictly direct method of measuring geologic time is through the built-in clock of isotopic decay, the proportion of radiogenic parent-to-daughter elements determining the elapsed time since the genesis (or closure) of the measured system, according to a known rate of decay; however, radiochronology is the most time-consuming and thus the least practical tool for routine age determination. Radiometric dates, nevertheless, can provide the basis to elevate other systems of gauging relative temporal order to practical but indirect time-measuring tools.

The most readily available method of detecting the relative antiquity of sediments is through biostratigraphy, i.e., the unique biologic events (the first and last occurrence of distinctive fossil taxa) that occur during the course of biologic evolution. Although biostratigraphy discriminates older from younger rocks, it cannot measure absolute time. To accomplish this, biostratigraphic events have to be age dated, either through correlation with radiometrically dated horizons, or indirectly through association with magnetic-polarity or climatic events that have been previously dated.

Magnetic-polarity reversal events have the distinctive attribute of being relatively numerous and globally synchronous. They are, therefore, most appropriate as precise global correlation criteria. Because polarity reversals are not unique events, however, they must be used in association with other unique events, such as biostratigraphic datums and/or radiometric dates.

Climatic events, as depicted by oxygen isotope variations, and other environmental events, such as productivity fluctuations as reflected in carbon isotope variations, are increasingly used for regional and global correlations. Like magnetic-polarity reversals, however, the isotopic variations can only be used in association with other unique events and, so far, detailed stable isotope "stage" stratigraphy has been developed only for the past 2 million years or so of the stratigraphic record.

Here, we must add a note about the potential of Sr-isotopic stratigraphy. Although Sr-isotopic stratigraphy holds much promise as a semi-independent system for age dating of both fossiliferous and nonfossiliferous marine sediments,

much work needs to be done to calibrate accurately Sr-isotopic variations to the chronostratigraphic schemes. The present state of the art (DePaolo and Ingram, 1985, Elderfield, 1986) does not permit the routine use of Sr-isotopic stratigraphy.

These limitations to various direct and indirect age-dating methods suggest that, within the framework of the tools presently available, a widely applicable chronologic framework has to be based on the most practical and readily available criteria of correlation (biostratigraphy), constrained as broadly as possible by absolute dates (radiochronology), and the precision of interregional correlations ensured by a system of globally synchronous events (magnetostratigraphy).

INTEGRATION PROCEDURE FOR THE CONSTRUCTION OF CYCLE CHARTS

The construction of the sea-level cycle charts is an integration process that involves many iterative steps (Fig. 1). Recent improvements in direct correlations between microplanktonic biohorizons and magnetic reversals (magnetic-polarity chrons) are of prime importance for the construction of accurate chronostratigraphy. Irrespective of the numerical calibration of magnetic-polarity reversals, such direct correlations between fossil datums and polarity chrons provide a reliable indication of the true ranges of fossil taxa, especially after the relationships have been ascertained in a series of sections from several different areas. Range stacking from different latitudinal locations, when possible, serves to document the maximum (chronostratigraphic) extent of the taxa and to elevate *biozones* into *biochronozones*. This magnetobiostratigraphic reconciliation is the first essential step in the construction of the global-cycle charts and the basis of all subsequent integration.

The magnetobiostratigraphic framework in turn allows the assignment of stratigraphically constrained radiometric dates to appropriate polarity chrons. The criteria for the selection of radiometric dates are that they are analytically sound, geochemically reliable, and biostratigraphically constrained. Through paleontologic correlation, they can then be placed within the polarity reversal framework, along with their limits of uncertainties (stratigraphic and analytical errors).

Following the assignment of radiometric dates to polarity chrons, these dates can be plotted against seafloor magnetic-anomaly profiles from different ocean basins (i.e., the distance of anomalies from the spreading center) to arrive at best-fit age models for the anomalies, constrained by inflection points preferably where seafloor spreading rate changes are predicted by a comparison of the seafloor magnetic-anomaly profile from different basins (Fig. 2). The resulting anomaly ages from various basins are then stacked to enhance the signal-to-noise ratio. In this way, the stacked mean ages were used to calibrate the late Cretaceous through Cenozoic magnetic-polarity scale on the cycle charts presented in this paper. This procedure reduces the noise from radiometric analytical techniques, as well as minor irregularities in seafloor spreading.

The next step in the development of the cycle charts in-

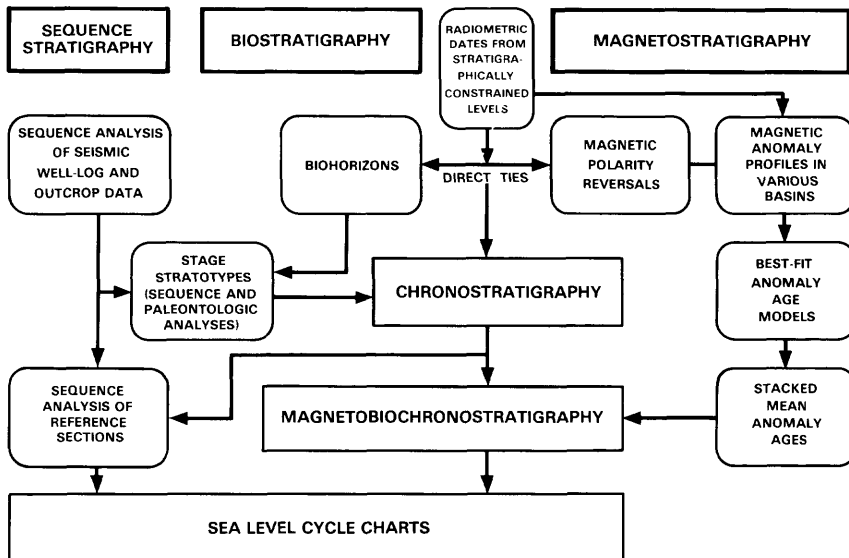


FIG. 1.—Flow chart of the iterative process of reconciliation of biostratigraphic, magnetostratigraphic, and radiometric data, leading to an integrated magnetobiochronostatigraphy. This framework is then combined with sequence-stratigraphic data from reference sections and stage stratotypes to produce sea-level cycle charts (Figs. 14–17).

volves the incorporation of the standard chronostratigraphic units (stages) in the magnetobiochronologic scheme. This integration involves two separate but related activities. First, the detailed biostratigraphic analyses of the stage stratotypes (and magnetostratigraphy or radiometric dates, when available) help determine the biochronostratigraphic extent of the stratotype. Second, the depositional-sequence analysis of the same sections assists in a more accurate positioning of the stages within a sequence-stratigraphic framework. The significance of the latter in the refinement of chronostratigraphy will become clear from the examples of field applications discussed in the following sections, especially the example from the neostratotype of the Lutetian Stage.

The final step in the construction of the cycle charts involves the integration of sea-level events with the magneto- and biochronostratigraphies. The sea-level changes interpreted through stratigraphic analyses of sequences in both subsurface and outcrop data from sections in various parts of the world, dated through their paleontologic and physical/stratigraphic relationships, are incorporated into the chronostratigraphic scheme to produce the sea-level cycle charts that are the ultimate purpose of this exercise.

In the ensuing sections, various aspects of this integration will be discussed in more detail. To communicate these concepts clearly, it is first necessary to review briefly the stratigraphic terminology utilized on the cycle charts.

Stratigraphic terminology.—

Table 1 summarizes the stratigraphic terminology employed in the text and on the cycle charts. As explained in the International Stratigraphic Guide (Hedberg, 1976), the distinction between rock (lithostratigraphic) and time (geochronologic) units is quite obvious. Time-rock (chronostratigraphic) units are often confused in the literature, however, and their nature needs to be clarified, especially when applied to depositional sequences. The cycle charts represent both time and rock data tied together by standard

chronostratigraphic units (stages). Depositional sequences are first identified in lithostratigraphic sections, and later, indirectly, tied to a linear time scale through their biostratigraphic and/or magnetostratigraphic relationships to establish their chronostratigraphic identity.

This underscores the need for a consistent and distinctive chronostratigraphic terminology for biostratigraphic, magnetostratigraphic, and sequence-stratigraphic units. For example, the biochronostratigraphic equivalent of a locally or regionally defined biostratigraphic zone (biozone) is a biochronozone. It represents the maximum temporal extent of the biozone world-wide, based on the total temporal ranges (or maximum first- or last-occurrence datums in the case of zones based on concurrent or partial ranges of taxa), as opposed to local ranges of the taxa on which the zone is defined. Because most taxa are environmentally, and thus areally, restricted, their geographic distribution at different times reflects the changes in their preferred environmental factors. A locally defined biostratigraphic zone (biozone) may therefore only span a part of the true temporal extent (biochronozone) of the taxa world-wide (see Table 1). Generally, most biostratigraphically useful taxa of the low and middle latitudes are environmentally excluded from the higher latitudes. Even in the tropical and temperate latitudes, however, considerable differences between biozonal and biochronozonal limits are possible as a result of circulation patterns, or other environmentally induced fluctuations (see also Loutit and others, this volume, for further discussion of biozones vs. biochronozones).

The distinction between magnetic-rock, time-rock, and time units has been made by Harland and others (1982), and we have adopted their terminology. We have also suggested a distinction between sequence-stratigraphic, sequence-chronostratigraphic and sequence-chronologic units (see Table 1). This terminology subdivides sequence-stratigraphic units into first-order (megasequence), second-order (supersequence), and third- or fourth-order (sequence) units, as well as into shorter term flooding events within se-

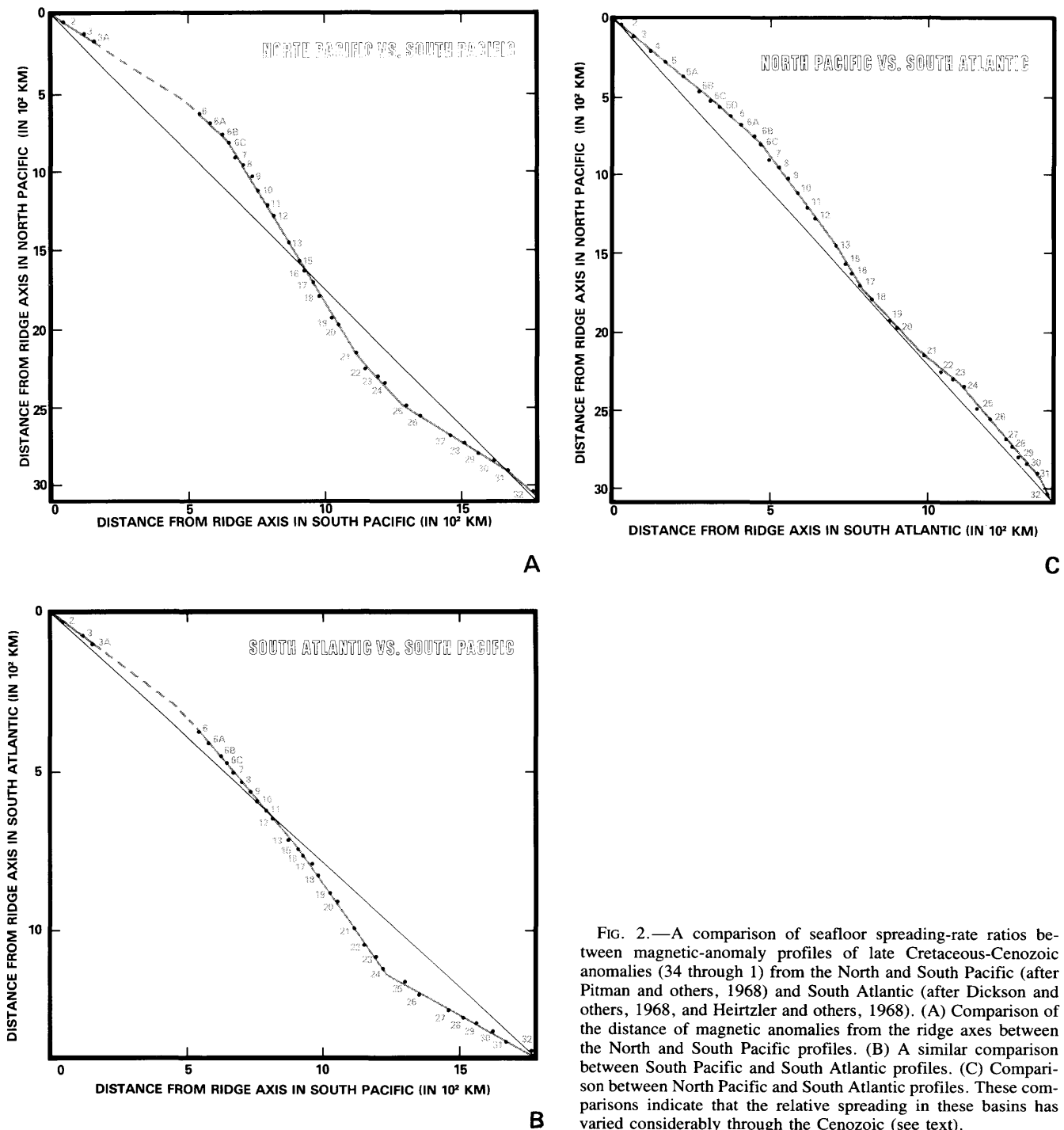


FIG. 2.—A comparison of seafloor spreading-rate ratios between magnetic-anomaly profiles of late Cretaceous-Cenozoic anomalies (34 through 1) from the North and South Pacific (after Pitman and others, 1968) and South Atlantic (after Dickson and others, 1968, and Heirtzler and others, 1968). (A) Comparison of the distance of magnetic anomalies from the ridge axes between the North and South Pacific profiles. (B) A similar comparison between South Pacific and South Atlantic profiles. (C) Comparison between North Pacific and South Atlantic profiles. These comparisons indicate that the relative spreading in these basins has varied considerably through the Cenozoic (see text).

quences that produce parasequences (Van Wagoner and others, this volume) and their chronostratigraphic and geochronologic equivalents.

BIOCHRONOSTRATIGRAPHIC AND MAGNETOCHRONOSTRATIGRAPHIC TIES

The progress in the calibration of biostratigraphic events to magnetostratigraphy in the last decade was first due to the availability of undisturbed piston cores of Neogene sedi-

ments, and more recently through the use of the Hydraulic Piston Corer (HPC) by the Deep Sea Drilling Project (DSDP) and its successor, the Ocean Drilling Program (ODP). Prior to the deployment of the HPC, the upper 200 m of softer sediments was usually too severely disturbed, as a result of the rotary action of the drill bit, to be suitable for magnetic or refined biostratigraphic analyses. HPC coring has provided the basis for direct ties between fossil datums and magnetic-polarity reversal events of pre-Neogene sedi-

TABLE 1.—STRATIGRAPHIC TERMINOLOGY SHOWING ROCK, TIME-ROCK, AND TIME UNITS.

Lithostratigraphy (Rock)	Chronostratigraphy (Time-Rock)	Geochronology (Time)
Group	Erathem	Era
Formation	System	Period
Member	Series	Epoch
Bed	Stage	Age
Biostratigraphy	Biochronostratigraphy	Biochronology
Superzone (Superbiozone)	Superbiochronozone	
Zone (Biozone)	Biochronozone	Biochron
Biohorizon	Biochronohorizon	
Magnetostratigraphy	Magnetochronostratigraphy	Magnetochronology
Polarity Superzone	Polarity Superchronozone	Polarity Superchron
Polarity Zone	Polarity Chronozone	Polarity Chron
Sequence Stratigraphy	Sequence Chronostratigraphy	Sequence Chronology
Megasequence (First Order)	Megasequence Chronozone	Megasechron-Megacycle
Supersequence (Second Order)	Supersequence Chronozone	Supersechron-Supercycle
Sequence (Third or Fourth Order)	Sequence Chronozone	Sechron-Cycle
Parasequence (Fourth and Higher Order)	Parasequence Chronozone	

The time-rock terminology (Chronostratigraphy, biochronostratigraphy, magnetochronostratigraphy, and sequence chronostratigraphy) adopted in the cycle charts (Figs. 14–17) is shown in the center column.

ments. In addition, magnetic/biostratigraphic studies in carbonate outcrops have also been critical in establishing a magnetobiostratigraphic framework for late Cretaceous and Paleogene intervals.

The desirability of assembling a magnetobiochronologic scheme of wide geographic applicability is quite obvious. Consequently, it is important to distinguish between the need to adopt *biochronozones*, wherever possible, as opposed to locally defined *biozones*, as previously mentioned.

To utilize the biozones in the amplified sense of *biochronozones*, it is essential that the biostratigraphic events on which the zones are based be compared to magnetic-polarity reversal stratigraphy in sections from different latitudes and hemispheres. So far, this is only possible for a very few biostratigraphic events. For instance, many of the late Cretaceous and early Cenozoic planktonic-datum events have been tied directly to polarity reversals in one or two sections and, rarely, in more than two sections. The optimization of the total-range information of the less well-constrained planktonic-datum events can sometimes be accomplished by cross-correlations of datums between taxa of the same group and between different groups. An illustrative example of such cross-correlations is provided by two early Oligocene datum events.

The last occurrence of the planktonic foraminifers *Pseudohastigerina* spp. and the first occurrence of nannofossil *Sphenolithus distentus* have been tied to the reversed-polarity interval of magnetic chron C12. Both of these are important datum events for the recognition of the Early Oligocene. Authors working in different areas, however, have recorded both a distinct overlap in the ranges of these taxa and a lack of such overlap. The cross-comparison of these taxa in all tropical and subtropical DSDP sites, where they have been jointly recorded, showed that a definite overlap existed in only 25 percent of the sites, a slight overlap was recorded in 56 percent of the sites, and a definite lack of overlap was recorded in 19 percent of the sites compared.

Whereas subtropical sites consistently show just a slight overlap, tropical sites show both a distinct overlap and a lack of overlap. Such biogeographic comparisons help ascertain the true maximum or biochronozonal extent of the taxa.

It is apparent that the temporal extent of many of the fossil zones as yet may not approximate their chronozonal limits, and ranges of marker taxa may have to be refined as more magneto- and biostratigraphic and paleobiogeographic data are compiled from different latitudes. This aspect of biostratigraphy, i.e., documentation of the true biochronozonal extent of marker taxa, needs a strong emphasis in the future, and major advances are to be expected in this area.

Recent paleomagnetic-biostratigraphic studies furnishing direct correlations between late Cretaceous and younger calcareous plankton datum events and polarity reversal events that form the basis of our magneto- and biochronostratigraphic framework include the following: Gartner (1973), Ryan and others (1974), Alvarez and others (1977), Haq and others (1977), Premoli-Silva (1977), Thierstein and others (1977), Haq and others (1980), Channell and Medizza (1981), Lowrie and others (1982), Poore and others (1982), Stradner and Allram (1982), Backman and others (1983), Napoleone and others (1983), Poore and others (1983), Berggren and others (1984), Hsü and others (1984), Shackleton and others (1984), Miller and others (1985), and Monechi and Thierstein (1985). In addition, recent publications by Berggren and others (1985 a,b) are a compilation of a wealth of data and reference sources on the state of the art of Cenozoic biostratigraphic magnetic polarity-reversal correlations.

For siliceous plankton, direct magnetobiostratigraphic correlations are limited to the Neogene. These studies include Burckle (1978), Theyer and others (1978), Burckle and Trainer (1979), and Barron (1985).

For the Late Jurassic and Early Cretaceous, direct ties

between fossil occurrences and magnetic reversals are provided by a few isolated studies. These include Alvarez and others (1977), Channell and others (1979), Lowrie and others (1980), Marton (1982), Marton and others (1980), Hörner and Heller (1983), Ogg (1983), Galbrun and Rasplus (1984), Ogg and others (1984), Steiner and others (1985), and Braecker (1987). These studies tie magnetic reversals to calcareous plankton datums, and occasionally ammonite bio-zones. It is obvious that for much of the Jurassic and Cretaceous considerable work needs to be done on magnetic-biostratigraphic relationships before the results can be considered adequate. Until then, such correlations should be considered more as provisional working schemes rather than as refined magneto-biostratigraphies.

TUNING OF THE NUMERICAL TIME SCALE

Ideally, a chronostratigraphic system should be based on the aggregate of reliable empirical data and must be consistent with known earth historical facts. It must also seek to minimize the elements of uncertainty in the data base and avoid unnecessary assumptions. In the past it has been customary to construct geochronologic schemes on the basis of a few selected radiometric dates. These dates are used as isolated constraints on the stratigraphic column, and the intervening segments are then subjected to interpolation, either according to sediment thickness or the distance of magnetic anomalies from spreading ridges. Inherent in such interpolation is the assumption of constancy of rates, whether sediment accumulation or seafloor spreading. These assumptions may not be always warranted, as will become clear in later discussion.

POTENTIAL SOURCES OF ERROR

Since radiometric, biostratigraphic, and magnetostratigraphic data supply the building blocks on which the global chronostratigraphic framework must be based, it may be instructive to review the scope of errors and the ultimate limits of refinement that each type of data offers.

Sources of error in radiometric data.—

In spite of the obvious advantages of basing a time scale on well-constrained radiometric dates, in practice radiometric data are severely limited by numerous sources of error inherent in the samples, as well as in the various radiometric techniques (see Odin, 1982b, for a summary of the sources of error in various techniques).

For example, unaltered plutonic rocks, which probably yield the most reliable radiometric dates because of their greater chemical stability, are often the most difficult to place stratigraphically. Moreover, the numbers obtained from plutonics will depend a great deal on the temperatures at which the various isotopes used to date the rock become 'fixed' in the crystal lattice (its closure temperature), as well as rate of cooling of the rock (Jäger and Hunziker, 1979). When this closure temperature is relatively low, as may often be the case, the subsequent reheating above this tem-

perature will reset the isotopic clock, and any results obtained from such samples only indicate the time of resetting (Gale, 1982). Thus, a careful petrological scrutiny to detect alteration and to ensure freshness of samples becomes an important prerequisite. Several analyses of the minerals in question may also be necessary for accurate age estimates.

Volcanic extrusives, such as lava flows, may suffer from similar sources of error as intrusives, but the presence of excessive radiogenic ^{40}Ar may be especially problematic in these rocks, which would lead to older apparent K/Ar age estimates. For example, in deep-sea lava flows, even when the rock is relatively fresh, excess radiogenic ^{40}Ar trapped during their formation often yields older apparent ages (Seidemann, 1977). Conversely, the presence of a recrystallized glassy component, common in whole-rock volcanic samples, would give younger age estimates (Odin 1982b). There is also the problem of inhomogeneity in samples of volcanic rocks, which could be a serious limitation. In general, however, fresh-acid volcanics that lack post-extrusive alteration can yield reliable Rb/Sr ages.

Bentonites, which are clay deposits formed by devitrification and chemical alteration of tuffs and volcanic ash (see Person, 1982), are generally better constrained stratigraphically than plutonics, but they have their own set of inherent sources of inaccuracies. For example, contaminations resulting from inherited crystal nuclei, and material from the volcanic vent and detrital material, as well as contamination introduced during hydrous alteration, combined with the effects of alteration from glass to clay (Baadsgaard and Lerbeckmo, 1982), can all introduce significant uncertainties in the dates obtained from bentonites. For bentonites as well, pooled dating of many samples from a single horizon may be needed to obtain better age estimates (Baadsgaard and Lerbeckmo, 1982).

Glauconites (or glaucony), marine authigenic minerals related to micas, are generally more abundant than plutonic rocks or bentonites and are best constrained stratigraphically; however, they require great caution in the choice of samples and in analysis. Glauconite grains are fraught with syngenetic and diagenetic sources of error that could alter the apparent ages obtained from them. The behavior of the relevant nuclides during formation and stabilization of the system, as well as the alteration of nuclide ratios since the time of the closure, will affect the ultimate age values (Keppens and Pasteels, 1982). In addition to such post-genetic factors as burial diagenesis, tectonism and reheating, and alteration due to weathering, which affect all types of minerals, the glauconites are also more susceptible to early- and late-diagenetic processes operating at low temperatures. Extra caution is therefore needed to ensure the reliability of dates obtained from glauconites. Glauconitic samples need to be chosen carefully to select grains in which the influence of alteration processes can be mineralogically discounted (Keppens and Pasteels, 1982).

In addition, each radiometric technique, depending on the isotopes being measured, has to contend with a string of special sources of uncertainty. These may be due to the presence of relatively high proportions of the original daughter isotope present in the rock sample at the time of the genesis and the addition or removal of parent or daugh-

ter isotopes since that time. In plutonic rock samples, the Rb/Sr system is generally considered more stable than in other rocks where radiogenic Sr may be removed more easily because of temperature rise. The presence of detrital contaminants, on the other hand, may mean the presence of excessive radiogenic Sr. There may also be a considerable inhomogeneity with respect to Sr in the rock itself (Clauer, 1982). Post-genetic alterations can be caused by leaching by ground water or by weathering by fresh and/or sea water. Exchange reactions resulting from groundwater circulation, however, seem to alter Rb/Sr ages more than K/Ar ages (Keppens and Pasteels, 1982). In general, K/Ar systems are less stable than Rb/Sr systems because Ar atoms carry no charge, are not well-bound chemically, and are subject to easier removal by alteration processes (Keppens and Pasteels, 1982).

Such common laboratory treatment of samples as ultrasonic cleaning or excessive heating prior to analysis may also significantly alter the apparent age of the rock by removal of Ar or Sr. Interlaboratory variations and instrument errors are additional sources of error that make the assessment of isotopic ages from literature an extremely difficult exercise (Webb, 1981).

Comparison of Rb/Sr and K/Ar analyses on the same plutonic rock show that K/Ar may yield ages that are some 4 to 9 million years younger than Rb/Sr (Shibata and Ishihara, 1979). This is attributed to the Rb/Sr system's representing the age of emplacement system's and K/Ar representing the age of cooling (Webb, 1981). An allowance for the age discrepancies may therefore have to be made when dealing with dates from the two systems in a data set. In glauconites, the Rb/Sr and K/Ar age discrepancies are attributed to the open-lattice mineral grains, which may represent alteration or incomplete glauconitization. Thus, there is a need to ascertain the closed-lattice nature of glauconitic minerals before analysis (Odin, 1982a). Good comparative results are obtained by the two methods on glauconites when it is ensured through careful petrographic/sedimentary examination that the samples have not been affected by temperature or pressure changes or by reworking (Keppens and Pasteels, 1982). When K/Ar analyses are performed on carefully chosen samples, a precision of as much as 2 to 3 percent at a 95 percent confidence level is possible (Webb, 1981).

These characteristics and analytical requirements of radiometric dating severely limit the usefulness of both high- and low-temperature radiometric dates, especially in obtaining reliable dates from stratigraphically constrained samples. Significant uncertainties may be involved with *all* types of dates, which underscores the need to use radiometric data with qualification. In our view, given the existing set of radiometric data, one cannot, as yet, achieve a consistent and widely acceptable resolution of the Paleogene and older linear time scales. A *qualified* use of a large set of analytically acceptable dates with known stratigraphic limits, however, can provide important constraints for chronostratigraphy that will lead to a time scale that, hopefully, better approximates reality than does the use of singular dates, used in isolation to nail down relatively long segments of the stratigraphic column.

Sources of error in biostratigraphic data.—

In biostratigraphic data, the most serious source of error that may go undetected is introduced by variations in the biogeographic distribution of marker taxa. Because distribution of taxa is environmentally controlled, their appearance or disappearance in an area may result from changes in environmental parameters rather than from evolutionary first appearance or extinction (see previous discussion on biozones vs. biochronozones). These biogeographic wrinkles can sometimes be ironed out through the aid of magnetostratigraphy or isotopic stratigraphy, but such documentation over large geographic areas exists for only a relatively small number of biohorizons.

The degree of biostratigraphic resolution and precision depends a great deal on the degree to which biostratigraphers can effectively communicate to other workers the morphologic changes they observe in fossils (Haq and Worsley, 1982). When biostratigraphic data are synthesized from widely different sources, a considerable uncertainty can be introduced as a result of differing taxonomic concepts among workers, differing levels of rigor in biostratigraphic work, and in recognizing and recording absolute first- and last-appearance levels in assemblages. Uncertainties can also be introduced by differing or inconsistent sampling intervals and because of undetected vertical discontinuities in sections, or because of reworking and dissolution (see Haq and Worsley, 1982, for further discussion).

Sources of error in magnetic data.—

Because the signal of the earth's individual magnetic-polarity reversal events is not unique, the potential of interpretive error is significant if the magnetostratigraphic data are not stratigraphically well constrained. The interpretation of polarity chronos is commonly dependent on radiometric or biostratigraphic control. Thus, all sources of error inherent in radiometric and biostratigraphic methodologies may ultimately bias the magnetostratigraphic data as well.

Like biostratigraphic data, the magnetostratigraphic data are also subject to sampling limitations and stratigraphic inconsistencies, which determine the ultimate limits of the temporal precision of polarity-reversal boundaries within any given section.

Magnetic-anomaly recognition on the sea floor may be hampered by a number of factors. Seafloor magnetic profiles are complicated by fracture zones, ridge jumps, changes in spreading centers, asymmetric spreading along opposite flanks of the spreading centers, and major plate reorganizations that punctuate the seafloor record. The low amplitude of some anomalies and anomaly skewness can also lead to misidentification of magnetic anomalies (Klitgord and Schouten, 1986). This heavy dependence on interpretation and synthesis may introduce a considerable element of uncertainty in the measurement of distances between anomalies.

In view of this array of sources of error and uncertainties in various types of techniques used in calibrating geologic time, the debates concerning the merits of using one technique over the other, and the criteria for selection of chron-

ologic data, seem spurious. One reaches the inescapable conclusion that a chronologic framework based on any singular technique or unduly restrictive-selection criteria could inherit considerable bias. Instead, an approach that is based on multiple correlative systems, and attempts to reconcile earth historic facts, without ignoring a large body of empirical and analytical data, has the potential of reducing inconsistencies introduced by any singular technique and of producing a more realistic and robust chronostratigraphy.

MAGNETO-BIOCHRONOSTRATIGRAPHY

As mentioned earlier, in the construction of our cycle charts, we have integrated radiometric, biostratigraphic and magnetostratigraphic data in an iterative manner, which produces a reconciliatory magneto-biochronostratigraphic model whose object is that it does not contradict known earth historic facts. For example, one assumption that is often made in the construction of time scales is the constancy of seafloor spreading rates for fairly long intervals of time. Does this assumption agree with the known spreading histories of the major ocean basins? This premise can be evaluated with a relatively simple test.

In Figures 2A–C we have compared the seafloor spreading profiles (i.e., the distances of magnetic anomalies 32 through 2 from the spreading centers) of three different ocean basins. Figure 2A shows a comparison between two North and South Pacific profiles (both after Pitman and others, 1968). Figure 2B shows a similar comparison between North Pacific and South Atlantic profiles (the latter after Dickson and others, 1968, and Heirtzler and others, 1968), and Figure 2C compares the South Atlantic profile with those of the South Pacific. If the spreading rates in these basins had been consistently uniform, these comparisons would have produced linear relationships (i.e., straight lines). Instead, the comparisons reveal that the relationships have varied considerably over time; therefore, spreading rates cannot be assumed to be uniform over the long term in at least two, and perhaps all three, of these basins.

Curry (1985) has also discussed the perils of the assumption of constant spreading rates over long periods of time in constructing time scales. He cites the widely used South Atlantic profile as an example and demonstrates the variability in the Cenozoic spreading rates between and within regions. Pitman and others (1968, fig. 8) made a similar comparison between the various profiles in the South Pacific and the composite North Pacific magnetic-anomaly profile and came to the conclusion that the ratio of spreading in the two basins varied during the Cenozoic; however, the similarities in the shapes of the spreading curves representing three different regions in the South Pacific suggested to them that spreading rates over these regions varied in a similar fashion, even though each region is bounded by different sets of fracture zones. Similarly, Klitgord and Schouten (1986, fig. 8) compared relative spreading between the magnetic-anomaly profile of the Cenozoic mid-Atlantic Ridge and a profile from the western flank of the Pacific-Antarctic Ridge. This comparison revealed distinct changes in the relative spreading of these two basins around anomalies 24/25, 21, 13, 5C, and 2.

Spreading rate comparisons in Figure 2 also indicate where the rate changes are most likely. For example, a consistent change in spreading rates is centered between anomalies 24 and 25, and additional changes may have occurred between anomalies 20 and 21, and 6C and 5C, which is consistent with the findings of Klitgord and Schouten (1986). Changes may also have occurred around anomaly 17 and between 13 and 15 in at least one of the basins. If a linear time scale is to reconcile spreading-rate data, it should be able to reproduce at least the most consistent of the spreading-rate changes (K. Klitgord, pers. commun., 1986). This provides us with important constraints in the integration of magnetostratigraphic data into a chronostratigraphic scheme. The comparison of seafloor spreading rates (Fig. 2) also demonstrates that, over the long term, constant spreading rates cannot be assumed for any one basin, and time scales based on such assumptions could inherit considerable error.

Because seafloor magnetic anomalies form the basis of magnetostratigraphy, the ultimate temporal fidelity of a chronostratigraphic scheme that includes magnetostratigraphy depends on a meaningful reconciliation of the magnetic-anomaly data from various basins. (See Ness and others, 1980, for a discussion and critique of various late Cretaceous-Cenozoic marine magnetic-anomaly scales.)

As mentioned earlier, our approach has been to assign analytically acceptable and biostratigraphically constrained radiometric dates to magnetic anomalies, through the known relationships of biostratigraphic events to magnetic-polarity reversals. The radiometric dates for the Cenozoic are listed in Appendix A. These dates have been plotted against the North Pacific marine magnetic-anomaly profile of Pitman and others (1968) in Figure 3. The same set of dates are plotted against the South Pacific profile (also after Pitman and others, 1968) in Figure 4, and against the South Atlantic profile of Dickson and others (1968) and Heirtzler and others (1968) in Figure 5. In each case the ages of the younger ends (tops) of the magnetic anomalies are calculated from the "best-fit" solution of the high- and low-temperature dates, which is weighted in favor of the older ranges of low-temperature dates when no high-temperature dates are available. Our rationale for using this weighted approach is that, when reliable high- and low-temperature dates are available for the same stratigraphic interval, the older range ends of low-temperature dates overlap with high-temperature dates (Figs. 3–6; see also the discussion on sources of error in radiometric data). As discussed previously, the anomalies where consistent changes in spreading rates are predicted (Fig. 2) can provide potential inflection points on the best-fit curves. Ages (Table 2) calculated from these solutions are then stacked to obtain a mean from the three profiles, which provides us with an integrated chronology of the magnetic anomalies. By stacking the curves, we have, in effect, attempted to reduce the noise due both to uncertainties in the radiometric analytical techniques and to minor irregularities in seafloor spreading patterns in any single basin. It also means that any individual spurious datum will have little effect on the overall validity of the stacked best-fit solution. In view of the inherent analytical uncertainties in radiometric techniques, however, we estimate that an average limit of uncertainty of about ± 1.4 million years can

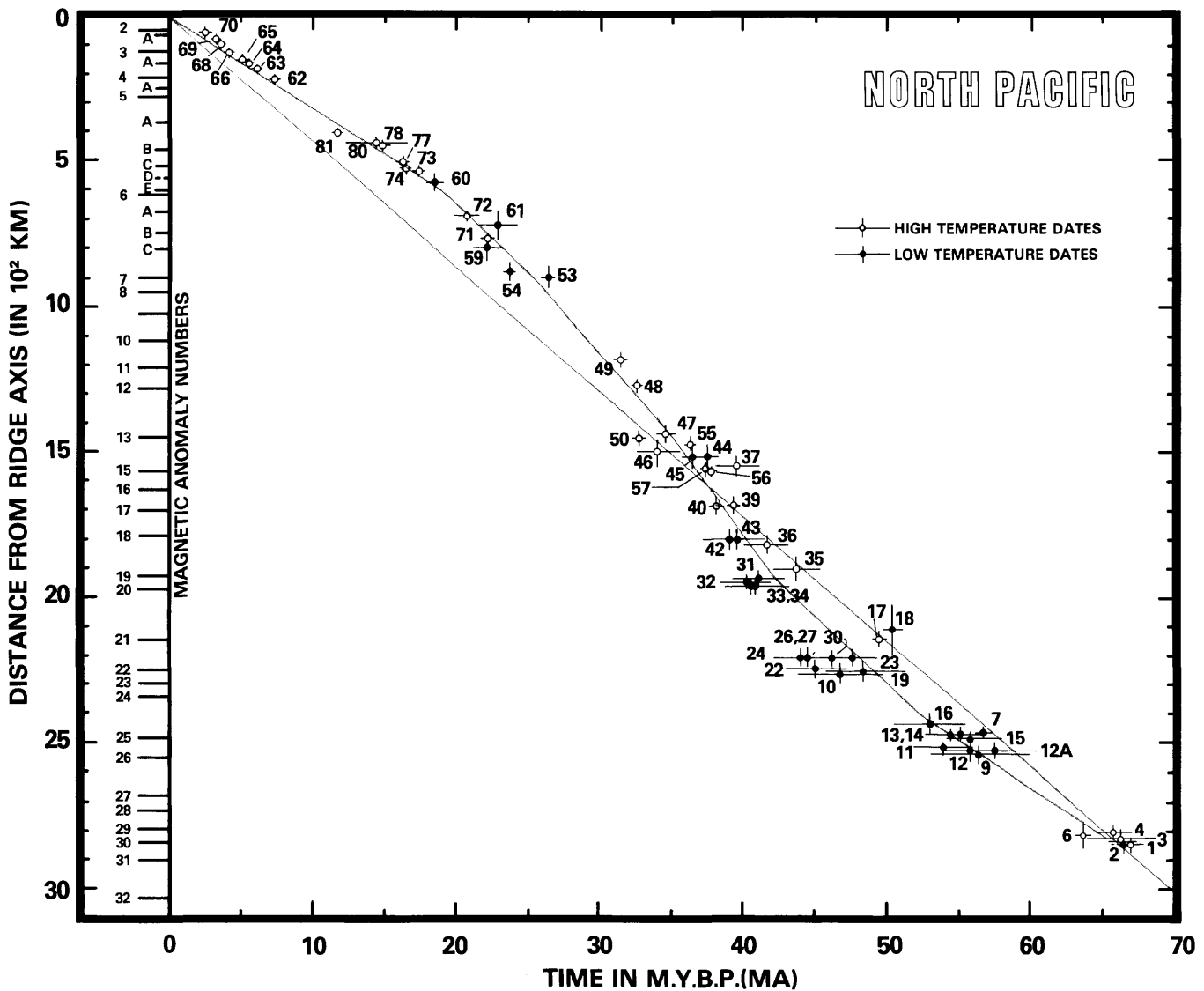


FIG. 3.—Cenozoic high- and low-temperature radiometric dates (see Appendix A for a complete listing) plotted against the composite North Pacific seafloor magnetic-anomaly profile of Pitman and others (1968). The dates are plotted both with their analytical limits of uncertainty (horizontal error bars) and their stratigraphic limits of uncertainty (vertical error bars). (Radiometric dates would align along the straight lines if the spreading rate in this basin were uniform over the Cenozoic.) The ages of the anomalies according to the segmented best-fit solution are given in Table 2 (see text for further explanation).

be ascribed to the Early Tertiary stage boundaries. The limits of uncertainty are considerably narrower for the Miocene stage boundaries (± 0.6 million years) and even more so for the Pliocene (in the range of ± 1.5 thousand years).

Because of the general lack of magneto-biostratigraphic constraints for the Mesozoic, a direct approach, similar to that used for the Cenozoic, cannot be employed for the Mesozoic. Existing chronologic schemes can be tested and improved, however, by using available stratigraphically constrained radiometric dates.

For example, the set of radiometric dates from the Jurassic and Cretaceous (Appendix B) can be compared to the time scale of Harland and others (1982) or to that of Kent and Gradstein (1985). Since the latter is a modified version of the former, and both are essentially similar (with the

exception of the post-Bathonian Jurassic), we have plotted the Jurassic-Cretaceous radiometric dates against the stage boundaries suggested by Harland and others (Fig. 6). Both high- and low-temperature dates have been plotted with their stratigraphic and analytical limits of uncertainty. It is obvious that the majority of the radiometric data older than Cenomanian implies consistently younger ages for the stage boundaries than that suggested by the time scale of Harland and others (1982) for this interval, which was based on the interpolation between two dates at the Aptian/Albian and Anisian/Ladinian boundaries. We propose a chronology of stage boundaries based on the best-fit solution (Fig. 6) through the entire set of data, again weighted in favor of older ends of the low-temperature dates when no high-temperature dates are available. Within each stage, where di-

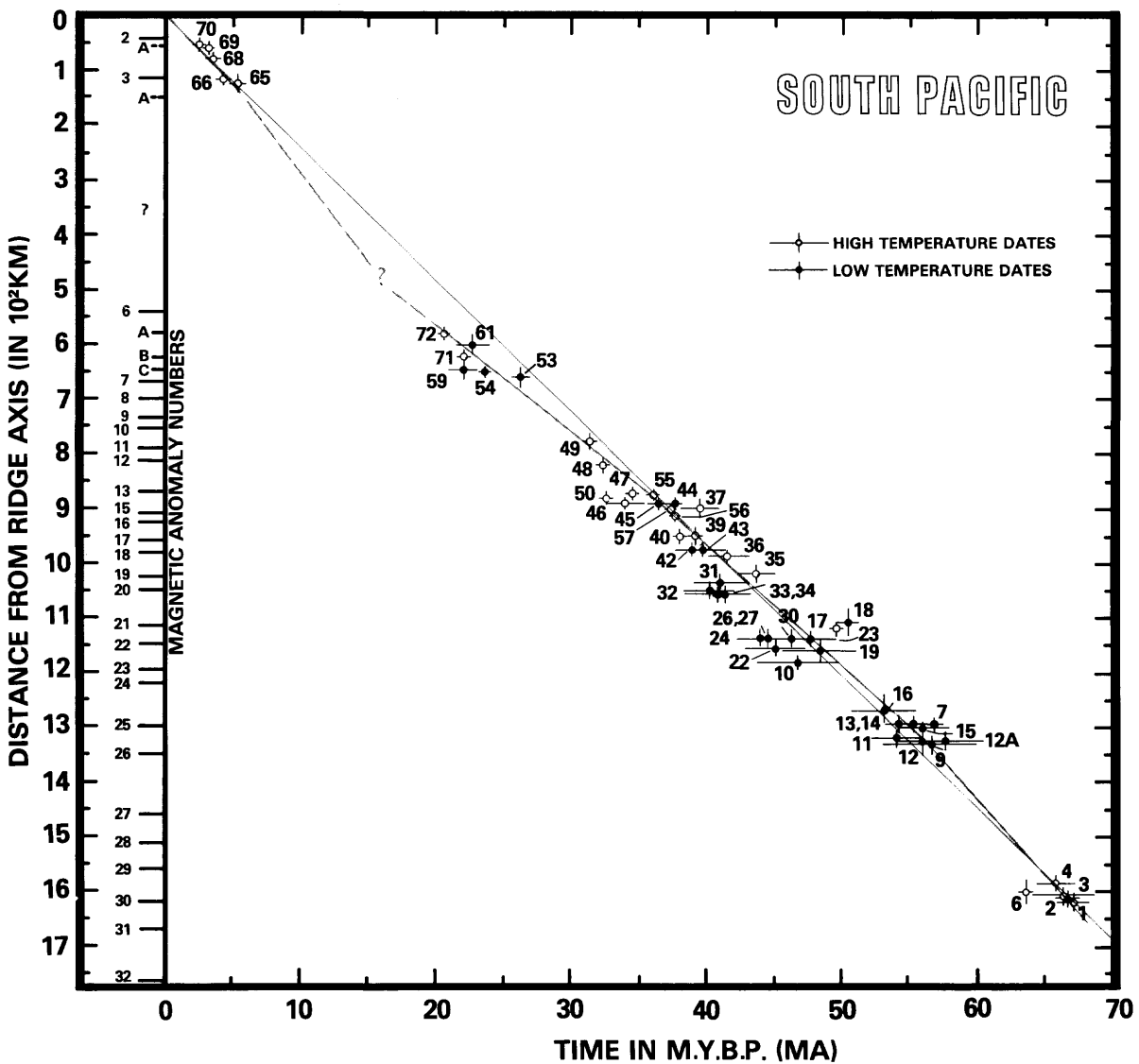


FIG. 4.—Cenozoic high- and low-temperature radiometric dates (same set of dates as in Fig. 3 and Appendix A) plotted against a South Pacific (EL-19S) seafloor magnetic-anomaly profile (after Pitman and others, 1968). Position of anomalies 4 through 5D is uncertain in this profile (see caption of Fig. 3 for explanation).

rect ties between biostratigraphic zonal boundaries and magnetic-polarity reversal events have not been established, we are forced to assign equal duration to biozones of such commonly used fossil groups as ammonites. Hallam and others (1985) have discussed the reason for assigning equal duration to ammonite zones (subzones) at some length. Our approach differs in that we have assigned equal duration to zones within each stage after assigning ages to stage boundaries from the radiometric best-fit solution, and only where no first- or second-order ties with magnetic reversals existed. This avoids the assumption of uniform evolutionary rates for ammonites over a very long period of time and restricts this element of uncertainty to shorter durations within the stage boundaries. The estimated average limits of uncertainty ascribed are ± 3.5 million years to the Jurassic stage boundaries, ± 3.0 million years to the Early

Cretaceous, and ± 1.75 million years to the Late Cretaceous.

The magnetic-polarity scale for the Callovian through Aptian interval is based on the marine magnetic-anomaly sequence that has been developed since the early 1970s. Larson and Chase (1972) and Larson and Pitman (1972) first published the late Jurassic-early Cretaceous M anomaly data based on the Hawaiian lineations in the Pacific. This sequence has since been added to and modified by Larson and Hilde (1975) and Cande and others (1978). The North Atlantic Mesozoic magnetic anomalies have been identified and were subsequently reinterpreted by Schouten and Klitgord (1977), Vogt and Einwich (1979), and Sundvik and others (1984), among others (see also Klitgord and Schouten, 1986, for a discussion of North and Central Atlantic magnetic-anomaly sequences). The correlations be-

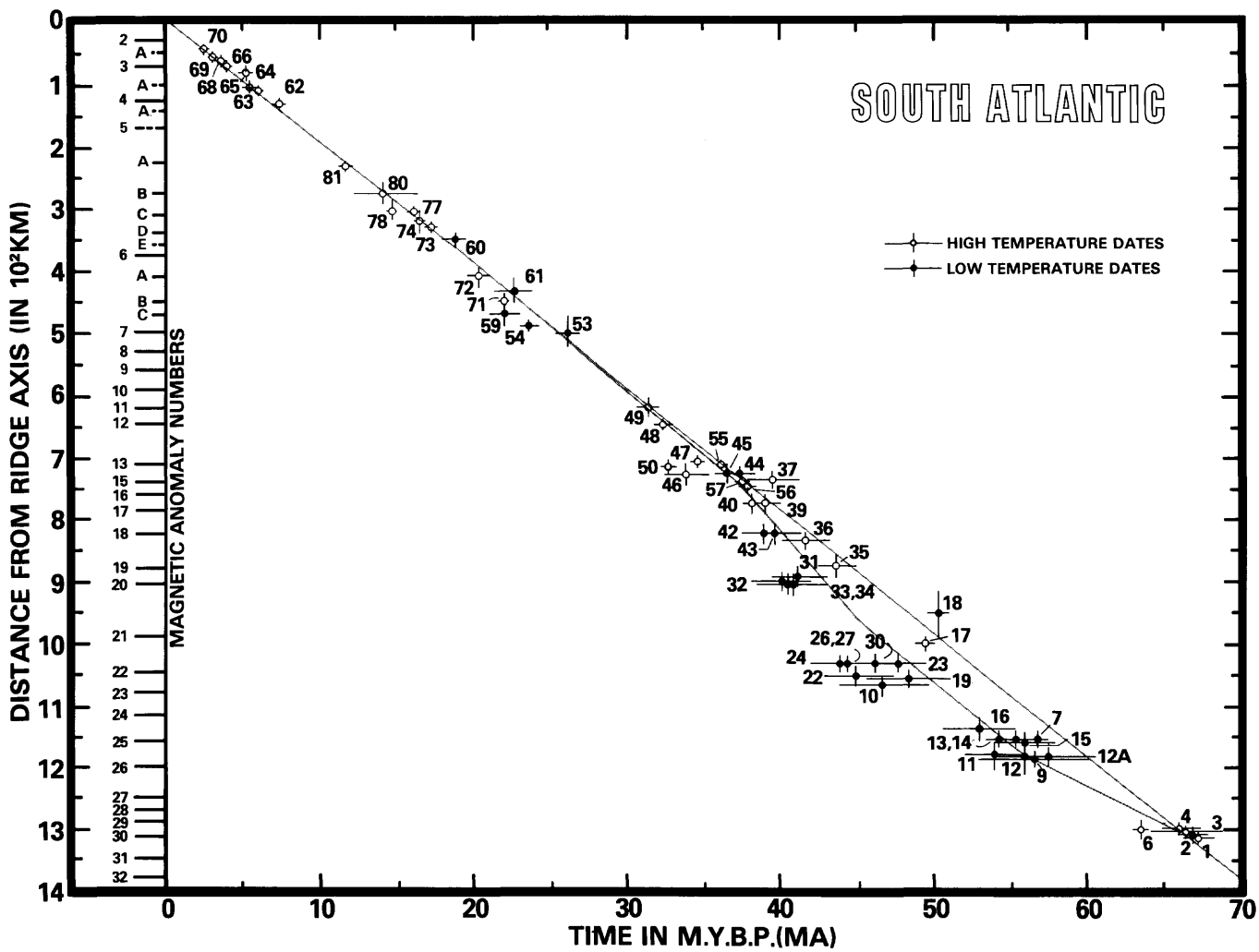


FIG. 5.—Cenozoic high- and low-temperature radiometric dates (same set of dates as in Fig. 3 and Appendix A) plotted against a South Atlantic (V20 S.A.) seafloor magnetic-anomaly profile (after Dickson and others, 1968, and Heirtzler and others, 1968). (See caption of Fig. 3 for explanation.)

tween stage boundaries and magnetic anomalies for the Callovian through Aptian interval have been discussed by Kent and Gradstein (1985).

How does the best-fit Jurassic-Cretaceous time scale of Figure 6 compare with the known magnetic-anomaly profiles in the Pacific and the North Atlantic? For such a comparison (Fig. 7), the ages of M anomalies as predicted by our best-fit solution of Figure 6 have been plotted against the profiles (distance of anomalies from anomaly M) in the North Pacific (after Hilde and others, 1975) and the western North Atlantic (after Klitgord and Schouten, 1986). The North Pacific basin, which has been spreading since Late Triassic-Early Jurassic time (Fig. 7A) shows a relatively constant spreading rate over this interval, with a slight change around anomaly M10N. The western North Atlantic, on the other hand, which began its consistent opening around Blake Spur Magnetic Anomaly (BSMA) time, sometime in the Bathonian-early Callovian, shows considerable variation in spreading rates. The early opening of the basin was relatively fast (Fig. 7B), then slowed down somewhat around

anomalies M25, M21, and M15 times, and accelerated slightly between anomalies M10N and M4. The changes at M21, M15, and around M10N are quite consistent with the changes in the plate kinematics of the North Atlantic as outlined by Klitgord and Schouten (1986; and M. Sundvik, pers. commun. 1984). The change predicted by our time scale at M25 may be entirely due to the relatively young age usually given to BSMA. Extrapolation of the trend between anomalies M22 and M25 to the position of the BSMA (dashed line), predicts a middle Bathonian age for this event and for the initiation of the seafloor spreading in this basin. This older age is more consistent with the middle Bathonian age for the opening of the Central and the North Atlantic as indicated by faunal and paleobiogeographic data from Europe, North America, and the southern Andes (Hallam, 1983). The slight acceleration in spreading around anomaly M10N in both the North Pacific and North Atlantic basins (Fig. 7) suggests that a possible plate reorganization event may have influenced both these basins at the same time.

A similar comparison of the late Cretaceous magnetic

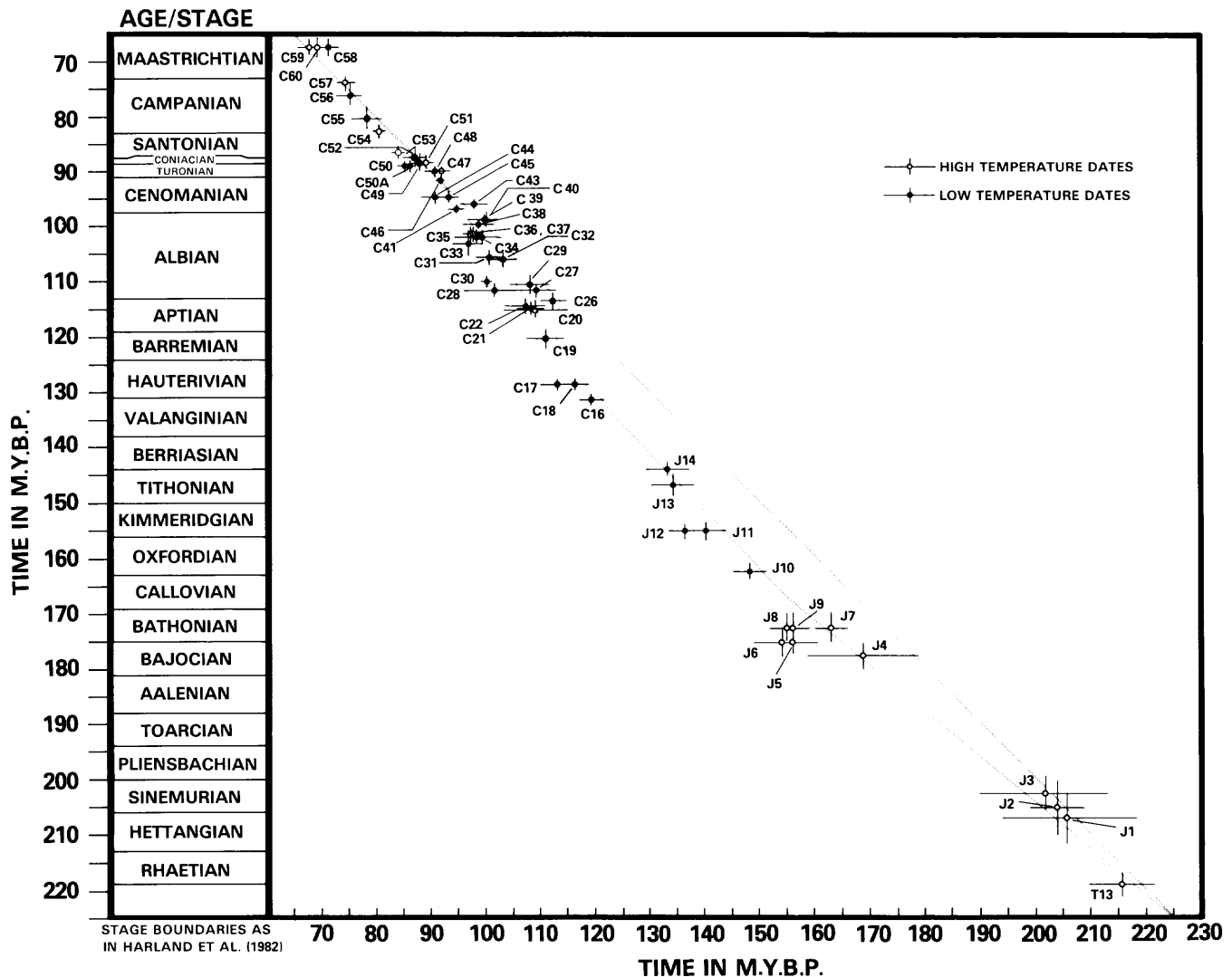


FIG. 6.—Late Triassic through Maastrichtian high- and low-temperature radiometric dates (see Appendix B for a complete list), with their analytical (horizontal error bars) and stratigraphic uncertainties (vertical error bars), plotted against the Jurassic-Cretaceous stage boundaries of the geologic time scale of Harland and others (1982). The segmented best-fit solution through this data set represents the stage boundary ages adopted here (see text for discussion).

profiles (Fig. 8) between anomalies 34 and 30 (younger than the Cretaceous Magnetic Quiet Zone) reveals that, whereas in the North and South Atlantic basins the sea-floor-spreading rates were relatively constant over this interval, those in the Indian Ocean and North and Southwest Pacific were intimately connected, showing a consistent acceleration between anomalies 32 and 31.

The pre-Callovian magnetostratigraphy is a provisional working model based on a synthesis of the existing paleomagnetic studies on sections in the Caucasus (Pechersky in Creer, 1971; Pechersky and Khramov, 1973), in the southern Alps (Channell and others, 1979, 1982), in Switzerland (Hörner and Heller, 1983), and in Hungary (Marton and others, 1980). Some of these studies also include ammonite zonal data that provide important constraints between biostratigraphic and magnetic reversal events. In Figure 9 all of the Jurassic and Cretaceous paleomagnetic studies of exposed marine sections available to us in 1985 have been

summarized. The pre-Callovian synthetic model will be subject to modifications as new and more detailed paleomagnetic data on this interval accumulate.

The radiometric data on the Triassic are sparse with relatively large analytical and stratigraphic uncertainties. The same set of data can be open to numerous differing interpretations, which could yield age estimates for the stage boundaries that differ by several millions of years. Thus, the Triassic linear time scale adopted by us must be considered provisional, with average limits of uncertainty for various stage boundaries of ± 5.0 million years. This time scale is essentially a compromise of the radiometric data and stratigraphic considerations presented by Armstrong (1982), Webb (1982), Harland and others (1982), Forster and Warrington (1985), Salvador (1985), and Snelling (1985). The Triassic magnetic-reversal stratigraphy and the adopted nomenclature synthesize the paleomagnetic studies of various stratigraphically constrained Triassic sections by

TABLE 2.—AGES OF YOUNGER ENDS (TOPS) OF CENOZOIC MAGNETIC ANOMALIES FROM NORTH AND SOUTH PACIFIC AND SOUTH ATLANTIC BASINS.

CHRON NUMBER (TOP NORMAL)	ANOMALY NUMBER	AGES FOR ANOMALY YOUNGER ENDS (IN MA)			
		NORTH PACIFIC PROFILE	SOUTH PACIFIC PROFILE	SOUTH ATLANTIC PROFILE	MEAN AGE FOR ANOMALY TOPS
C2	2	1.65	1.65	1.65	1.65
C2A	2A	2.50	2.50	2.50	2.50
C3	3	3.90	3.90	3.90	3.90
C3A	3A	5.40	U	5.40	5.40
C4	4	6.80	N	6.60	6.70
C4A	4A	7.90	C	7.70	7.80
C5	5	8.90	E	9.00	8.95
C5A	5A	11.60	R	11.80	11.70
C5B*	5B	14.20	T	14.20	14.20
C5C	5C	16.20	A	16.00	16.10
C5D	5D	17.40	I	17.60	17.50
C5E	5E	18.60	N	18.40	18.50
C6	6	19.30	19.30	19.30	19.30
C6A	6A	20.70	20.80	20.90	20.80
C6B	6B	22.40	22.60	22.80	22.60
C6C	6C	23.70	23.75	23.80	23.75
C7	7	25.60	25.60	25.40	25.53
C8	8	26.30	27.10	26.90	26.76
C9	9	27.60	28.70	28.40	28.23
C10	10	29.50	29.80	29.80	29.70
C11	11	31.20	31.50	31.40	31.36
C12	12	32.30	32.70	32.50	32.50
C13	13	35.20	35.60	35.50	35.43
C15	15	36.90	37.30	37.10	37.10
C16	16	37.90	38.20	38.10	38.06
C17	17	38.60	39.40	38.90	38.96
C18	18	40.20	40.30	40.10	40.20
C19	19	42.30	42.20	42.20	42.23
C20	20	43.20	43.10	43.00	43.10
C21	21	46.90	46.30	46.50	46.56
C22	22	49.20	48.50	48.90	48.86
C23	23	50.30	50.40	50.40	50.36
C24	24	51.30	51.50	52.30	51.70
C25	25	55.40	54.90	54.80	55.03
C26	26	57.10	57.00	57.75	57.28
C27	27	61.40	61.00	61.70	61.36
C28	28	63.00	63.10	63.30	63.13
C29	29	65.00	64.80	64.95	64.91
C30	30	66.80	67.00	67.10	66.96

* NORMAL POLARITY INTERVAL JUST ABOVE C5B (ABOVE ANOMALY 5B)

Ages are derived from the best-fit solutions of radiometric dates (Figs. 3–5). The right column shows stacked mean ages for the anomaly tops adopted in the Cenozoic-cycle chart (Fig. 14).

Helsley (1969), Burek (1970), Pechersky (in Creer, 1971), McElhinney and Burek (1971), and Pechersky and Khramov (1973). Like the pre-Callovian Jurassic, the Triassic magnetostratigraphy will be subject to modifications in the future as new data become available.

DOCUMENTATION OF SEA-LEVEL CHANGES

The interpretation of sea-level changes in marine outcrops has been facilitated by the development of sequence-stratigraphic concepts. The *depositional sequence* (Mitchum and others, 1977; Van Wagoner and others, this volume) is a relatively conformable succession of genetically related strata bounded by unconformities, or their correlative conformities. A sequence is interpreted to have been deposited during a complete cycle of sea-level change. A complete cycle of sea-level change includes two relative falls of sea level and extends from the inflection point of the maximum rate of sea-level fall to the subsequent rise, followed by the next fall. *Sequence stratigraphy* is that branch

of stratigraphy which subdivides the rock record using a succession of depositional sequences composed of genetically related strata as regional and interregional correlative units.

Sedimentary patterns along continental margins are controlled by sediment supply, rate of subsidence, and sea-level change. The combined effects of regional tectonics and eustasy determine the accommodation potential for the sediments (Jervey, and Posamentier and others, this volume) and the distribution of facies within the genetically related packages (see Posamentier and Vail, and Van Wagoner and others, this volume). The rate of relative fall in sea level determines the type of sequence boundary that will terminate the sequence. If the rate of eustatic fall exceeds the rate of subsidence at the depositional-shoreline break (Van Wagoner and others, this volume), the entire shelf may be exposed, and a type 1 sequence boundary will result. In deep-water basins with a sand source, type 1 boundaries are commonly characterized by canyon cutting on the slope and fluvial incision on the shelf. When the rate of relative sea-level fall is less than the rate of subsidence at the depositional-shoreline break, the shelf seaward of the depositional-shoreline break will not be exposed, and a type 2 sequence boundary will result.

A complete cycle of sea-level change is interpreted to be represented in the rock record by a depositional sequence. A sequence is interpreted to begin with a relative sea-level fall. In the type 1 sequence, sea level falls beyond the depositional-shoreline break, beginning fluvial incision of the shelf. Sea-level falls of major magnitude are characterized by canyon-cutting events on the shelf and slope. The incised-river system may feed a lowstand fan that is most likely to be deposited offshore during this time (Fig. 10).

When the rate of regional subsidence begins to exceed the rate of eustatic fall, relative sea level begins to rise. During this time, the lowstand wedge portion of the lowstand systems tract is deposited as an overlapping wedge seaward of the shelf break (Fig. 10). This wedge is characterized by a deep-water debris flow/leveed-channel system. In most cases, this system is eventually overlain by the prograding complex of the lowstand wedge. When sea level begins to rise in more rapidly, the sea transgresses over the shelf and back-stepping parasequences of the transgressive-systems tract begin to accumulate (see Van Wagoner and others, this volume). Following the time of maximum flooding, the parasequences in the transgressive-systems tract are overlain by a progradational stack of parasequences of the highstand systems tract. The highstand systems tract builds basinward over the transgressive-systems tract and lowstand wedge (Fig. 10). The parasequences in all systems tracts are interpreted to be formed by higher frequency flooding events and intermittent times of slower sea-level rise.

If the termination of the sequence is a type 2 boundary, relative sea level does not fall at the deposition-shoreline break, the whole shoreface is not exposed, and lowstand fan and the leveed-channel complexes do not develop. Instead, a shelf margin wedge (shelf margin systems tract) may prograde directly over the shelf break and onto the slope (Fig. 10).

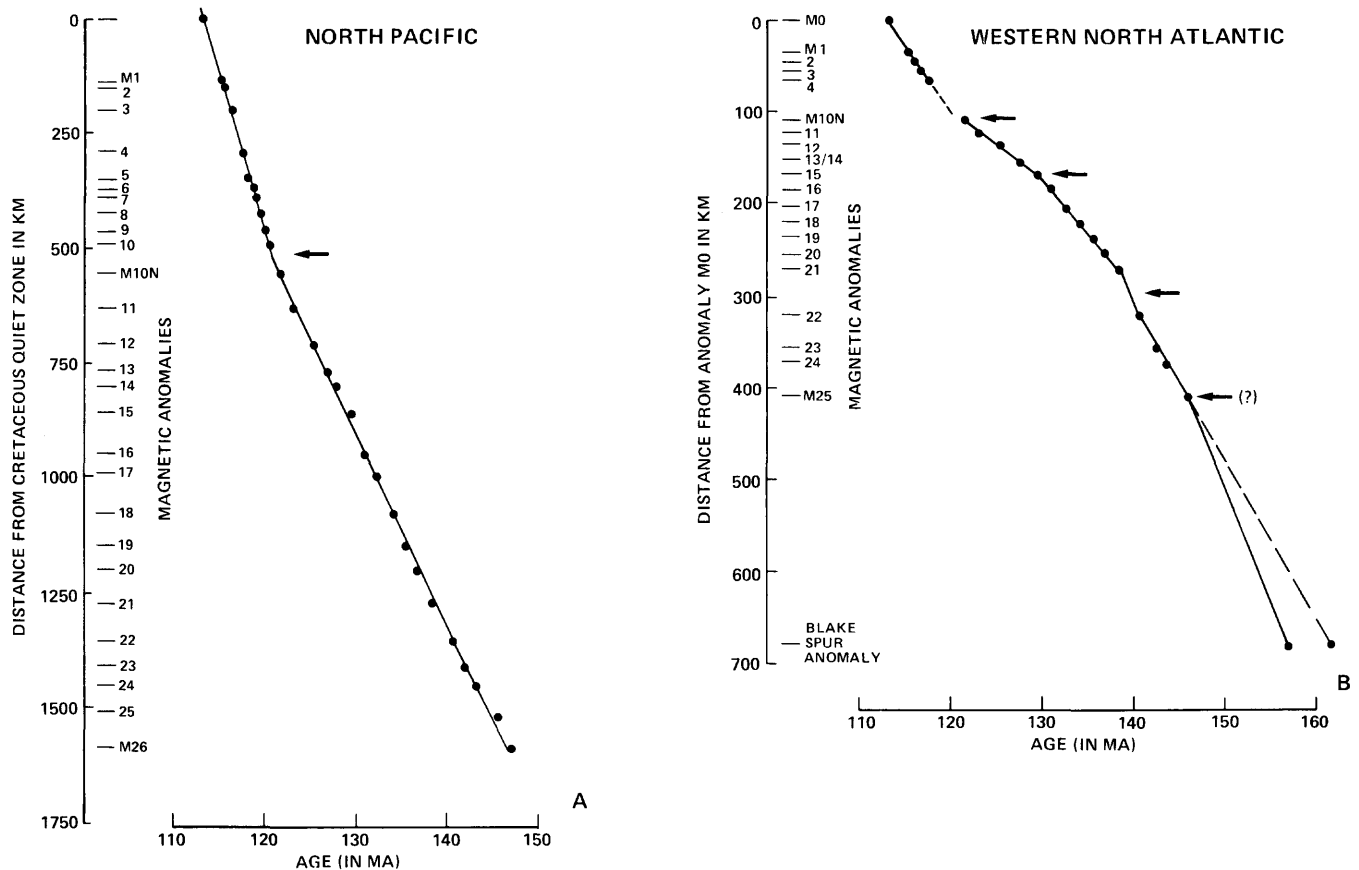


FIG. 7.—The ages of M-series magnetic anomalies, as predicted by the best-fit solution time scale plotted against the seafloor magnetic-anomaly profiles in the North Pacific (after Hilde and others, 1975) and western North Atlantic (after Schouten and Klitgord, 1982, and Klitgord and Schouten, 1986). (A) Anomalies M26 through M1 are shown with their distance from the Cretaceous Magnetic Quiet Zone. (B) The distance of Blake Spur and M25 through M1 anomalies is shown from anomaly M0. Points represent ages on the anomalies as estimated from the best-fit time scale of Figure 6. In the North Pacific, this time scale predicts an essentially uniform seafloor spreading rate, with a slight acceleration between anomalies M10 and M10N. In the western North Atlantic, the same time scale suggests changes at anomalies marked by arrows. The dashed line between M25 and Blake Spur anomalies represents the continuation of the spreading-rate trend of the interval between M22 and M25 to Blake Spur. This would date the Blake Spur anomaly and the beginning of the opening of the North Atlantic at about 162 Ma (mid-Bathonian). (See text for discussion.)

During the course of a complete cycle of sea-level change, lowstand, transgressive, and highstand facies are all well defined, although lowstand and highstand facies are generally represented by relatively thicker sections, and transgressive facies by thinner sections.

In outcrop sections, the lowstand, shelf margin, transgressive-, and highstand systems tracts can be identified between three prominent depositional surfaces. The first is the “transgressive surface” (Fig. 10), which occurs at the top of the lowstand systems tract. The transgressive surface is the first flooding surface marking the beginning of the more rapid sea-level advance over the shelf. This surface is usually marked by conspicuous lithologic changes, for example, from marginal marine below to nearshore marine above, or from more terrigenous to less terrigenous sediments on the outer shelf and slope. The lowstand deposits below the transgressive surface are characterized by the sediments of the most regressive phase of the sequence. When lowstand deposits are lacking, the transgressive surface may coincide with the underlying unconformable portion of the sequence boundary.

The second readily recognizable surface in outcrops of shelf strata is the “surface of maximum flooding” of the shelf. This surface manifests itself as a “downlap surface” on seismic profiles. It is associated with the period of depositional starvation on the outer shelf and slope, when depocenters have moved landward in response to rapidly rising sea level. The sediment starvation produces a physically condensed section (see Loutit and others, this volume, for a detailed discussion of condensed sections and their stratigraphic importance). The condensed section forms partly within the transgressive- and partly within the highstand systems tracts of the sequence. Because of the lack of terrigenous input, the condensed section may compromise a zone of high pelagic-fossil concentration, rich glauconitic or phosphatic layers, or a hardground caused by lithification. The relative duration of sediment starvation within a condensed section increases basinward, until beyond the area of terrigenous influence, the biogenic deposition in the deeper basins occurs as a series of stacked condensed sections. The downlap surface separates the transgressive- from the highstand systems tracts, and the accompanying prominent faunal

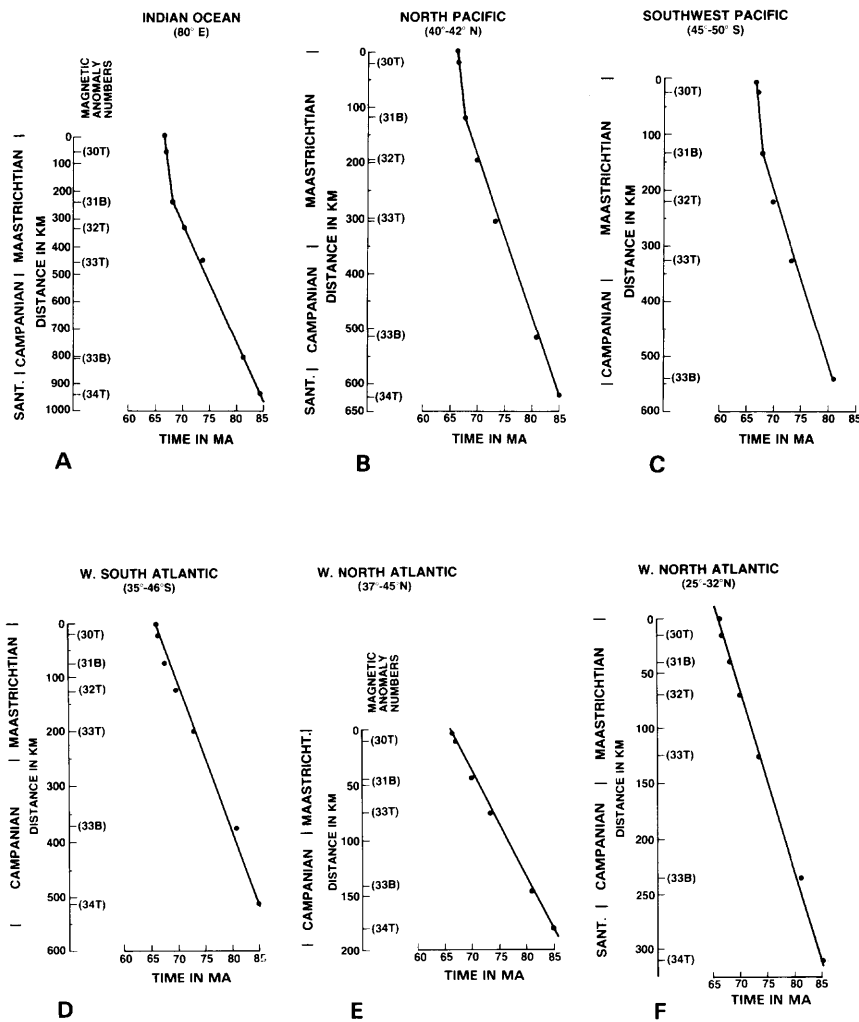


FIG. 8.—Tops (younger ends) and bottoms (older ends) of the latest Cretaceous (younger than Cretaceous Magnetic Quiet Zone) magnetic anomalies in different basins plotted against the ages of the anomalies predicted by the Cretaceous time scale adopted here (Fig. 6). All profiles are after Cande and Kristoffersen (1977, fig. 5).

and lithologic changes at this surface also often lead to confusion between the downlap surface and the sequence boundary.

The third surface is the sequence boundary, expressed as the downward (basinward) shift of the coastal-onlap pattern, or by truncation on seismic profiles. In outcrops the sequence boundary may be an obvious unconformity or its correlative conformity, depending on the position of the section along the shelf-to-basin profile and the rate of sea-level fall. For example, if the position of a section is proximal (landward) on the shelf, the probability of lowstand deposition in the area is reduced or precluded. In such a case, the sequence boundary may be an unconformity that coincides with the transgressive surface (Fig. 10). Basinward, the sequence boundary becomes conformable and may be typified by a change from interbedded progradational deposits to more massive, aggradational, deposits.

The outcrop interpretation of the Cenozoic and Mesozoic sea-level cycles, using the sequence-stratigraphic principles outlined previously (and detailed in Jersey, and Posamentier and others, this volume), has been made on continental margin and interior sections in various parts of the world. The bulk of the documentation so far, however, comes from

sections in western Europe, the United States Gulf and Atlantic coasts, and the United States Western Interior. Sections in New Zealand, Australia, and Pakistan, and in the Arctic islands of Bjørnøya and Svalbard have also contributed to the documentation. Lists of sections that have contributed to the documentation of the sequences on the cycle charts can be found in Appendix C for Cenozoic strata, Appendix D for Cretaceous strata, Appendix E for Jurassic strata, and Appendix F for Triassic strata.

Some examples of outcrop studies.—

To illustrate the sequence-stratigraphic analysis of outcrop sections in different settings, we include three examples of outcrop studies. The first example is from the neostratotype of the Lutetian stage in the Paris Basin, the second from the type area of the Cenomanian, and the third from a reference section of Scythian age from the Salt Range in Pakistan. Other examples of identification of systems tract boundaries in outcrop sections are enumerated in this volume by Sarg; Donovan and others; Greenlee and others (and in prep.); Loutit and others; and Baum and others. Examples discussed in the above studies and those given below provide a broad overview of the application of sequence-

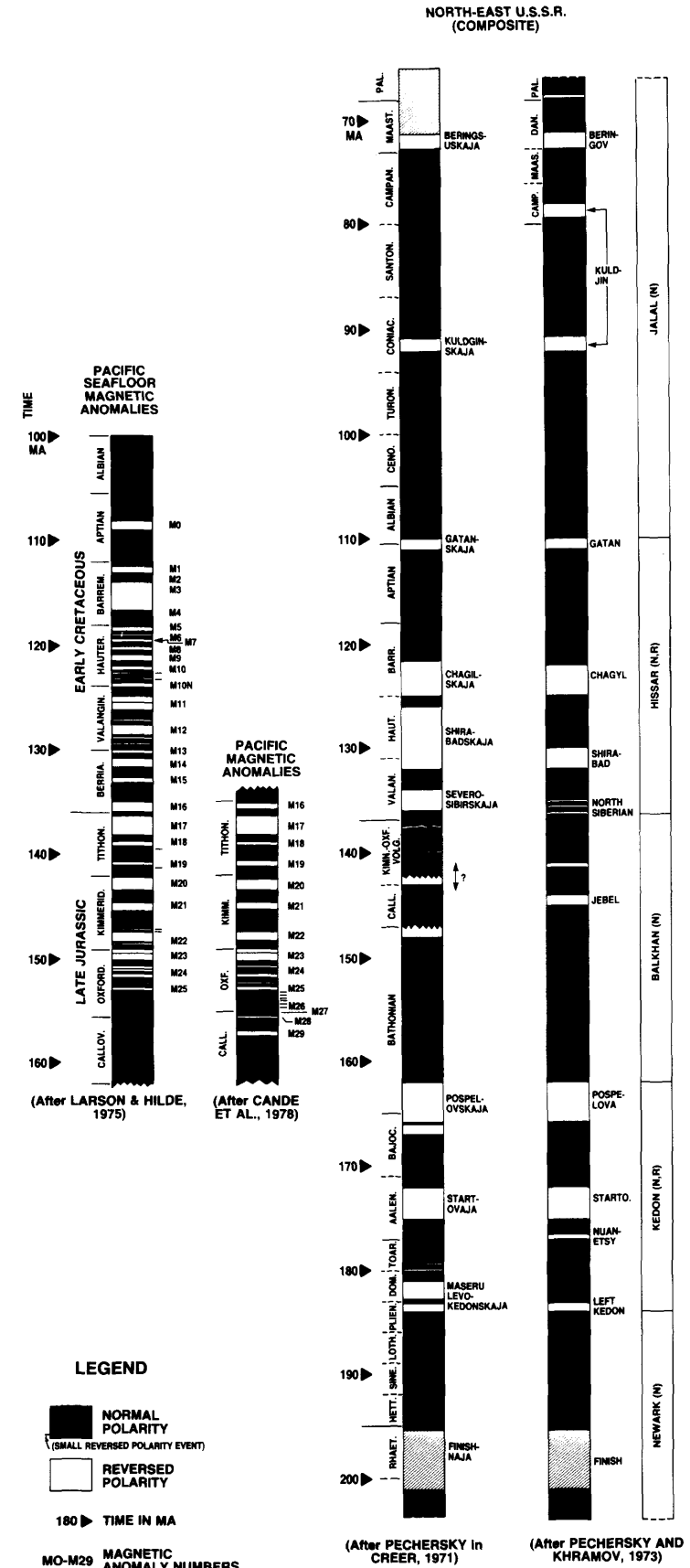
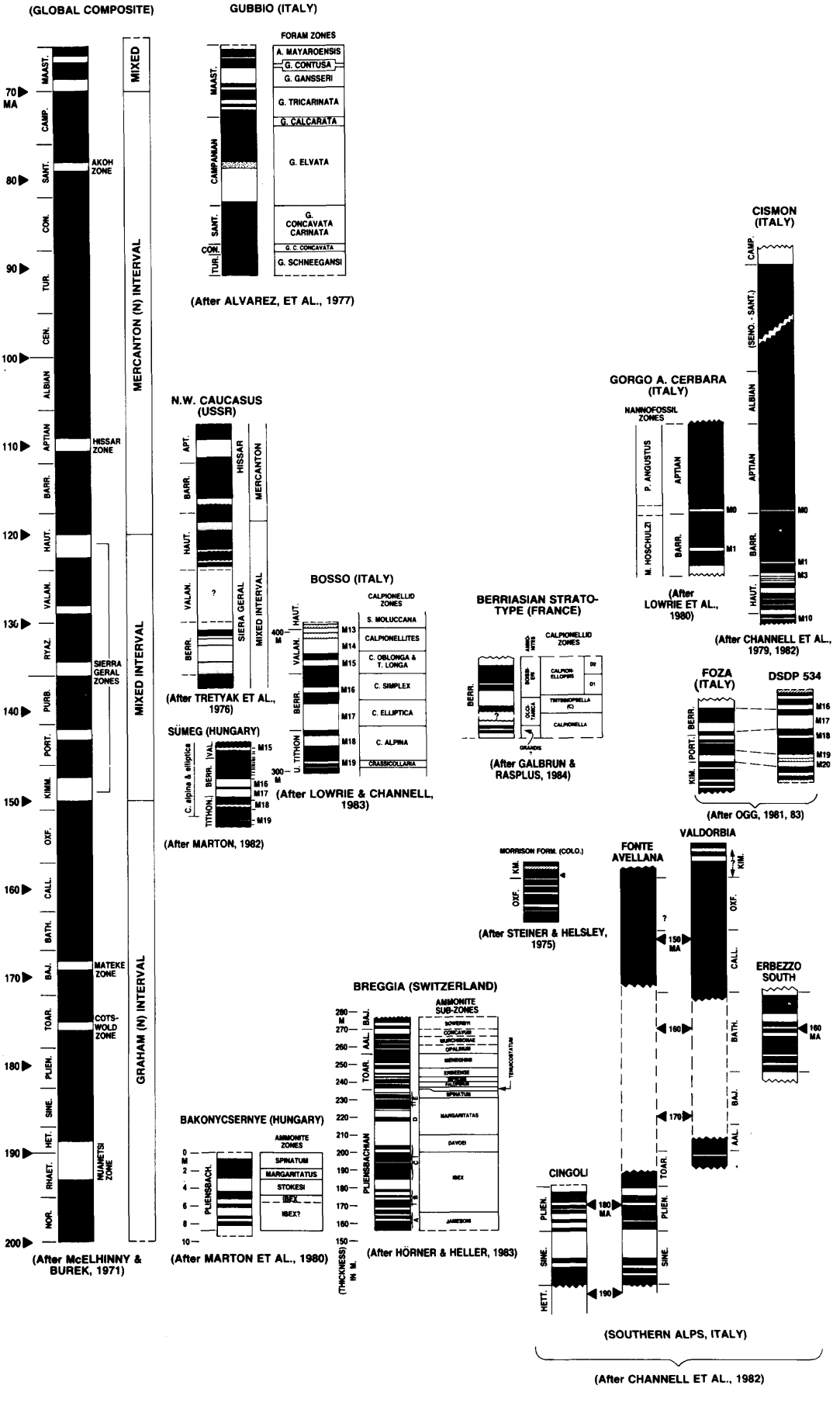


FIG. 9.—A paleomagnetic composition of known magnetic-polarity reversal data from sections in the U.S.S.R. and central Europe (France, Italy, Switzerland, and Hungary). The Pacific seafloor magnetic-anomaly data (Larson and Hilde, 1975; Cande and others, 1978) and a global composite (of McElhinny and Burek, 1971) are also plotted. The provisional pre-Callovian polarity reversal model (Fig. 16) is based on a synthesis of the paleomagnetic data of the same interval shown here.



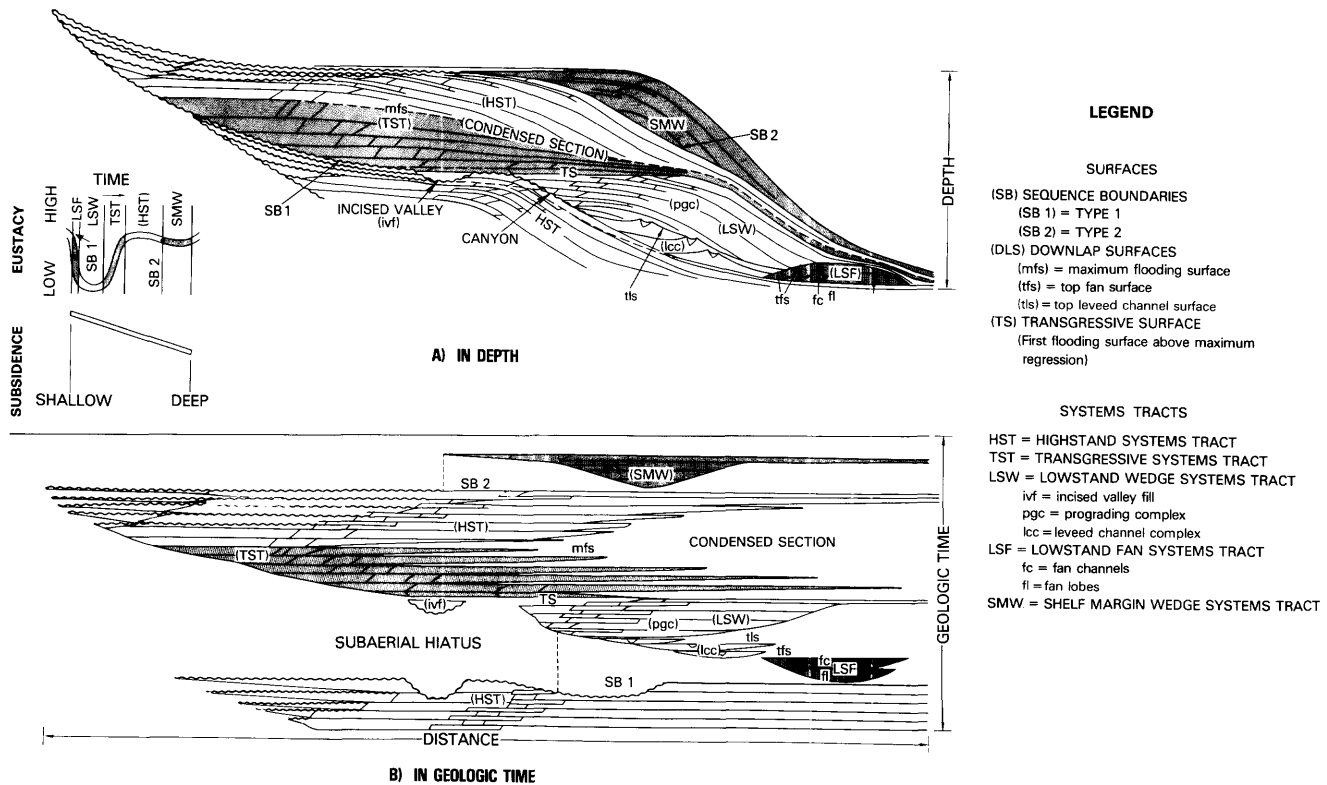


FIG. 10.—Stratigraphic sequence depositional model showing depositional-systems tracts and their bounding surfaces. The model shows systems tracts associated with type 1 sequence boundary (i.e., lowstand fan, lowstand wedge, transgressive-, and highstand systems tracts). Shelf margin wedge systems tract develops following a type 2 sequence boundary (see text). (A) The geometry of the systems tracts with depth. (B) The same features as in A in relationship to geologic time.

stratigraphic concepts in identifying cycles of sea-level change.

The identification of depositional surfaces and sequence boundaries in the outcrop is based on the premise that changes in relative sea level affect facies relationships in the sediments. A correct analysis of the depositional facies is easiest in areas with pronounced changes in lithofacies. Facies changes in shallow-water clastic settings are often more obvious than those in carbonate settings. The preliminary sequence interpretation in the three examples given here is based on available facies analyses from published information and subsequent visits to the outcrops. It must be emphasized, however, that a more precise positioning of the depositional surfaces needs to be confirmed by more detailed litho- and biofacies analyses of such sections on a broader, regional basis.

The first example, the neostratotype of the Lutetian, the “standard” stage of the lower Middle Eocene, is based on a composite section from the lower Lutetian at St. Leu d’Esserent and the middle and upper Lutetian at St. Vaast-les-Mello in the Paris Basin (Blondeau, 1980; Blondeau and Renard, 1980). The lower Lutetian is composed of approximately 12 m of coarse sands, dolomitic and glauconitic limestone, and the middle and upper Lutetian of 33 m of limestones and alternating limestones, marls, and clays, overlain by Quaternary sands (Fig. 11). Four sequence boundaries can be identified.

The lowest sequence boundary (49.5 Ma) is placed between micaceous sands attributed to the Cuisian Stage and coarse glauconitic sands with bryozoans and shark teeth which form the transgressive base of onlapping lower Lutetian deposits. The sequence boundary and the transgressive surface are interpreted to coincide at the St. Leu d’Esserent locality, as indicated by the presence of an unconformity between the Cuisian and Lutetian in this area. The sandy transgressive deposits of the lower Lutetian become more calcareous upward. The downlap surface is not well exposed at this locality. Thus, the base of the Lutetian in the type section falls between the sequence boundary at 49.5 Ma and the downlap surface at 49.0 Ma.

The next sequence boundary (48.5 Ma) can be identified in the upper part of the lower Lutetian, where sandy, calcareous deposits are overlain by glauconitic sands containing *Nummulites laevigatus*. The transgressive surface is marked by a highly glauconitic sandy limestone with very abundant *N. laevigatus*. This transgressive surface with its abundant fossil content has traditionally been considered the boundary between the lower and middle Lutetian (Blondeau, 1980). The sandy glauconitic deposits between the sequence boundary and the transgressive surface are interpreted here as a thin shelf margin wedge. The transgressive deposits overlying the transgressive surface consist of coarse calcarenites with abundant molluscan molds. The downlap surface can best be seen at St. Vaast-les-Mello, at the base

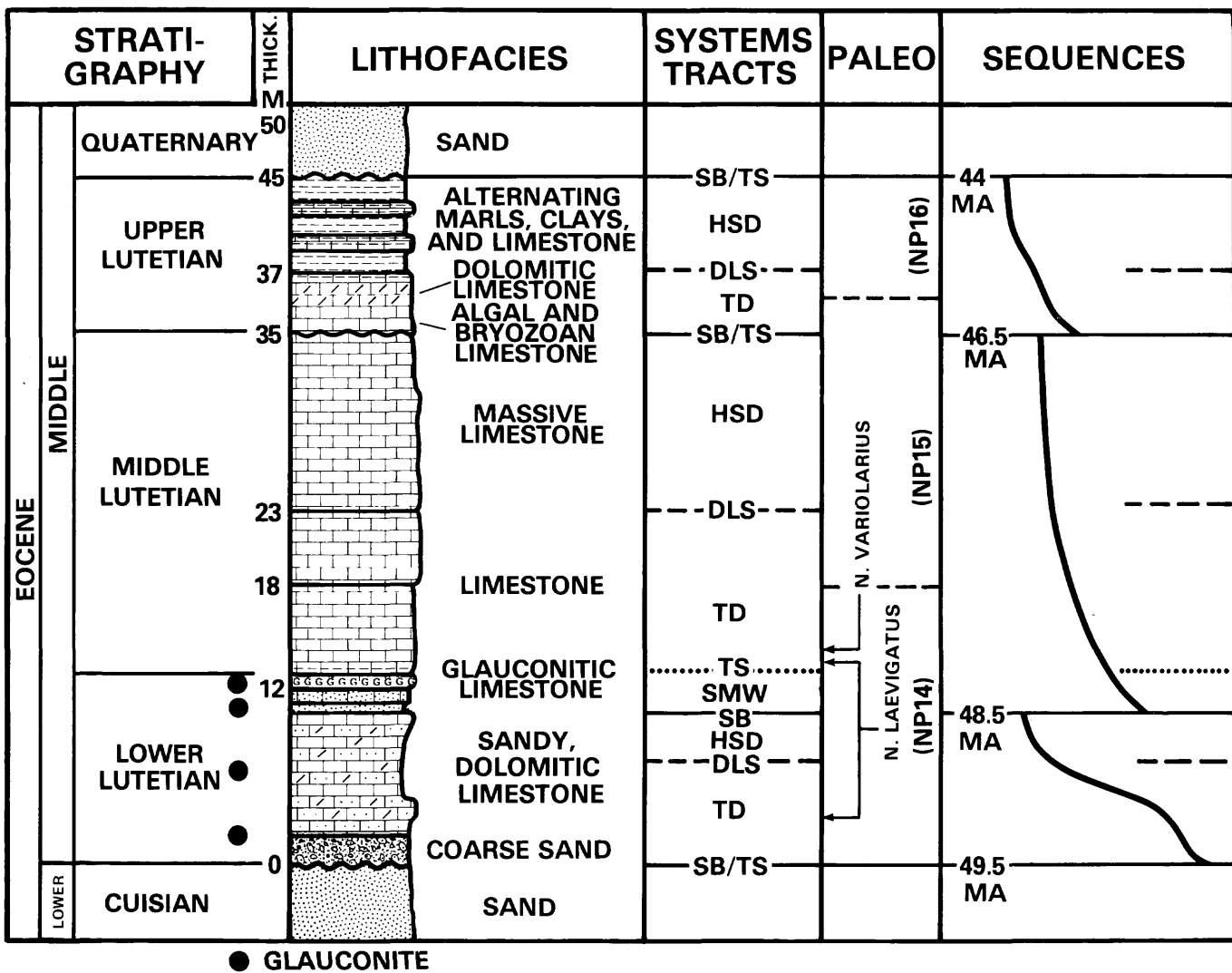


FIG. 11.—Lithofacies, biostratigraphy, and sequence stratigraphy of the neostratotype sections of the Lutetian (middle Eocene) Stage in the Paris Basin. The section is a composite of the lower Lutetian from St. Leu d'Esserent and middle and upper Lutetian from St. Vaast-les-Mello (stratigraphic subdivisions and lithologic sections after Blondeau, 1980, and Blondeau and Renard, 1980, and indirect nannofossil zonal assignments in the paleo column after Bouche, 1962, and Aubry, 1983). Symbols in the systems tracts column are as follows: SB: Sequence boundary; TS: Transgressive surface; TD: Transgressive deposits; HSD: Highstand deposits; SMW: Shelf-margin wedge. (See text for further explanation.)

of a massive 12-m-thick, fine calcarenite bed with abundant miliolids ("Banc Royal"), which represents the highstand deposits of this sequence.

The 46.5-Ma sequence boundary is placed above the "Banc Royal" at the base of a coarser grainstone high in the middle Lutetian. The downlap surface in this sequence is marked by the transition from higher energy grainstones in the transgressive-systems tract to interbedded marls and fine limestones in the highstand systems tract. The fourth sequence boundary, at 44 Ma, lies between the alternating marls, clays, and limestones of the upper Lutetian and the transgressive sands of the Auversian. The later sequence boundary is not exposed at St. Vaast because Quaternary sediments unconformably overlie the upper Lutetian.

Indirect calcareous nannofossil information from the Lutetian elsewhere in the Paris Basin (Bouché, 1962; Au-

bry, 1983) permits the correlation and positioning of these four sequences relative to the cycle chart.

The second outcrop study example comes from the region of the type Cenomanian in the southeastern Paris Basin. In sections in the Le Mans-Ballon and the Theligny-St. Calais areas, the uppermost Albian rests unconformably on Oxfordian limestone, which marks the lowest sequence boundary in the area (98 Ma). In Figure 12, composite sections (compiled by P. Juignet) from the two areas are shown along with lithostratigraphy, biostratigraphy (ammonite zones after Amédro, 1980, 1986; Wright and Kennedy, 1984) and sequence-stratigraphic interpretations based on broader, regional considerations of the depositional facies relationships.

Both the Le Mans-Ballon and Theligny-St. Calais sections are composed of 115 to 120 m of glauconitic

marls, sands, chalks, and limestones. The next sequence boundary (96.5 Ma) lies within the upper Albian glauconitic marls that contain *Ostrea vesiculosa*. Although discernable on a regional basis, this boundary is very subtle in both of the sections shown in Figure 12. The downlap surface within this sequence is marked by the deeper, chalier facies in the Theligny-St. Calais section. The third- and fourth-sequence boundaries (95.5 and 94 Ma, respectively) are less subtle and can be identified by the change from late highstand marly and interbedded-limestone facies below to shelf margin sands above. Shelf margin facies are well developed in the lower of these two sequences and consist of sands that grade upward into the more calcareous facies of the transgressive phase. Highstand deposits consist of alternating marls and thin-bedded limestones.

The highest sequence boundary in the Cenomanian (93 Ma) is a minor sequence placed at the base of *Catopygus obtusus* sands. These sands, interpreted as shelf margin wedge facies, mark a brief return of shallow clastic deposition to an overall deepening depositional setting. The downlap surface lies just above the Cenomanian-Turonian boundary in the *Inoceramus labiatus* chalk.

The well-established ammonite zonation of the sections helps place the sequence and systems tract boundaries within

a chronostratigraphic framework. Such studies on stage stratotypes or their equivalents, where they exist, are good examples of how the sequence-stratigraphic approach can help position the eustatic cycles more precisely within the global chronostratigraphic framework.

The third outcrop study example is from the Scythian (Lower Triassic) of the Salt Range in Pakistan (Fig. 13). The Late Permian to Early Triassic succession is a well-exposed succession in the Salt Range, and a series of easily accessible sections provide an excellent Tethyan paleontologic and sea-level record of this interval. For this reason, the Salt Range has achieved the status of a global reference section for the latest Permian and Early Triassic interval.

The Scythian (Mianwali Formation) of the Salt Range (Nakazawa and others, 1985) consists of a mixed clastic and carbonate section whose relative position along the shelf-to-slope profile (outer shelf, near the depositional-shelf edge) is such that the sequence boundaries are conformable and lithologically very subtly expressed. The transgressive surfaces, however, are marked by prominent lithologic changes, and downlap surfaces are also readily identified by association with the conspicuous physical features typical of such surfaces (Fig. 13).

The Permo-Triassic boundary in this section (between the

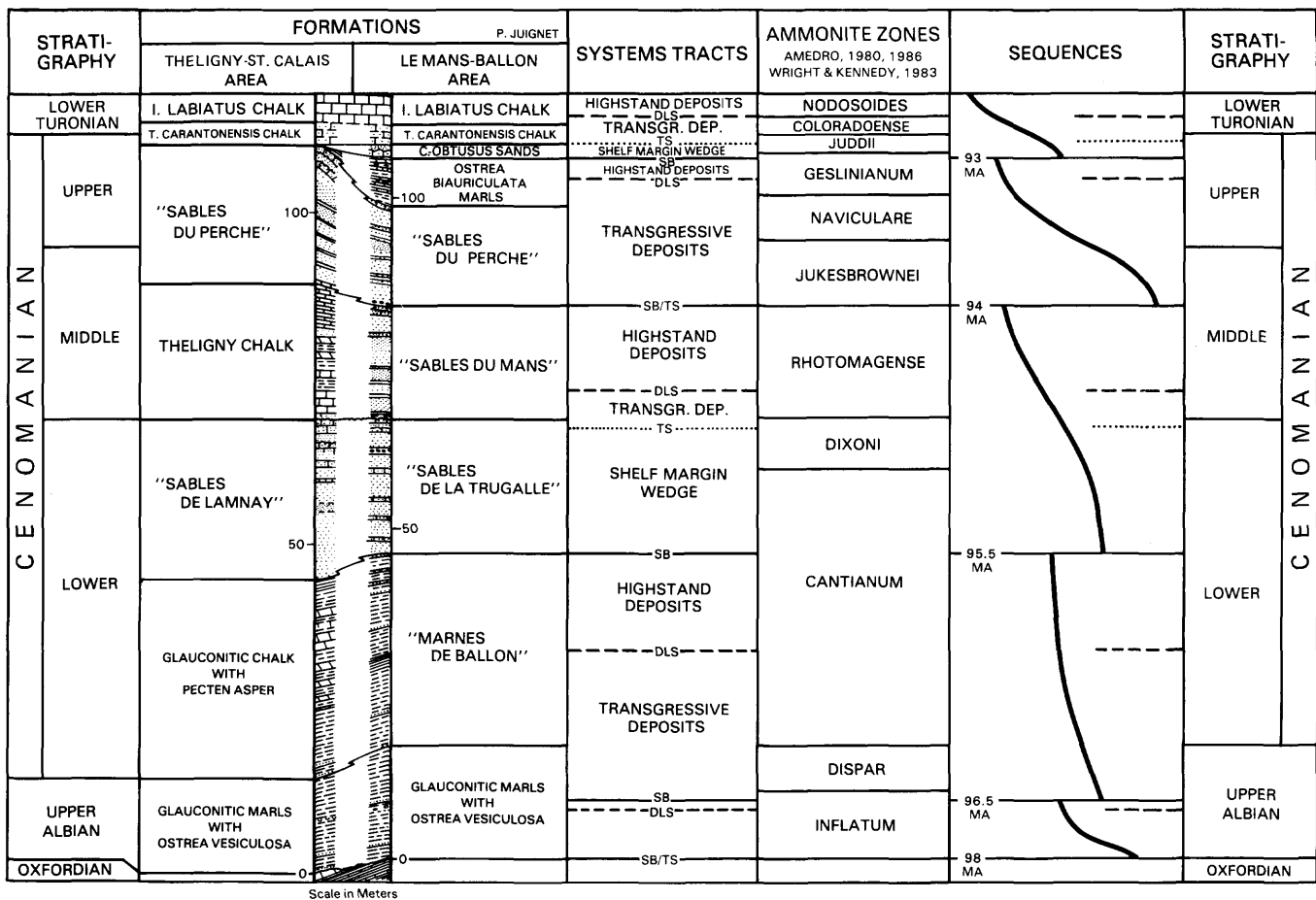


FIG. 12.—A composite section from the type region of the Cenomanian Stage (Theligny-St. Calais and Le Mans-Ballon areas), showing lithostratigraphy (compiled by P. Juignet), biostratigraphy (after Amedro, 1980, 1986, and Wright and Kennedy, 1983), and sequence-stratigraphic interpretations. For symbols in systems tracts column, see caption for Figure 11.

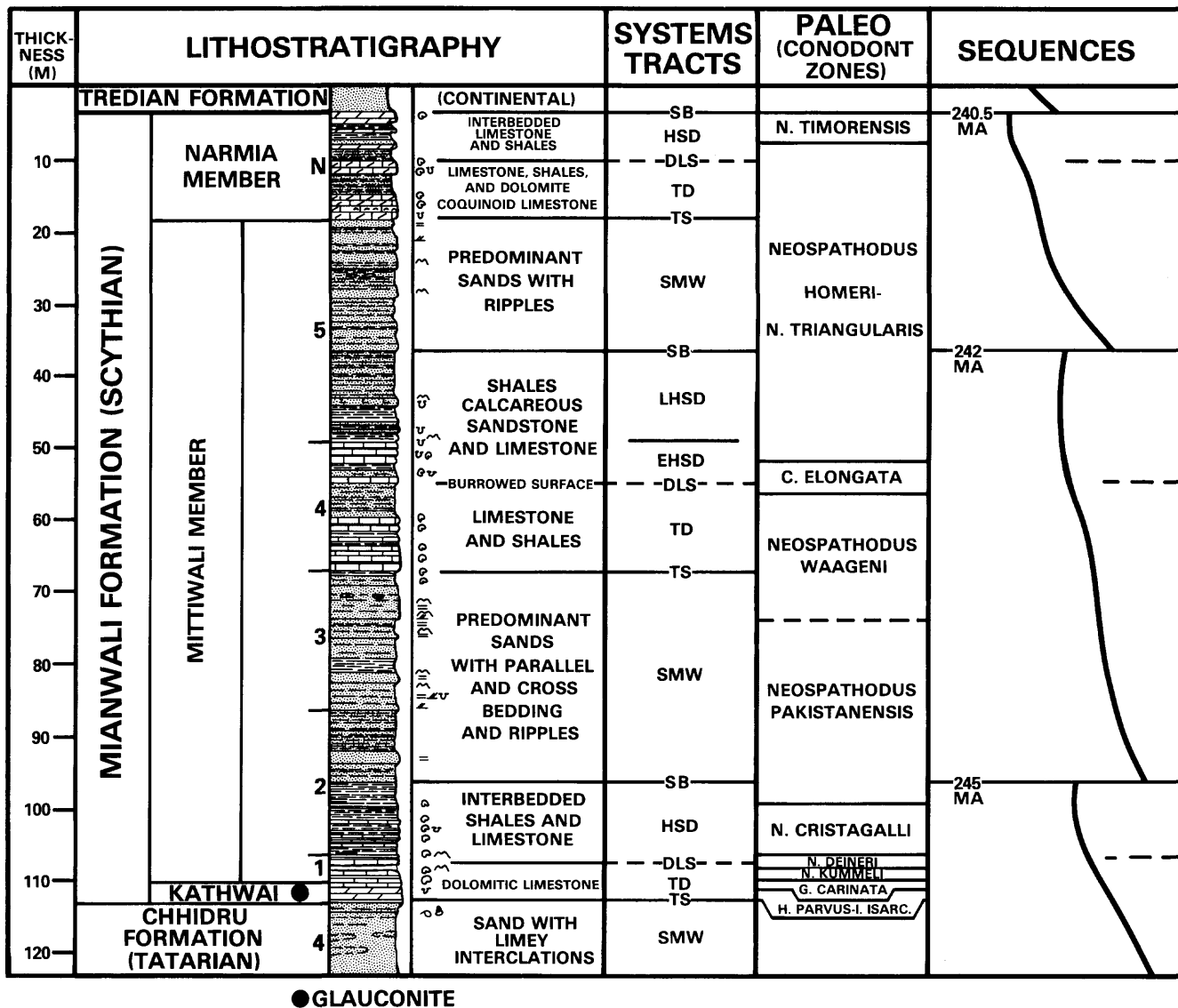


FIG. 13.—Lithostratigraphic, paleontologic, and sequence-stratigraphic data of the Scythian (Lower Triassic) section at Nammal Gorge, Salt Range, Pakistan. Lithostratigraphy after Nakazawa and others (1985) and paleontologic zonation after Matsuda (1985). For symbols in systems tracts column, see caption for Figure 11. EHSD: Early highstand deposits; LHSD: Late highstand deposits.

Chhidru and Mianwali formations; see Figure 13) is a prominent transgressive surface which is marked by a change from sands of the shelf margin wedge facies below to transgressive dolomitic limestones above. The transgressive deposits are relatively thin and mark the passage into highstand facies of interbedded shales and limestones through a condensed section marked by a burrowed surface. The overlying sequence boundary is rather subtle lithologically but shows an increased terrigenous input of coarser grained sandstones.

The next younger sequence is composed of a relatively thick shelf margin wedge with a series of stacked parasequences of sandstones with parallel bedding and cross-bedding. The top of the shelf margin facies is indicated by a conspicuous change from sandstones below to limestones and shales of the transgressive-systems tracts above. These

grade upward into calcareous sandstones and limestones of the highstand systems tracts. The intervening downlap surface is marked by burrows. The early highstand systems tracts deposits are predominantly limestone, whereas late highstand facies consist of interbedded shales and sandstones.

The overlying sequence boundary is once again very subtle in the field, although terrigenous input increases below and above this boundary. The shales and sandstones of the relatively thick shelf margin systems tracts are abruptly overlain by limestones, shales, and dolomitic and coquinoïd limestones of the transgressive-systems tracts. The highstand facies of this sequence consist of interbedded limestone and shales. These are in turn overlain by continental deposits of the Tredian formation, the change marking the youngest sequence boundary in the section.

The excellent fossil record of the Salt Range sections includes conodonts, ammonites, ostracodes, and dinoflagellates. These groups have been extensively studied and tied to global stratigraphy (e.g., Matsuda, 1985; Nakazawa and others, 1985) and permit the accurate dating of the transgressive and downlap surfaces and sequence boundaries.

DESCRIPTION OF THE CYCLE CHARTS

Figures 14 and 17 present the chronology of sea-level fluctuations in the Cenozoic, Cretaceous, Jurassic and, Triassic. A large-scale composite chart outlining the chronostratigraphy and eustatic cycles of the Mesozoic and Cenozoic is also included (in pocket). The cycle charts combine the linear time scale (in Ma, or millions of years before present, repeated on the left, center, and right of the charts for convenience) with magnetostratigraphy, standard chronostratigraphy, biochronostratigraphy, and sequence chronostratigraphy.

Magnetostratigraphy includes the polarity reversal sequence, seafloor magnetic-anomaly numbers (from Oxfordian to Recent), and the numeric terminology of polarity chrono-zones (*sensu* Harland and others, 1982). The late Cretaceous and Cenozoic chron numerology is adopted from Tauxe and others (1983) and the Callovian through Aptian from LaBrecque and others (1983). The old system of Neogene polarity "epochs" (LaBrecque and others, 1977, 1983) is also included, for correlation purposes with the older literature. In the present version, however, the correlation of epochs 7 through 14 with magnetic anomalies has been updated following Barron and others (1985).

The magnetostratigraphy adopted for the cycle charts is a combination of four types of paleomagnetic data of varying quality. For the past 6.5 Ma, an accurate geomagnetic-polarity scale tied to reliable radiometric dates of lavas is available (McDougall and others, 1976, 1977; Mankinen and Dalrymple, 1979). The Cenozoic polarity reversal scale (older than 6.5 Ma and up to magnetic anomaly 32) is based on the stacked mean ages of marine magnetic anomalies from three ocean basins, as discussed earlier. The composite-polarity scale for this interval has developed from the marine magnetic-anomaly scale of Heirtzler and others (1968) with later refinements suggested by LaBrecque and others (1977) and Lowrie and Alvarez (1981). The Oxfordian through Barremian polarity scale has been adopted by calibrating the M-series magnetic anomalies and standard stages against a best-fit numerical scale based on available Jurassic-Cretaceous radiometric dates (see Fig. 6). The M-series magnetic-anomaly scale has developed through the studies of Larson and Pitman (1972), Larson and Hilde (1975), and Cande and others (1978). An update of the relationship of these anomalies to stage boundaries has been recently discussed by Kent and Gradstein (1985). Here, however, we have included a minor reversed-polarity event near the top of the Aptian (above MO), following the finding of Lowrie and others (1980). For the pre-Callovian Jurassic and the Triassic, for which no seafloor magnetic anomaly data are available, the polarity reversal sequence has been synthesized from the paleomagnetic studies of Helsley (1969), Burek (1970), McElhinny and Burek (1971),

Perchesky (in Creer, 1971), Perchesky and Kramov (1973), Helsley and Steiner (1974), Marton and others (1980), Channell and others (1982), and Hörner and Heller (1983). The magnetic zonal terminology for this interval is largely after Burek (1970), McElhinny and Burek (1971), and Perchesky and Kramov (1973).

The chronostratigraphic section includes hierarchical subdivisions of system, series, and stage. We have adopted the commonly used European stage nomenclature because it has become the "standard" for world-wide correlations. The suprastage designations, such as Buntsandstein, Muschelkalk, Keuper, Lias, Dogger, Malm, Neocomian, and Senonian, that are still frequently used in regional stratigraphic literature, are also included in the stage columns, but no formal status is implied. The Jurassic/Cretaceous boundary has been placed between the Portlandian and Ryazanian stages (at 131 Ma), following the common North Sea usage. Alternative boundary placement is between the Tithonian and Berriasian stages (at 134 Ma), which is also common in the continental European literature.

The third section of the cycle charts includes biochronostratigraphy. This section incorporates two types of information: zonal schemes, where zones have been formally defined, and first- and last-occurrence events (biohorizons) of some fossil taxa whose formal zonal schemes have not been established. The included zonal schemes vary for each cycle chart, depending on the relative usefulness of the fossil groups for each interval. All four cycle charts include palynomorph biohorizons (mostly dinoflagellates, with the exception of some spore and pollen in the early Triassic) that have been synthesized and compiled by palynologists of Exxon Production Research Company (L. E. Stover, M. Milliod, N. S. Ioannides, R. Jan de Chêne, Y. Y. Chen, J. D. Shane, and B. E. Morgan). These data are based mostly on information from western Europe and the North Sea area.

On the Cenozoic-cycle chart (Fig. 14) the biochronostratigraphic data include planktonic foraminiferal zones after Blow (1969), Berggren (1972), Stainforth and others (1975); calcareous nannofossil zones after Martini (1971), Okada and Bukry (1980) and Bukry (1981); radiolarian zones after Sanfilippo and others (1981, 1985); and diatom zones after Gombos (1982), Gombos and Ciesielski (1983), Fenner (1985), and Barron (1985).

The Cretaceous biochronostratigraphic data (Fig. 15) include zonal schemes of planktonic foraminifera after Premoli-Silva and Bolli (1973), Premoli-Silva and Boersma (1977), van Hinte (1976), Robaszynski and others (1979, 1983), and Caron (1985); calpionellids after Alleman and others (1971) and Remane (1978, 1985); calcareous nannofossils after Thierstein (1976), Sissingh (1977), Manivit and others (1977), and Roth (1978, 1983). Cretaceous boreal macrofossil zones (mostly ammonoids and belemnoids, but also some echinoids in the Late Cretaceous) are after Rawson and others (1978) and Kennedy (1984). Tethyan ammonoid zones are after various authors in Cavalier and Rogers (1980), Busnardo (1984), Amedro (1980, 1981, 1984), Kennedy (1984), Robaszynski and others (1983), and Clavel and others (1986).

The Jurassic biochronostratigraphy (Fig. 16) includes radiolarian events and preliminary zones after Pessagno (1977),

Pessagno and Blome (1980), Baumgartner (1985), and Pessagno and others (1987a,b) and calcareous nannofossil zones after Barnard and Hay (1974), Medd (1982), Hamilton (1982), and Roth and others (1983). Boreal ammonoid zones and subzones are from Cope and others (1980).

The Triassic-cycle chart (Fig. 17) includes radiolarian zones after Blome (1984) and conodont zones after Mosher (1970), Sweet and others (1971), and Matsuda (1985). The Tethyan ammonoid zones are after Tozer (1984) and North American ammonoids after Silberling and Tozer (1968).

The fourth section of the cycle charts consists of sequence chronostratigraphy, which includes sequence chrono-zones. The first-order sequence chrono-zones include megasequence and megasequence set chrono-zones. The Phanerozoic is divided into two megasequence set chrono-zones (lower and upper), and all of the interval from the Late Permian through the Recent fits within the Upper Phanerozoic megasequence set. The Mesozoic and Cenozoic, however, are composed of three megasequence chrono-zones (the upper part of the Absaroka, the Zuni, and the Tejas). The sequence chronozone terminology adopted here is based on the sequence terminology of Sloss (1963). The megasequences are subdivided into second-order supersequence and supersequence set chrono-zones. Seven supersequence sets include 27 super-sequences, all of which terminate with sequence boundaries of major magnitude. The sequence chronozone terminology is followed by scaled relative change in coastal onlap associated with each third-order sequence chronozone. The third-order sequence chrono-zones include sequences that terminate with major, medium, and minor boundaries, and these boundaries are distinguished as such on the cycle charts. A total of 120 sequence chrono-zones has been identified from the base of the Triassic to Recent. Of these, 19 begin with major-magnitude falls of sea level, 43 with relatively medium-magnitude falls, and 58 with minor sea-level falls. Generally, only the major- and some medium-magnitude cycles can be identified at seismic stratigraphic resolution level. Detailed well-log and/or outcrop studies are necessary to resolve the minor cycles.

Alongside the coastal-onlap column, the ages of the sequence boundaries and downlap surfaces are indicated in separate columns, as are the depositional systems tracts. Boundaries where lowstand fans have been observed are indicated by "F." The unshaded triangle within each coastal-onlap cycle represents the condensed sections within that sequence (see Loutit and others, this volume). The shape of the triangle depicts the interval of slow deposition on the shelf and slope, following a rapid rise of sea level, the relative duration of which increases basinward. The relative magnitude of the condensed sections (major, medium, or minor) is also identified by the relative thickness of the lines representing the downlap surface associated with each condensed section.

The long- and short-term eustatic curves complete the cycle charts. The scale represents our best present estimate of sea-level rises and falls compared to the modern average mondial sea level. The relative magnitude of long-term sea-level variations is estimated following the methods described in Hardenbol and others (1981), with a high value (in the Turonian) adopted from Harrison (1986). The rel-

ative magnitude of the short-term sea-level changes is a best estimate from seismic and sequence-stratigraphic data. Although we believe these estimates to be within realistic ranges, they may have to be modified as better, more rigorous methods of determining the magnitude of sea-level changes become available. Today's long- and short-term sea-levels diverge because the long-term eustatic curve is estimated assuming an ice-free world.

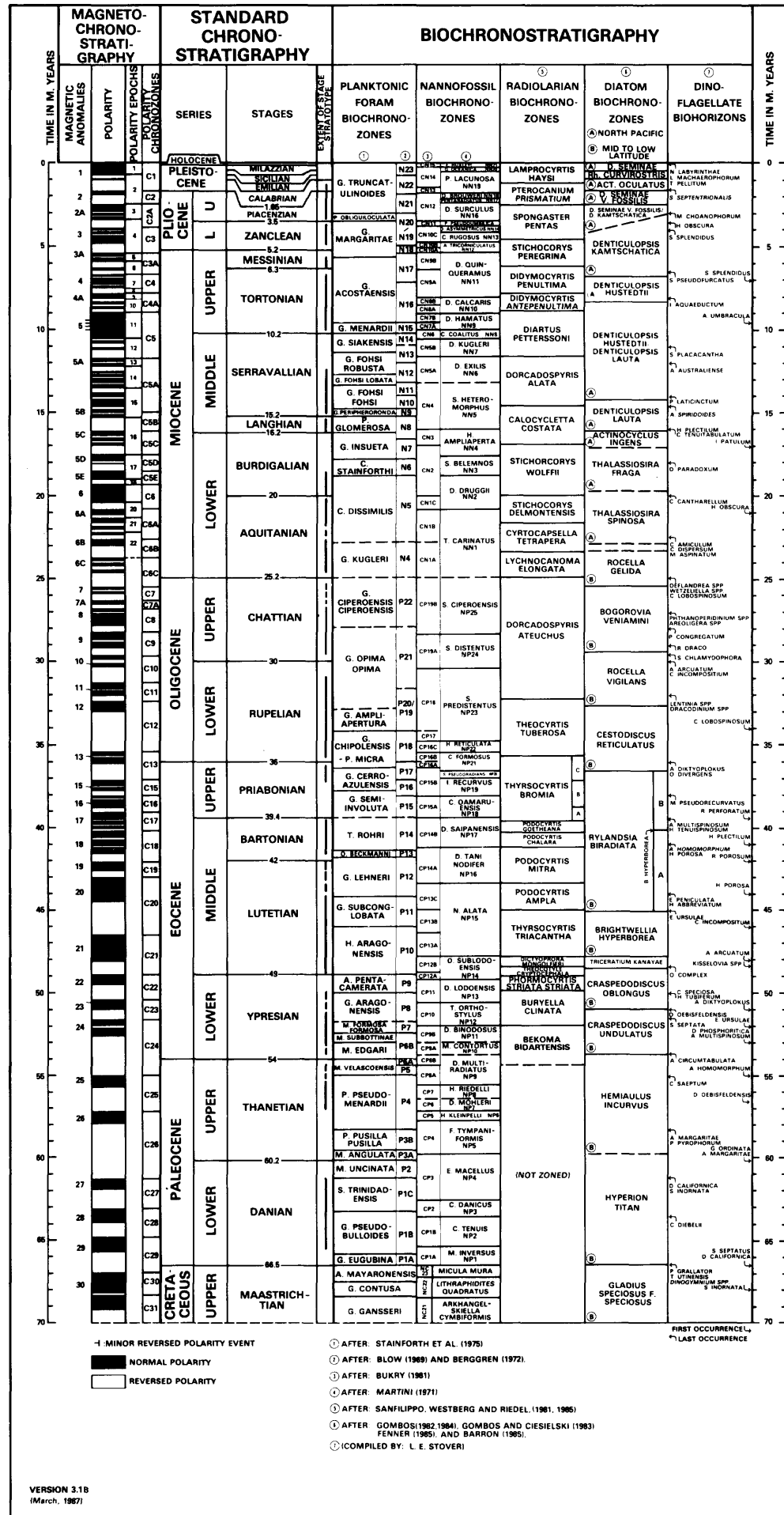
In the long term, the low-sea levels of the Late Paleozoic reached their lowest point in Tatarian (Late Permian). This trend continued into the Triassic and Early Jurassic. The Hettangian saw another marked drop, and the levels remained generally low through most of the Early and Middle Jurassic, with a slight rise in the Bajocian. The trend finally reversed itself in the Callovian, and the sea level continued a long-term rise through the Oxfordian, reaching a Jurassic peak in the Kimmeridgian.

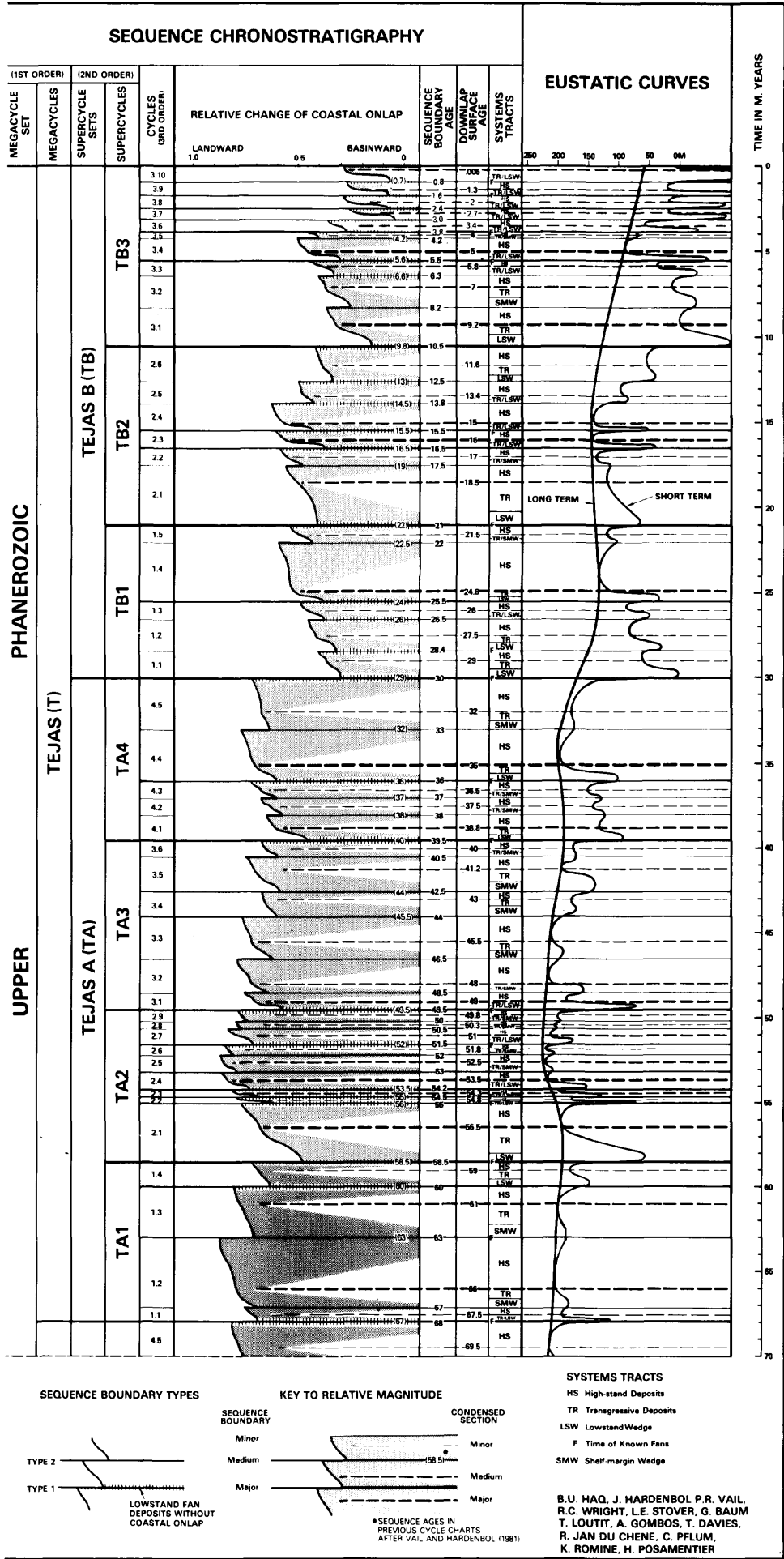
After a marked decline in the Valanginian, the sea level began rising once again, reaching its Mesozoic-Cenozoic peak in the Turonian. A gradual decline began in the latest Cretaceous and continued through the Cenozoic. With the exception of short-lived highs in the Danian, Ypresian, Rupelian, Langhian-early Serravallian, and Zanclean, this trend toward lower sea level has continued through to the present.

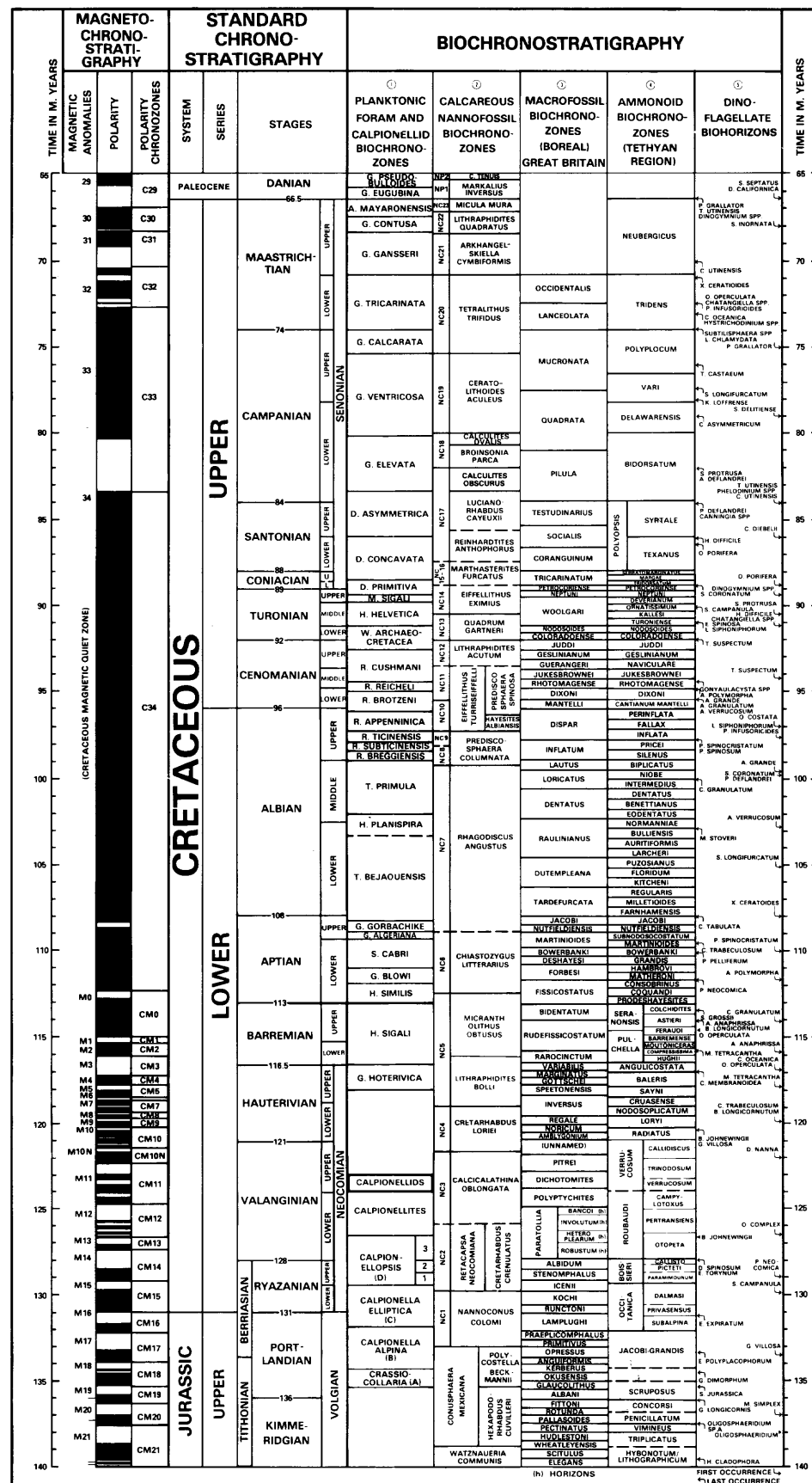
In the short term, major sea-level falls occurred in the early Portlandian, early Aptian, mid-Cenomanian, latest Ypresian, and latest Bartonian, near the Rupelian/Chattian boundary, in the Burdigalian-Langhian, in the late Serravallian, and throughout the late Pliocene-Pleistocene. These marked sea-level falls are often associated with world-wide major unconformities and frequently with canyon-cutting events on the shelves. At least since the Oligocene, sea-level falls are in part due to the increasing influence of glaciation. This is displayed by the relatively higher amplitude variations of the short-term sea level since the Oligocene.

ACKNOWLEDGMENTS

We are grateful to many colleagues for stimulating discussions about magnetostratigraphy, biostratigraphy, and radiochronology, which convinced us that a truly robust chronostratigraphy requires a broad integration of all reliable empirical and analytical data. In particular, we acknowledge our discussions at various stages of this work with J. A. Barron, W. A. Berggren, D. V. Kent, K. D. Klitgord, J. L. LaBrecque, K. G. Miller, N.-A. Mörner, G. S. Odin, E. A. Pessagno, Jr., R. Z. Poore, P. H. Roth, A. Salvador, H. Schouten, N. J. Shackleton, and E. L. Winterer. This paper was reviewed by J. A. Barron, C. A. Ross, J. Van Wagoner, R. M. Mitchum, and S. R. May, who improved the quality of the text. The following provided invaluable assistance in the field in different parts of the world with the special knowledge of their areas: F. Amédro, G. Badillet, A. Blondeau, R. Busnardo, B. Clavel, C. Collette, M. Delamette, R. Demyttenaere, A. Donovan, P. J. Felder, J. Ferrer, J. C. Fouchet, S. Gartner, R. C. Glenie, A. Hallam, J. Hooker, P. Juignet, E. Kaufman, P. Laga, E. Mancini, N. Morris, A. Mork, S. Nathan, C. Pomerol, L. Pray, K. Akhtar Qureshi, S. Mahmood Raza,







VERSION 3.1A
(January, 1987)

FIG. 15.—Cretaceous chronostratigraphic- and eustatic-cycle chart. (See Fig. 14 caption and text for explanation.)

- (i) AFTER: ALLEMAN ET AL. (1971), PREMOLI-SILVA AND BOLLI (1973), VAN Hinte (1976), PREMOLI-SILVA AND BOERSMA (1977), REMANE (1978), ROBASZYNSKI ET AL. (1979, 1983), AND CARON (1986).
- (j) AFTER: THIERSTEIN (1978), SISsingh (1977), MANIVIT ET AL. (1977), ROTH (1978, 1983), AND MONECHI AND THIERSTEIN (1985).
- (k) AFTER: RAWSON ET AL. (1978), AND KENNEDY (1984).
- (l) AFTER: VARIOUS AUTHORS IN CAVALIER AND ROGERS (1980), AMEDRO (1980, 1981, 1984), ROBASZYNSKI ET AL. (1983), KENNEDY (1984), AND CLAVEL (1986).
- (m) COMPILED BY: Y.Y. CHEN, N. IOANNIDES, M. MILLIOUD, J. SHANE, L. STOVER

FIRST OCCURRENCE →

LAST OCCURRENCE ←

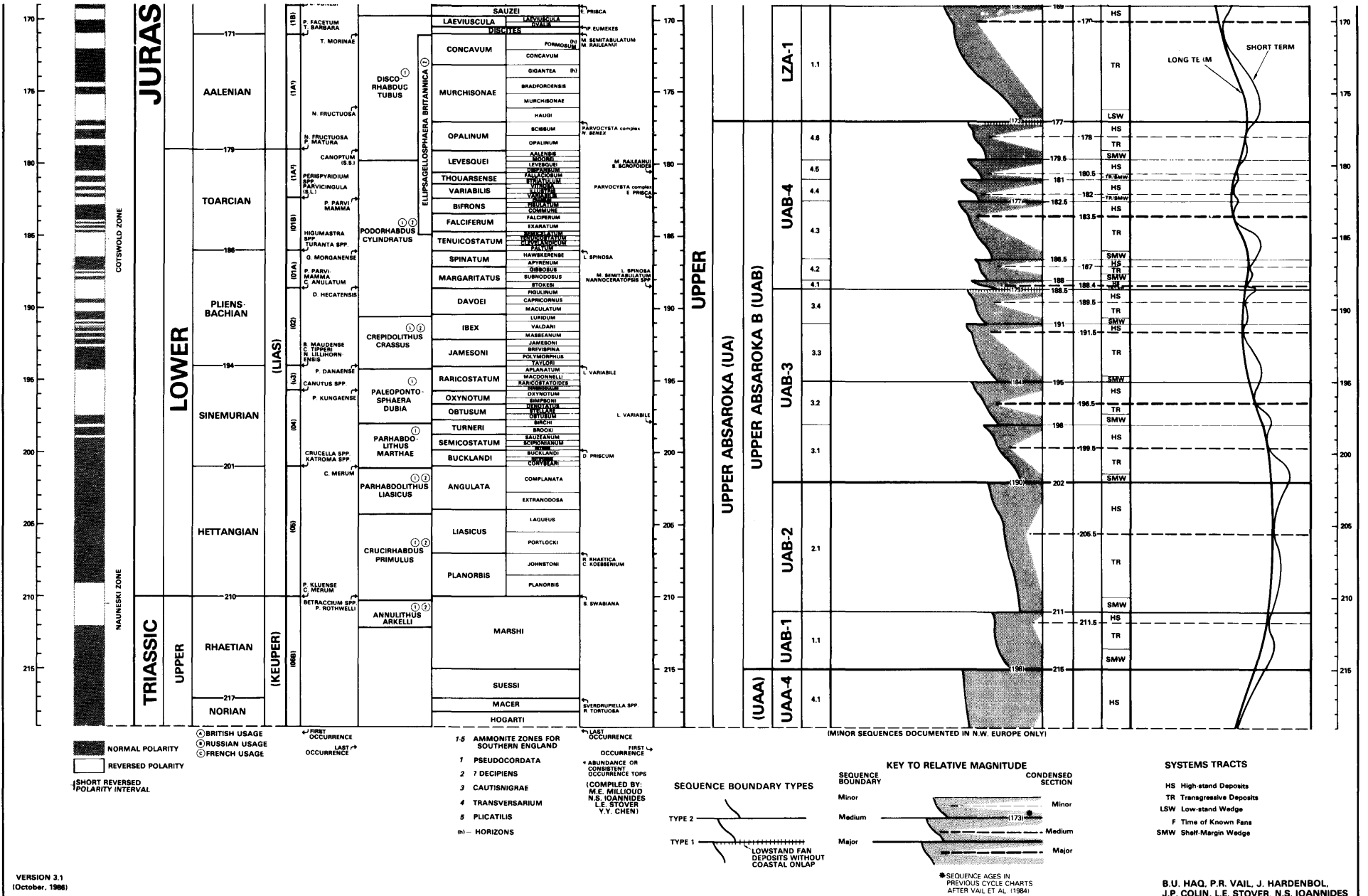
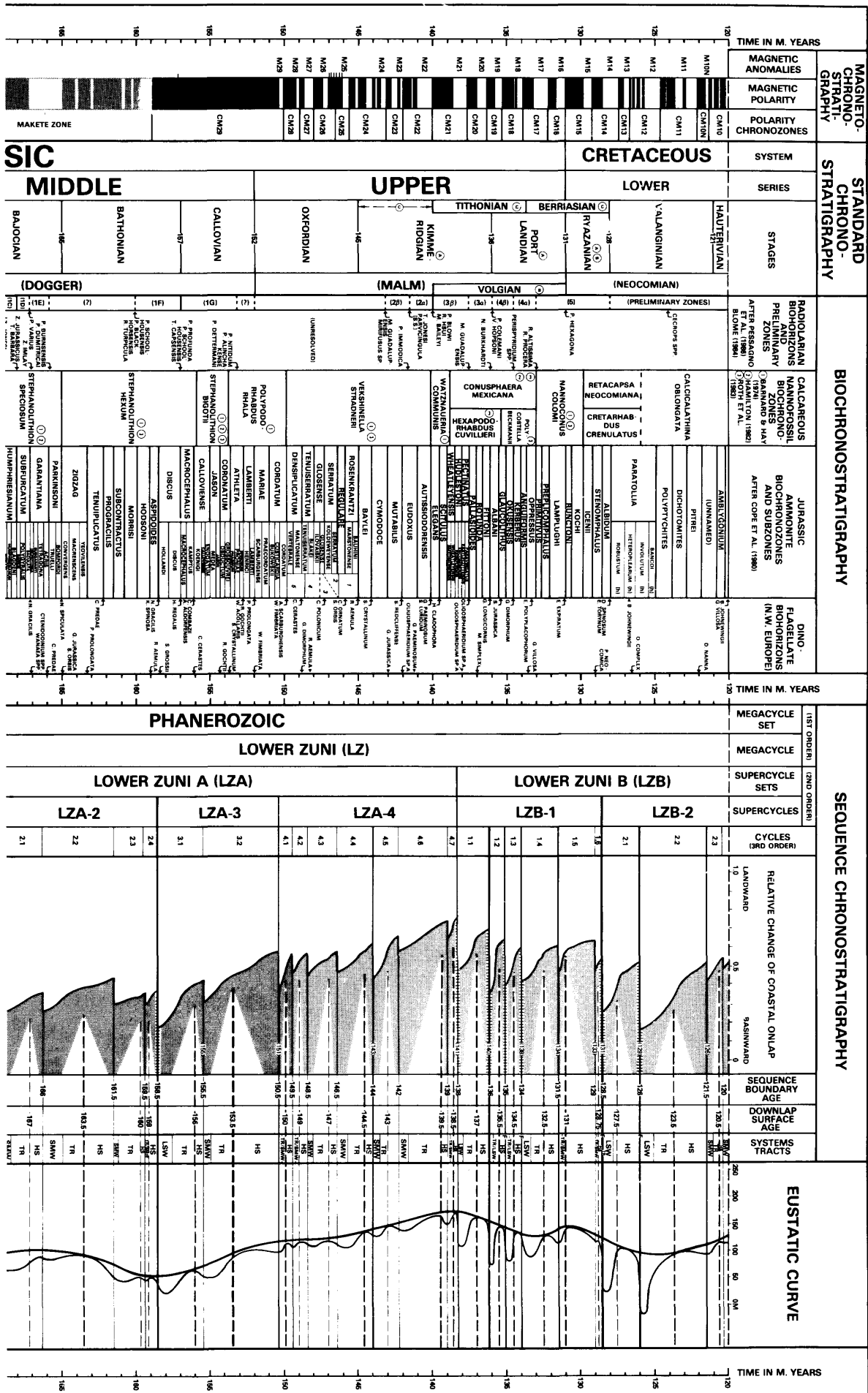


FIG. 16.—Jurassic chronostratigraphic- and eustatic-cycle chart (see Fig. 14 caption and text for explanation). The provisional pre-Callovian magnetic-polarity reversal pattern (shown in gray and white) is synthesized from known paleomagnetic data and may be subject to modification as more data become available from this interval.



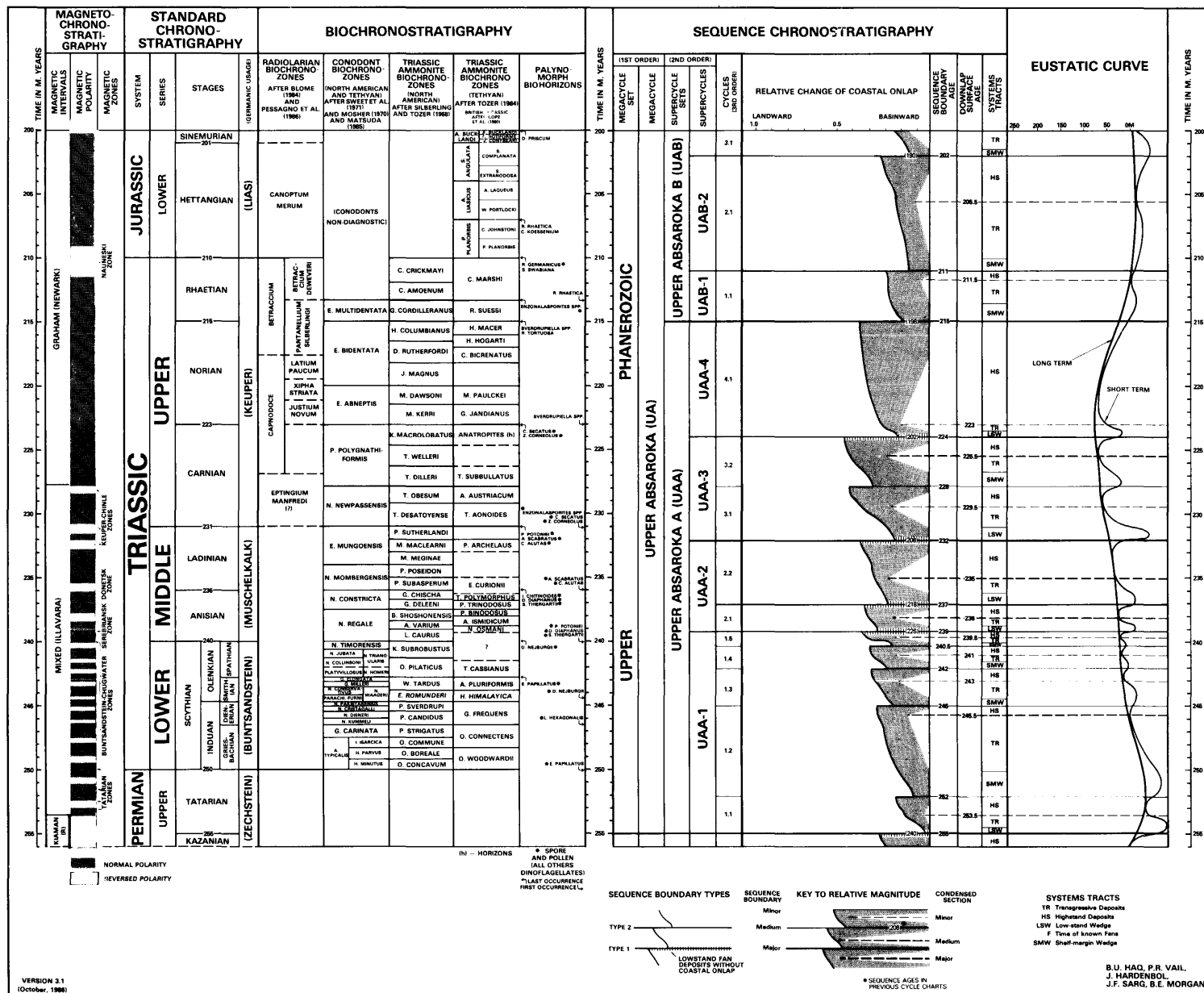


FIG. 17.—Triassic chronostratigraphic- and eustatic-cycle chart (see Fig. 14 caption and text for explanation). The Triassic magnetic-polarity reversal model is synthesized from available paleomagnetic data and is provisional, subject to modification in the future as new data are accumulated from this interval.

F. Robaszynski, M. Seroni-Vivien, A. Strasser, P. Strong, B. Thompson, and N. Vandenberghe. We acknowledge Exxon Production Research Company for permission to publish this article.

REFERENCES

- ABELE, C., AND PAGE, R. W., 1974, Stratigraphic and isotopic ages of basalts at Maude and Aureys Inlet, Victoria, Australia: Royal Society of Victoria, Proceedings, v. 86, p. 143–150.
- ADAMS, C. J. D., 1975, New Zealand potassium-argon age list-2: New Zealand Journal of Geology and Geophysics, v. 18, p. 443–467.
- ALLEMAN, F., CATALANO, R., FARES, F., AND REMANE, J., 1971, Standard calpionellid zonation (Upper Tithonian-Valanginian) of the western Mediterranean Province: 2nd Planktonic Conference, Proceedings, Rome, v. 2, p. 1337–1340.
- ALVAREZ, W., ARTHUR, M., FISHER, A., LOWRIE, W., NAPOLEONE, G., PREMOLI-SILVA, I., AND ROGENTHEN, W., 1977, Upper Cretaceous-Paleocene magnetic stratigraphy at Gubbio, Italy: Geological Society of America Bulletin, v. 88, p. 367–389.
- AMEDRO, F., 1980, Synthèse biostratigraphique de l'Aptien et Santonien du Boulonnais à partir de sept groupes paleontologiques: Revue de Micropaleontologie, v. 2, p. 195–321.
- , 1981, Actualisation des zonations d'ammonites dans le Crétacé Moyen du Bassin Anglo-Parisien: Cretaceous Research, v. 2, p. 261–269.
- , 1984, Nouvelles données paleontologique (ammonites) sur l'Abîme la Bordure Nord-est du Bassin de Paris: Bulletin de la Société de la Géologie Normandie et Amis Museum du Harve, v. 71, p. 17–30.
- , 1986, Biostratigraphie des craies cenomaniennes du Boulonnais par les ammonites: Annales Société Géologique du Nord, v. CV, p. 159–167.
- ARMSTRONG, R. L., 1982, Late Triassic—early Jurassic time scale calibration in British Columbia, Canada, in Odin, G. S., ed., Numerical Dating in Stratigraphy: Wiley, New York, p. 509–513.
- AUBRY, M.-P., 1983, Biostratigraphie du Paleogene epicontinentale de l'Europe du Nord-Quest. Etude fondée sur les nannofossiles calcaires: Documents Laboratoire de Géologie Lyon, 89, 317 p.
- BAADSGAARD, H., AND LERBEKMO, J. F., 1982, The dating of bentonite beds, in Odin, G. S., ed., Numerical Dating in Stratigraphy: Wiley, New York, p. 423–440.
- BACKMAN, J., SHACKLETON, N. J., AND TAUXE, L., 1983, Quantitative nannofossil correlation to open ocean deep-sea sections from Plio-Pleistocene boundary at Vrica, Italy: Nature, v. 304, p. 156–158.
- BANDY, O. L., HORNIBROOK, N. de B., AND SCHOFIELD, J. C., 1970, Age relationships of the *Globigerinoides trilobus* zone and the andesite at Muriwai Quarry, New Zealand: New Zealand Journal of Geology and Geophysics, v. 13, p. 980–995.
- BARNARD, T., AND HAY, W. W., 1974, On Jurassic coccoliths: a tentative zonation of Jurassic of southern England and North France: Eclogae Geologicae Helvetiae, v. 67, p. 563–585.
- BARRON, J. A., 1985, Miocene to Holocene planktic diatoms, in Bolli, H. M., Saunders, J. B., and Perch-Nielsen, K., eds., Plankton Stratigraphy: Cambridge University Press, Cambridge, p. 763–809.
- , KELLER, G., AND DUNN, D. A., 1985, A multiple microfossil biochronology for the Miocene: Geological Society of America memoir 163, p. 21–36.
- BAUMGARTNER, P. O., 1985, Summary of Middle Jurassic and Early Cretaceous radiolarian biostratigraphy of DSDP Site 534 (Blake-Bahama basin) and correlations to Tethyan sections: Initial Reports of the Deep Sea Drilling Project, v. 76, p. 569–571.
- BERGGREN, W. A., 1972, A Cenozoic time-scale—some implications for regional geology and paleobiogeography: Lethaia, v. 5, p. 195–215.
- , HAMILTON, N., JOHNSON, D. A., PUJOL, C., WEISS, W., CEPEK, P., AND GAMBOA, A., 1984, Magnetostratigraphy of DSDP Leg 72 Sites 515–518: Initial Reports of the Deep Sea Drilling Project, v. 72, p. 675–713.
- , KENT, D. V., AND FLYNN, J. J., 1985a, Jurassic to Paleogene: Part 2. Paleogene geochronology and chronostratigraphy, in Snelling, N. J., ed., The Chronology of the Geological Record: Blackwell Scientific Publishing, Oxford, and Geological Society of London Memoir 10, p. 141–195.
- , —, AND VAN COUVERING, J. A., 1985b, The Neogene: Part 2. Neogene geochronology and chronostratigraphy, in Snelling, N. J., ed., The Chronology of the Geological Record: Blackwell Scientific Publishing, Oxford and Geological Society of London Memoir 10, p. 211–260.
- BLOME, C. D., 1984, Upper Triassic Radiolaria and radiolarian zonation of western North America: Bulletin of American Paleontology, v. 85, p. 5–88.
- BLONDEAU, A., 1980, Lutetien, in Cavelier, C., and Roger, J., eds., Les étages Français et leurs stratotypes: Bureau de Recherches Géologiques et Minières, Mémoire, v. 109, p. 211–223.
- , AND RENARD, M., 1980, Le Lutetien stratotypique de la région de Creil (Oise): Bulletin de Information Géologique du Bassin de Paris, no. h-s, Excursion B-15 du 26eme Congress Géologique International, p. B15-1–B15-11.
- BLOW, W. H., 1969, The late Middle Eocene to Recent planktonic foraminiferal biostratigraphy: 1st Planktonic Conference, Proceedings, Geneva, 1967, p. 199–422.
- BOUCHÉ, P., 1962, Nannofossiles calcaires du Lutetian du Bassin de Paris: Revue de Micropaleontologie, v. 5, p. 75–103.
- BRALOWER, T. J., 1987, Valanginian to Aptian calcareous nannofossil stratigraphy and correlation with the upper M-sequence magnetic anomalies: Marine Micropaleontology, v. 11, p. 293–310.
- BUKRY, D., 1981, Cenozoic coccoliths from the Deep Sea Drilling Project: Society of Economic Paleontologists and Mineralogists Special Publication 32, p. 335–353.
- BURCKLE, L. H., 1978, Early Miocene to Pliocene diatom datum levels from the equatorial Pacific: 2nd Working Group Meeting, Biostratigraphic datum-planes of the Pacific Neogene, Proceedings: International Geological Correlation Program, Project 114, Bandung, 1977, Special Publication of the Geological Research and Development Center, no. 1, p. 25–44.
- , AND TRAINER, J., 1979, Middle and Late Pliocene diatom datum levels from the central Pacific: Micropaleontology, v. 25, p. 281–293.
- BUREK, P. J., 1970, Magnetic reversals: their applications to stratigraphic problems: American Association of Petroleum Geologists Bulletin, v. 54, p. 1120–1139.
- BURKE, W. H., DENISON, R. E., HETHERINGTON, E. A., KOEPNICK, R. B., NELSON, H. F., AND OTTO, J. B., 1982, Variation of seawater 87-Sr/86-Sr throughout Phanerozoic time: Geology, v. 10, p. 516–519.
- BUSNARDO, R., 1984, Ammonites, in Cretace Inferieur: Bureau de Recherches Géologiques et Minières, Mémoire, v. 125, p. 292–294.
- CANDE, S. C., AND KRISTOFFERSEN, Y., 1977, Late Cretaceous magnetic anomalies in the North Atlantic: Earth and Planetary Science Letters, v. 35, p. 215–224.
- , LARSON, R. L., AND LABRECQUE, J. L., 1978, Magnetic lineations in the Pacific Jurassic quiet zone: Earth and Planetary Science Letters, v. 41, p. 436–440.
- CARON, M., 1985, Cretaceous planktonic foraminifera, in Bolli, H. M., Saunders, J. B., and Perch-Nielsen, K., eds., Plankton Stratigraphy: Cambridge University Press, Cambridge, p. 11–86.
- CAVALIER, C., AND ROGERS, J., 1980, Les étages Français et leurs stratotypes: Bureau Recherches Géologiques et Minières Mémoire, v. 109, 295 p.
- CHANNELL, J. E. T., AND MEDIZZA, F., 1981, Upper Cretaceous and Paleogene magnetic stratigraphy and biostratigraphy from Venetian (southern) Alps: Earth and Planetary Science Letters, v. 55, p. 419–432.
- , LOWRIE, W., AND MEDIZZA, F., 1979, Middle and early Cretaceous magnetic stratigraphy from the Cismon section, northern Italy: Earth and Planetary Science Letters, v. 42, p. 153–166.
- , OGG, J. G., AND LOWRIE, W., 1982, Geomagnetic polarity in the Early Cretaceous and Jurassic: Philosophical Transactions of the Royal Society of London, Series A, v. 306, p. 137–146.
- CLAUER, N., 1982, The rubidium-strontium method applied to sediments: certitudes and uncertainties, in Odin, G. S., ed., Numerical Dating in Stratigraphy: Wiley, New York, p. 245–276.
- CLAVEL, B., 1986, Précisions stratigraphiques sur le Crétacé inférieur basal du Jura méridional: Eclogae Geologicae Helvetiae, v. 79, p. 319–341.
- COPE, J. C. W., GETTY, T. A., HOWARTH, M. K., MORTON, N., TORRENS, H. S., DUFF, K. L., PARSONS, C. F., WIMBLEDON, W. A., AND WRIGHT

- J. K., 1980, Jurassic, Parts 1 and 2: Geological Society of London, Special Reports, no. 14, 15, 73 and 109 p.
- CREER, K. M., 1971, Mesozoic paleomagnetic reversal column: *Nature*, v. 233, p. 545–546.
- CURRY, D., 1985, Oceanic magnetic lineaments and the calibration of late Mesozoic-Cenozoic time scales, in Snelling, N. J., ed., *The Chronology of the Geological Record*: Blackwell Scientific Publishing, Oxford, and Geological Society of London, Memoir, 10, p. 269–272.
- DEPAOLO D. J., AND INGRAM, B. L., 1985, High-resolution stratigraphy with strontium isotopes: *Science*, v. 227, p. 938–941.
- DICKSON, G. O., PITMAN, W. C., AND HEITZLER, J. R., 1968, Magnetic anomalies in the South Atlantic and ocean floor spreading: *Journal of Geophysical Research*, v. 73, p. 2087–2100.
- ELDEFIELD, H., 1986, Strontium isotope stratigraphy: *Palaeogeography, Palaeoclimatology, Palaeoecology*, v. 57, p. 71–90.
- EMRY, R. J., 1973, Stratigraphy and preliminary biostratigraphy of the Flagstaff Rim area, Natrona County, Wyoming: *Smithsonian Contributions to Paleobiology*, v. 18, p. 1–42.
- EVERNDEN, J. F., SAVAGE, D. E., CURTIS, G. H., AND JAMES, C. T., 1964, Potassium-argon dates and the Cenozoic mammalian chronology of North America: *American Journal of Science*, v. 262, p. 145–198.
- FENNER, J., 1985, Late Cretaceous to Oligocene planktic diatoms, in Bolli, H. M., Saunders, J. B., and Perch-Nielsen, K., eds., *Plankton Stratigraphy*: Cambridge University Press, Cambridge, p. 713–762.
- FITCH, F. J., HOOKER, P. J., MILLER, J. A., AND BRERETON, N. R., 1978, Glauconite dating of Paleocene-Eocene rocks from East Kent and the time-scale of Paleogene volcanism in North Atlantic region: *Journal of the Geological Society of London*, v. 135, p. 499–512.
- FLYNN, J. J., 1981, Magnetic polarity stratigraphy and correlation of Eocene strata from Wyoming and southern California (abs.): *EOS, American Geophysical Union Transactions*, v. 62, p. 264.
- FORSTER S. C., AND WARRINGTON, G., 1985, Geochronology of the Carboniferous, Permian and Triassic, in Snelling, N. J., ed., *The Chronology of the Geological Record*: Blackwell Scientific Publishing, Oxford and Geological Society of London, Memoir 10, p. 99–113.
- GALBRUN, B., AND RASPLUS, L., 1984, Magnetostratigraphie du stratotype du Berriasien, premiers résultats: *Comptes Rendus, Académie des Sciences, Paris*, v. 298, p. 219–222.
- GALE, N. H., 1982, The dating of plutonic events, in Odin, G. S., ed., *Numerical Dating in Stratigraphy*: Wiley, New York, p. 441–453.
- GARTNER, S., 1973, Absolute chronology of the Late Neogene calcareous nannofossil succession in the equatorial Pacific: *Geological Society of America Bulletin*, v. 84, p. 2021–2034.
- GHOSH, P. K., 1972, Use of bentonites and glauconites in potassium-40/argon-40 dating in Gulf Coast stratigraphy: unpublished Ph.D. Dissertation, Rice University, Houston, Texas, 136 p.
- GOMBOS, A. M., Jr., 1982, Early and middle Eocene diatom evolutionary events: *Bacillaria*, v. 5, p. 225–236.
- , 1984, Late Paleocene diatoms in the Cape Basin: Initial Reports of the Deep Sea Drilling Project, v. 73, p. 495–512.
- , CIESIELSKI, P. F., 1983, Late Eocene to early Miocene diatoms from the southwest Atlantic: Initial Reports of the Deep Sea Drilling Project, v. 71, p. 583–634.
- HALLAM, A., 1983, Early and mid-Jurassic molluscan biogeography and the establishment of the central Atlantic seaway: *Palaeogeography, Palaeoclimatology, Palaeoecology*, v. 43, p. 181–193.
- , HANCOCK, J. M., LABRECQUE, J. L., LOWRIE, W., AND CHANNELL, J. E. T., 1985, Jurassic to Paleogene: Part 2, Jurassic and Cretaceous geochronology and Jurassic to Paleogene magnetostratigraphy, in Snelling, N. J., ed., *The Chronology of the Geological Record*: Blackwell Scientific Publishing, Oxford, and Geological Society of London, Memoir 10, p. 118–140.
- HAMILTON, G. B., 1982, Triassic and Jurassic and Jurassic nannofossils, in Lord, A. R., ed., *A Stratigraphic Index of Calcareous Nannofossils*: Ellis Horwood, Chichester, p. 17–39.
- HAQ, B. U., BERGGREN, W. A., AND VAN COUVERING, J. A., 1977, Corrected age of the Pliocene-Pleistocene boundary: *Nature*, v. 269, p. 483–289.
- , HARDENBOL, J., AND VAIL, P. R., 1987, The chronology of fluctuating sea level since the Triassic: *Science*, v. 235, p. 1156–1167.
- , AND WORSLEY, T. R., 1982, Biochronology—biological events in time resolution, their potential and limitations, in Odin, G. S., ed., *Numerical Dating in Stratigraphy*: Wiley, New York, p. 19–36.
- , —, BURCKLE, L. H., DOUGLAS, R. G., KEIGWIN, L. D., Jr., OPDYKE, N. D., SAVIN, S. M., SOMMER, M. A., II, VINCENT, E., AND WOODRUFF F., 1980, The Late Miocene carbon isotopic shift and the synchronicity of some phytoplanktonic biostratigraphic datums: *Geology*, v. 8, p. 427–431.
- HARDENBOL, J., AND BERGGREN, W. A., 1978, A new Paleogene numerical time scale: *American Association of Petroleum Geology, Studies in Geology*, v. 6, p. 213–234.
- , VAIL, P. R., AND FERRER, J., 1981, Interpreting paleoenvironments, subsidence history, and sea-level changes of passive margins from seismic and biostratigraphy: *Oceanologica Acta, Suppl. to v. 3*, p. 33–44.
- HARLAND, W. B., COX, A. V., LLEWELLYN, P. G., PICKTON, C. A. G., SMITH, D. G., AND WALTERS, R., 1982, *A geologic time scale*: Cambridge University Press, Cambridge, 131 p.
- HARRISON, C. G. A., 1986, Long-term eustasy and epeirogeny in continents: *National Academy of Sciences, Studies in Geophysics*: p. 111–131.
- HEDBERG, H. D., ed., 1976, *International Stratigraphic Guide*: Wiley, New York, 200 p.
- HEITZLER J. R., DICKSON, G. O., HERRON, E. M., PITMAN W. C., III, AND LEPICHON, X., 1968, Marine magnetic anomalies, geomagnetic field reversals, and motions of ocean floor and continents: *Journal of Geophysical Research*, v. 73, p. 2119–2136.
- HELLSEY, C. E., 1969, Magnetic stratigraphy of the Lower Triassic Moenkopi Formation of western Colorado: *Geological Society of America Bulletin*, v. 80, p. 2431–2450.
- , AND STEINER, M. B., 1974, Paleomagnetism of the Lower Triassic Moenkopi Formation: *Geological Society of America Bulletin*, v. 85, p. 457–464.
- HILDE, T. W. C., ISEZAKI, N., AND WAGEMAN, J. M., 1975, Mesozoic sea-floor spreading in the North Pacific, in Sutton, G. H., Mangnani, M. H., and Moberly, R., *The Geophysics of the Pacific Ocean Basin and its Margins*: American Geophysical Union Monograph 19, p. 205–226.
- HÖRNER, F. AND HELLER, F., 1983, Lower Jurassic magnetostratigraphy at the Breggia Gorge (Ticino, Switzerland) and Alpe Turati (Como, Italy): *Journal of the Royal Astronomical Society of London*, v. 73, p. 705–718.
- HSÜ, K. J., PERCIVAL S. F., Jr., WRIGHT, R. C., AND PETERSEN, N., 1984, Numerical ages of magnetostratigraphically calibrated biostratigraphic zones: *Initial Reports of the Deep Sea Drilling Project*, v. 73, p. 623–635.
- JAGER, E., AND HUNZIKER, J. C., 1979, *Isotope Geology*: Springer-Verlag, Heidelberg, 329 p.
- KAWAI, N., AND HIROOKA, K., 1966, Some age results on Cenozoic igneous rocks from southwest Japan (abs.): *Symposium on Age of Formation for Japanese Acid Rocks by Dating Results*: Geological Society of Japan, p. 5.
- KENNEDY, W. J., 1984, Ammonite faunas and the ‘standard zones’ of the Cenomanian to Maastrichtian stages in their type areas, with some proposals for the definition of stage boundaries by ammonites: *Bulletin of the Geological Society of Denmark*, v. 33, p. 147–161.
- KENT, D. V., AND GRADSTEIN, F. M., 1985, A Cretaceous and Jurassic geochronology: *Geological Society of America Bulletin*, v. 96, p. 1419–1427.
- KEPPENS, E., AND PASTEELS, P., 1982, A comparison of rubidium-strontium and postassium-argon apparent ages on glauconites, in Odin, G. S., ed., *Numerical Dating in Stratigraphy*: Wiley, New York, p. 225–239.
- KLITGORD, K. D., AND SCHOUTEN, H., 1986, Plate kinematics of the central Atlantic, in Vogt, P. R., and Tucholke, B. E., eds., *The Geology of North America: Geological Society of America*, v. M, p. 351–378.
- LABRECQUE, J. L., HSU, K. J., CARMAN, M., KARPOFF, A.-M., MCKENZIE, J., PERCIVAL, S., PETERSEN, N., PISCOTTO, K., SCHREIBER, E., TAUZE, L., TUCKER, P., WEISSERT, H., AND WRIGHT, R., 1983, DSDP Leg 73: Contributions to Paleogene stratigraphy in nomenclature, chronology and sedimentation rates: *Palaeogeography, Palaeoclimatology, Palaeoecology*, v. 42, p. 91–125.
- , KENT, D. V., AND CANDE, S. C., 1977, Revised magnetic polarity time scale for Late Cretaceous and Cenozoic time: *Geology*, v. 5, p. 330–335.
- LARSON, R. L., AND CHASE, C. G., 1972, Late Mesozoic evolution of the

- western Pacific: Geological Society of America Bulletin, v. 83, p. 3627–3644.
- , AND HILDE, T. W. C., 1975, A revised time scale of magnetic reversals for early Cretaceous, late Jurassic: Journal of Geophysical Research, v. 80, p. 2586–2594.
- , AND PITMAN, III, W. C., 1972, World-wide correlation of Mesozoic magnetic anomalies and its implications: Geological Society of America Bulletin, v. 83, p. 3645–3662.
- LOWRIE, W., AND ALVAREZ, W., 1981, 100 million years of geomagnetic polarity history: Geology, v. 9, p. 392–397.
- , —, NAPOLEONE, G., PERCH-NIELSEN, K., PREMOLI-SILVA, I., AND TOUMARKINE, M., 1982, Paleogene magnetic stratigraphy in Umbrian pelagic carbonate rocks: The Contessa sections, Gubbio: Geological Society of America Bulletin, v. 93, p. 414–432.
- , —, PREMOLI-SILVA, I., AND MONECHI, S., 1980, Lower Cretaceous magnetic stratigraphy in Umbrian pelagic carbonate rocks: Geophysical Journal of the Royal Astronomical Society, v. 60, p. 263–281.
- , —, AND CHANNELL, J. E. T., 1983, Magnetostratigraphy of the Jurassic-Cretaceous boundary in the Maiolica Limestone (Umbria, Italy): Geology, v. 12, p. 44–47.
- MANIVIT, H., PERCH-NIELSEN, K., PRINS, B., AND VERBEEK, J. W., 1977, Mid-Cretaceous calcareous nannofossil biostratigraphy: Koninklijke Nederlandse Akademie van Wetenschappen, v. B80, p. 109–181.
- MANKINEN, E. A., AND DALRYMPLE, G. B., 1979, Revised late Cenozoic geomagnetic polarity time scale: U.S. Geological Survey Professional Paper 1100, 167 p.
- MARTINI, E., 1971, Standard Tertiary and Quaternary calcareous nanoplankton zonation: 2nd Plankton Conference Proceedings, Rome, 1969, v. 2, p. 739–785.
- MARTON, E., 1982, Late Jurassic/early Cretaceous magnetic stratigraphy from the Sumeg section, Hungary: Earth and Planetary Science Letters, v. 57, p. 182–190.
- , MARTON, P., AND HELLER, F., 1980, Remnant magnetization of a Pliensbachian limestone sequence at Bakonycsernye (Hungary): Earth and Planetary Science Letters, v. 48, p. 218–226.
- MATSUDA, T., 1985, Late Permian to early Triassic conodont paleobiogeography in the 'Tethys Realm', in Nakazawa, K., and Dickins, J.M., eds., *The Tethys—Her Paleogeography and Paleobiogeography from the Paleozoic to Mesozoic*: Tokai University Press, Tokyo p. 157–170.
- MCDougall, I., SAEMUNDSSON, K., JOHANNESSEN, H., WATKINS, N.D., AND KRISTJANSSON, L., 1977, Extension of the geomagnetic polarity time scale to 6.5 m.y.: K-Ar dating, geological and paleomagnetic study of a 3,500 m lava succession in western Iceland: Geological Society of America Bulletin, v. 88, p. 1–15.
- , WATKINS, N.D., WALKER, G.P.L., AND KRISTJANSSON, L., 1976, Potassium-argon and paleomagnetic analysis of Icelandic lava flows—limits on the age of anomaly 5: Journal of Geophysical Research, v. 81, p. 1505–1512.
- MCELHINNY, M.W., AND BUREK, P.J., 1971, Mesozoic paleomagnetic stratigraphy: Nature, v. 232, p. 98–102.
- MCKEE, E.H., 1975, K-Ar ages of deep-sea basalts, Benham Rise, W. Philippine Basin, Leg 31: Initial Reports of the Deep Sea Drilling Project, v. 31, p. 599–611.
- MEDD, A.W., 1982, Nannofossil zonation of the English Middle and Upper Jurassic: Marine Micropaleontology, v. 7, p. 73–95.
- MILLER, K.G., KHAN, M.J., AUBRY, M.-P., BERGGREN, W.A., KENT, D.V., AND MELILLO, A., 1985, Oligocene-Miocene biostratigraphy, magnetostratigraphy, and isotopic stratigraphy of western North Atlantic: Geology, v. 13, p. 257–261.
- MITCHUM, R.M., VAIL, P.R., AND THOMPSON, S., 1977, The depositional sequence as a basic unit for stratigraphic analysis: American Association of Petroleum Geologists Memoir 26, p. 53–62.
- MONECHI, S., AND THIERSTEIN, H., 1985, Late Cretaceous—Eocene nannofossil and magnetostratigraphic correlations near Gubbio, Italy: Marine Micropaleontology, v. 9, p. 419–440.
- MOSHER, L.C., 1970, New conodont species as Triassic guide fossils: Journal of Paleontology, v. 44, p. 737–742.
- NAKAZAWA, K., ALI, S.T., BANDO, Y., ISHII, K., OKIMURA, Y., QURESHI, K.A., AND SHUJA, T.A., 1985, Permian and Triassic Systems in the Salt Range and Surghar Range, Pakistan, in Nakazawa, K., and Dickins, J.M., eds., *The Tethys—Her Paleogeography and Paleobiogeog-*
- raphy from Paleozoic to Mesozoic: Tokai University Press, Tokyo, p. 221–312.
- NAPOLEONE, G., PREMOLI-SILVA, I., HELLER, F., CHELI, P., COREZZI, S., AND FISCHER, A. G., 1983, Eocene magnetic stratigraphy at Gubbio, Italy, and its implications for Paleogene geochronology: Geological Society of America Bulletin, v. 94, p. 181–191.
- NESS, G., LEVI, S., AND COUCH, R., 1980, Marine magnetic anomaly time scales for the Cenozoic and late Cretaceous: a précis, critique, and synthesis: Reviews of Geophysics and Space Physics, v. 18, p. 753–770.
- NEWMAN, K. R., 1979, Cretaceous/Tertiary boundary in Denver Formation at Golden, Colorado, USA, in Christensen, W. K., and Birkenlund, T., eds., *Cretaceous-Tertiary Boundary Events*: University of Copenhagen, Sweden, v. 2, p. 246–248.
- OBRADOVICH, J. D., AND COBBAN, W. A., 1975, A time-scale for the Late Cretaceous of the Western Interior of North America, in Caldwell, W. G. E., ed., *The Cretaceous System in the Western Interior of North America*: Geological Association of Canada, Special Paper 13, p. 31–54.
- ODIN, G. S., ed., 1982a, *Numerical Dating in Stratigraphy*: Wiley, New York, 1040 p.
- , 1982b, The Phanerozoic time scale revisited: Episodes, no. 3, p. 3–9.
- OGG, J. G., 1981, Sedimentology and paleomagnetism of Jurassic pelagic limestones ('Ammonitico Rosso' facies): Unpublished Ph.D. Dissertation, University of California, San Diego, California, 203 p.
- , 1983, Magnetostratigraphy of Upper Jurassic and lowest Cretaceous sediments, Deep Sea Drilling Project Site 534, western North Atlantic: Initial Reports of the Deep Sea Drilling Project, v. 76, p. 685–697.
- , STEINER, M. B., OLORIZ, F., AND TAVERA, J. M., 1984, Jurassic magnetostratigraphy, I. Kimmeridgian-Tithonian of Sierra Gorda and Carcabuey, southern Spain: Earth and Planetary Science Letters, v. 71, p. 147–162.
- OKADA, H., AND BUKRY, J., 1980, Supplementary modification and introduction of code numbers to low-latitude coccolith biostratigraphic zonation (Bukry, 1973; 1975): Marine Micropaleontology, v. 5, p. 321–326.
- PECHERSKY, D. M., AND KHRAMOV, A. N., 1973, Mesozoic paleomagnetic scale of the U.S.S.R.: Nature, v. 244, p. 499–501.
- PERSON, A., 1982, The genesis of bentonites, in Odin, G. S., ed., *Numerical Dating in Stratigraphy*: Wiley, New York, p. 407–422.
- PESSAGNO, E. A., Jr., 1977, Upper Jurassic Radiolaria and radiolarian biostratigraphy of the California Coast Range: Micropaleontology, v. 23, p. 56–133.
- , AND BLOME, C. D., 1980, Upper Triassic and Jurassic Pantanellinae from California, Oregon and British Columbia: Micropaleontology, v. 26, p. 225–273.
- , —, CARTER, E. S., MACLEOD, N., WHALEN, P. A., AND YEH, K.-Y., 1987b, Part 2. Preliminary radiolarian zonation for the Jurassic of North America: Cushman Foundation for Foraminiferal Research, Special Publication, no. 23, p. 1–18.
- , LONGORIA, J. F., MACLEOD, N., AND SIX, W. M., Jr., 1987a, Part 1. Upper Jurassic (Kimmeridgian—Upper Tithonian) Pantanellidae from the Taman Formation, east-central Mexico: tectonostratigraphic, chronostratigraphic and phylogenetic implications: Cushman Foundation for Foraminiferal Research, Special Publication, no. 23, p. 1–51.
- PITMAN, III, W. C., HERRON, E. M., AND HEIRTZLER, J. R., 1968, Magnetic anomalies in the Pacific and sea floor spreading: Journal of Geophysical Research, v. 73, p. 2069–2085.
- POORE, R. Z., TAUZE, L., PERCIVAL, S., JR., AND LABRECQUE, J. L., 1982, Late Eocene—Oligocene magnetostratigraphy and biostratigraphy at South Atlantic DSDP Site 552: Geology, v. 10, p. 508–511.
- , —, —, —, WRIGHT, R., PETERSEN, N., SMITH, C., AND HSU, K., 1983, Late Cretaceous-Cenozoic magnetostratigraphic and biostratigraphic correlations of South Atlantic Ocean (DSDP Leg 73): Palaeogeography, Palaeoclimatology, Palaeoecology, v. 42, p. 127–149.
- PREMOLI-SILVA, I., 1977, Upper Cretaceous-Paleocene magnetic stratigraphy at Gubbio, Italy, II. Biostratigraphy: Geological Society of America Bulletin, v. 88, p. 371–374.
- , AND BOERSMA, A., 1977, Cretaceous planktonic foraminifers—

- DSDP Leg 39 (South Atlantic): Initial Reports of the Deep Sea Drilling Project, v. 39, p. 615–631.
- , AND BOLLI, H. M., 1973, Late Cetaceous to Eocene planktonic foraminifera and stratigraphy of Leg 15 Sites in the Caribbean Sea: Initial Reports of the Deep Sea Drilling Project, v. 15, p. 499–547.
- PROTHERO, D. R., DENHAM, C. R., AND FARMER, H. G., 1982, Oligocene calibration of the magnetic polarity time scale: *Geology*, v. 10, p. 650–653.
- RAWSON, P. F., CURRY, D., DILLEY, F. C., HANCOCK, J. M., KENNEDY, W. J., NEALE, J. W., WOOD, C. J., AND WORSSAM, B. C., 1978, Cretaceous: Geological Society of London Special Report no. 9, 70 p.
- REMANE, J., 1978, Calpionellids, *in* Haq, B. U., AND Boersma, A., eds., *Introduction to Marine Micropaleontology*: Elsevier, New York, p. 161–170.
- , 1985, Calpionellids, *in* Bolli, H. M., Saunders, J. B., and Perch-Nielsen, K., eds., *Plankton Stratigraphy*: Cambridge University Press, Cambridge, p. 555–572.
- ROBASZYNSKI, F., CARON, M., AND THE EUROPEAN WORKING GROUP ON PLANKTONIC FORAMINIFERA, 1979, Atlas des foraminifères planktoniques du Crétacé Moyen (Mer Boréale et Téthys): Cahiers de Micropaleontologie, no. 1, 2, 185 and 181 p.
- , CARON, M., GONZALES, J. M., AND WONDER, A., 1983, Atlas of Late Cretaceous planktonic foraminifera. *Reviews of Micropaleontology*, v. 26, p. 145–305.
- ROTH, P. H., 1978, Cretaceous nannoplankton biostratigraphy and oceanography of the northwestern Atlantic Ocean: Initial Reports of the Deep Sea Drilling Project, v. 44, p. 731–759.
- , 1983, Jurassic and Lower Cretaceous nannofossils in the western North Atlantic (Site 534): Initial Reports of the Deep Sea Drilling Project, v. 76, p. 587–621.
- , MEDD, A. W., AND WATKINS, D. K., 1983, Jurassic calcareous nannofossil zonations, an overview with new evidence from Deep Sea Drilling Project Site 534: Initial Reports of the Deep Sea Drilling Project, v. 76, p. 573–579.
- RYAN, W. B. F., CITA, M. B., DREYFUS RAWSON, M., BURCKLE, L. H., AND SAITO, T., 1974, A paleomagnetic assignment of Neogene stage boundaries and the development of isochronous datum planes between the Mediterranean, the Pacific and the Indian Ocean in order to investigate the response of the world ocean to Messinian Salinity Crisis: *Rivista Italiana Paleontologica e Stratigrafia*, v. 80, p. 631–688.
- SALVADOR, A., 1985, Chronostratigraphic and geochronometric scales in COSUNA stratigraphic correlation charts of the United States: *American Association of Petroleum Geologists Bulletin*, v. 69, p. 181–189.
- SANFILIPPO, A., WESTBERG, M. J., AND RIEDEL, W. R., 1981, Cenozoic radiolarians at Site 462, DSDP leg 61: Initial Reports of the Deep Sea Drilling Project, v. 61, p. 495–505.
- , —, AND —, 1985, Cenozoic Radiolaria, *in* Bolli, H. M., Saunders, J. B., and Perch-Nielsen, K., eds., *Plankton Stratigraphy*: Cambridge University Press, Cambridge, p. 631–712.
- SCHOUTEN, H., AND KLITGORD, K. D., 1977, Map showing Mesozoic magnetic anomalies, western North Atlantic: U.S. Geological Survey Miscellaneous Field Studies, Map MF-915, scale 1:2,000,000.
- , AND —, 1982, The memory of the accreting plate boundary and the continuity of fracture zones: *Earth and Planetary Science Letters*, v. 59, p. 255–266.
- SEIDEMANN, D. E., 1977, Effects of submarine alteration on K-Ar dating of deep-sea igneous basalts: *Geological Society of America Bulletin*, v. 88, p. 1660–1666.
- SHACKLETON, N. J., AND SHIPBOARD SCIENTIFIC PARTY, 1984, Accumulation rates in Leg 74 sediments: Initial Reports of the Deep Sea Drilling Project, v. 74, p. 621–637.
- SHIBATA, K., 1973, K-Ar ages of volcanic rocks from the Hokuriku Group: *Geological Society of Japan, Memoir* 8, p. 143–149.
- , AND ISHIHARA, S., 1979, Rb-Sr whole rock and K-Ar mineral ages of granitic rocks in Japan: *Geochemical Journal*, v. 13, p. 113–119.
- , NISHIMURA, S., AND CHINZEI, K., 1984, Radiometric dating related to Pacific Neogene planktonic datum planes, *in* Ikebe, N., and Tsuchi, R., eds., *Pacific Neogene Datum Planes*: University of Tokyo Press, Tokyo, p. 85–89.
- , AND NOZAWA, T., 1967, K-Ar ages of granitic rocks from the Outer Zone of S.W. Japan: *Geochemical Journal*, v. 1, p. 131–137.
- , SATO, H., AND NAKAGAWA, M., 1981, K-Ar ages of Neogene volcanic rocks from the Noto Peninsula: *Japan Association of Petrology, Mineralogy, and Economic Geology, Journal*, v. 76, p. 248–252.
- , UCHIUMI, S., AND NAKAGAWA, T., 1979, K-Ar age results-1: *Geological Society of Japan Bulletin*, v. 30, p. 675–686.
- SILBERING, N. J., AND TOZER, E. T., 1968, Biostratigraphic classification of the marine Triassic in North America: *Geological Society of America Special Paper*, no. 110, 63 p.
- SISSINGH, W., 1977, Biostratigraphy of Cretaceous calcareous nannoplankton: *Geologie en Mijnbouw*, v. 56, p. 335–350.
- SLOSS, L. L., 1963, Sequences in the cratonic interior of North America: *Geological Society of America Bulletin*, v. 64, p. 93–113.
- SNELLING, N. J., ed., 1985, *The Chronology of the Geological Record*: Blackwell Scientific Publishing, Oxford and Geological Society of London, Memoir 10, 343 p.
- STAINFORTH, R. M., LAMB, J. L., LUTERBACHER, H., BEARD, J. H., AND JEFFORDS, R. M., 1975, Cenozoic planktonic foraminiferal zonation and characteristic index forms: *University of Kansas, Paleontological Contributions*, v. 62, Lawrence, Kansas, 425 p.
- STEINER, M. B., AND HELSLEY, C. E., 1975, Late Jurassic magnetic polarity sequence: *Earth and Planetary Science Letters*, v. 27, p. 108–112.
- , OGG, J. G., MELENDEZ, G., AND SEQUEIROS, L., 1985, Jurassic magnetostratigraphy, 2. Middle-Late Oxfordian of Aguilón, Iberian Cordillera, northern Spain: *Earth and Planetary Science Letters*, v. 76, p. 151–166.
- STRADNER, H., AND ALLRAM, F., 1982, The nannofossil assemblage of DSDP Leg 66, Middle America Trench: Initial Reports of the Deep Sea Drilling Project, v. 66, p. 589–639.
- SUNDVIK, M., LARSON, R. L., AND DETRICK, R. S., 1984, Rough-smooth basement boundary in the western North Atlantic basin: evidence for seafloor-spreading origin: *Geology*, v. 12, p. 31–43.
- SWEET, W. C., MOSHER, L. C., CLARK, D. L., COLLINSON, J. W., AND HASENMUELLER, W. A., 1971, Conodont biostratigraphy of the Triassic: *Geological Society of America Memoir*, 126, p. 441–465.
- TAUXE, L., TUCKER, P., PETERSEN, N. P., AND LABRECQUE, J. L., 1983, The magnetostratigraphy of Leg 73 sediments: *Palaeogeography, Palaeoclimatology, Palaeoecology*, v. 42, p. 65–90.
- THEYER, F., HAMMOND, S. R., AND MATO, Y., 1978, Paleomagnetic and geochronologic calibration of latest Oligocene to Pliocene radiolarian events, Equatorial Pacific: *Marine Micropaleontology*, v. 3, p. 337–395.
- THIERSTEIN, H. R., 1976, Mesozoic calcareous nannoplankton biostratigraphy of marine sediments: *Marine Micropaleontology*, v. 1, p. 325–362.
- , GETZENAUER, K. R., MOLFINO, B., AND SHACKLETON, N. J., 1977, Global synchrony of late Quaternary coccolith datum levels—validation by oxygen isotopes: *Geology*, v. 5, p. 400–404.
- TOZER, E. T., 1984, The Triassic and its ammonoids, evolution of a time scale: *Geological Survey of Canada, Miscellaneous Reports*, v. 35, 171 p.
- TREYAK, A. H., VIGILYANSKAYA, L. I., AND SHEMPELEV, A. G., 1976, Paleomagnitny Razrez Nizhnego mela Severo-Zapadnogo Kavkaza, *in* Mikhylova, N. P., ed., *Paleomagnetizm, Magnetizm, Geomagnitnoye Pole*: Izd. Nauk Dumka, Moscow, p. 38–42.
- VAIL, P. R., AND HARDENBOL, J., 1979, Sea-level changes during the Tertiary: *Oceanus*, v. 22, p. 71–79.
- , —, AND TODD, R. G., 1984, Jurassic unconformities, chronostratigraphy and sea level changes from seismic stratigraphy and biostratigraphy: *Third Annual Conference, Gulf Coast Society and Society of Economic Paleontologists and Mineralogists, Proceedings*, p. 347–364.
- , MITCHUM, R. M., JR., TODD, R. G., WIDMIER, J. M., THOMPSON, S., III, SANGREE, J. B., BUBB, J. N., AND HATLELID, W. G., 1977, Seismic stratigraphy and global changes of sea level: *American Association of Petroleum Geologists Memoir*, 26, p. 49–212.
- VAN HINTE, J. E., 1976, A Cretaceous time scale: *American Association of Petroleum Geologists Bulletin*, v. 60, p. 498–516.
- VOGT, P. R., AND EINWICH, A. M., 1979, Magnetic anomalies and sea-floor spreading in the western North Atlantic, and a revised calibration of Keathly (M) geomagnetic reversal chronology: *Initial Repots of the*

Deep Sea Drilling Project, v. 43, p. 857-876.

WEBB, J. A., 1981, A radiometric time scale of the Triassic: Journal of the Geological Society of Australia, v. 28, p. 107-121.

—, 1982, Triassic radiometric dates from eastern Australia, in *Odin*,

G. S., ed., *Numerical Dating in Stratigraphy*: Wiley, New York, p. 515-522.

WRIGHT, C. W. AND KENNEDY, W. J., 1983, The Ammonoidea of the Lower Chalk, Part 1: Palaeontographical Society, 126 p.

**APPENDIX A.—RADIOMETRIC DATES PLOTTED AGAINST SEAFLOOR MAGNETIC-ANOMALY PROFILES (FIGS. 3-5)
FOR BEST-FIT SOLUTION OF MAGNETIC-ANOMALY AGES.**

Number	Date (in MA)	High-/Low-Temperature Date	Magnetic Anomaly (Assignment Through Paleo)	Reference(s) (*Reference in <i>Odin</i> , 1982a)
1	67.1 ± 1.0	H	30N	Obradovich and Cobban, 1975
2	66.7 ± 1.0	L	Above 30N	*Harris, p. 604
3	66.4 ± 2.5	H	Within 29R	Evernden and others 1964; Obradovich and Cobban, 1975; Newman, 1979
4	65.8 ± 1.4	H	Below 29N	*Odin and Obradovich, p. 768
6	63.5 ± 0.4	H	Between 30N and 29N	*Baadsgaard and Lerbekmo, p. 797
7	56.8 ± 0.8	L	Just above 25N	Fitch and others, 1978
9	56.6 ± 3.4	L	Above 26N	*Harris, p. 604
10	46.7 ± 3.0	L	Above 23N	*Harris, p. 604
11	54.1 ± 2.0	L	Between 26N and 25N	*Curry and Odin, p. 685
12	56.0 ± 2.1	L	Between 26N and 25N	*Curry and Odin, p. 673
12A	57.5 ± 3.0	L	Between 26N and 25N	*Curry and Odin, p. 674
13	54.2 ± 1.9	L	Just above 25N	*Curry and others, p. 694
14	55.2 (?)	L	Just above 25N	*Curry and others, p. 695
15	56.0 ± 1.9	L	Just above 25N	*Curry and Odin, p. 695
16	53.0 ± 2.4	L	Above 25	*Bigot and others, p. 693
17	49.5 ± (?)	H	Top 21N	Flynn, 1981
18	50.3 ± 0.7	L	Between 21N and 20 N	*Kreuzer, p. 932
19	48.3 ± 2.7	L	22N	*Curry and Odin, p. 691
22	45.0 ± 2.2	L	22N	*Curry and Odin, p. 681
23	47.7 ± 1.6	L	Between 22N and 21N	*Curry and Odin, p. 682
24	43.9 ± 2.0	L	Between 22N and 21N	*Curry and Odin, p. 665
26	44.4 ± 2.3	L	Between 22N and 21N	*Curry and Odin, p. 665
27	44.4 ± 2.3	L	Between 22N and 21N	*Curry and Odin, p. 686
30	46.2 ± 1.6	L	Between 22N and 21 N	*Curry and Odin, p. 689
31	41.0 ± 1.8	L	20N to 19N	*Curry and Odin, p. 680
32	40.1 ± 1.8	L	20N to 19R	*Curry and Odin, p. 663
33	40.7 ± 1.7	L	20N to 19R	*Curry and Odin, p. 663
34	40.8 ± 2.3	L	20N to 19R	*Curry and Odin, p. 679
35	43.7 ± 1.5	H	19N to 18R	Ghosh, 1972; Hardenbol and Berggren, 1978
36	41.6 ± 1.5	H	18N	Ghosh, 1972; Hardenbol and Berggren, 1978
37	39.5 ± 0.5	H	Between 15N and 13N	Ghosh, 1972; Hardenbol and Berggren, 1978
39	39.1 (?)	H	17N to 16N	McKee, 1975
40	38.0 (?)	H	17N to 16N	McKee, 1975
42	38.9 ± 1.8	L	18N/17R	*Curry and Odin, p. 659
43	39.6 ± 1.8	L	18N/17R	*Curry and Odin, p. 661
44	37.5 ± 0.7	L	13N/R	*Curry and Odin, p. 696
45	36.4 ± 0.7	L	13N/R	*Curry and Odin, p. 696
46	33.9 ± 1.5	H	13N/R	*Baubron and Cavelier, p. 893
47	34.6 (?)	H	Top 13N	Evernden and others, 1964; Prothero and others, 1982
48	32.4 (?)	H	12N	Evernden and others, 1964; Prothero and others, 1982
49	31.3 ± 0.3	H	11N to 10N	*Hartung and others, p. 896
50	32.6 ± 0.3	H	13N	*Hartung and others, p. 896
53	26.2 ± 0.5	L	7N to 6CN	*Kreuzer and Gramann, p. 794
54	23.6 ± 0.2	L	Above 7N	*Kreuzer, p. 793
55	36.1 (?)	H	Mid-13N	Emry, 1973; Prothero and others, 1982
56	37.7 (?)	H	Top 15N	Emry, 1973; Prothero and others, 1982
57	37.4 (?)	H	Above 15N	Emry, 1973; Prothero and others, 1982
59	22.0 ± 1.1	L	6CR to 6BN	*Odin, p. 699
60	18.6 ± 0.7	L	5EN to 5DN	*Odin, p. 702
61	22.6 ± 1.2	L	6BN to 6A	*Odin, p. 703
62	7.24 (?)	H	Top 4N	McDougall and others, 1977
63	5.93 (?)	H	Below 3AN	McDougall and others, 1977
64	5.40 (?)	H	Just below 3AN	McDougall and others, 1977
65	5.07 (?)	H	Lower 3N	McDougall and others, 1977
66	3.99 (?)	H	Upper 3N	McDougall and others, 1977
68	3.55 (?)	H	Just below 2AN	McDougall and others, 1977
69	2.99 (?)	H	Mid-2A	McDougall and others, 1977
70	2.48 (?)	H	Just above 2A	McDougall and others, 1977
71	22.0 ± 0.3	H	6BN	Abele and Page, 1974; Shibata and others, 1984
72	20.4 ± 0.3	H	Mid-6A	Adams, 1975; Shibata and others, 1984
73	17.2 ± 0.4	H	Just below 5C	Bandy and others, 1970; Shibata and others, 1984
74	16.4 ± 0.9	H	Just below 5C	Shibata, 1973
77	16.1 ± 0.4	H	Between 5C and 5B	Shibata and others, 1981
78	14.7 ± 0.4	H	Just above 5B	Kawai and Hirooka, 1966; Shibata and others, 1964
80	14.3 ± 2.1	H	Just above 5B	Shibata and Nozawa, 1967
81	11.6 ± 0.4	H	Below 5AN	Shibata and others, 1979

High-temperature dates are K/Ar or Rb/Sr dates on tuffs, bentonites, lavas, or other high temperature minerals. Low-temperature dates are K/Ar dates on glauconites. See individual references for stratigraphic and analytical details. All dates have been converted to new decay constants (if not already converted).

APPENDIX B.—RADIOMETRIC DATES USED TO OBTAIN A BEST-FIT NUMERICAL TIME SCALE FOR THE JURASSIC-CRETACEOUS (FIG. 6).

Number	Date (in MA)	High-/Low-Temperature Date	Stratigraphic Level	References (In Odin, 1982a)
T13	216.0 ± 2.0	H	Late Norian—early Rhaetian	Priem, Abstract 137, p. 814
J1	206.0 ± 12.0	H	Early Lias	Webb, Abs. 202, p. 876
J2	204.0 ± 5.0	H	Sinemurian—early Pliensb.	Armstrong, Abs. 181, p. 857
J3	202.0 ± 12.0	H	Between early and mid-Lias.	Webb, Abs. 203, p. 877
J4	169.0 ± 10.0	H	Bajocian	Odin and Obradovich, Abs. 102, p. 766
J5	156.0 ± 5.0	H	Bajocian/Bathonian transition	Baubron and Odin, Abs. 214, p. 891
J6	154.0 ± 5.0	H	Bajocian/Bathonian transition	Baubron and Odin, Abs. 214, p. 891
J7	163.0 ± 3.0	H	Bathonian	Kreuzer, Abs. 149, p. 831
J8	155.0 ± 3.0	H	Bathonian	Kreuzer, Abs. 149, p. 831
J9	156.0 ± 3.0	H	Bathonian	Kreuzer, Abs. 149, p. 831
J10	148.0 ± 3.0	L	Oxfordian	Odin and McDowell, Abs. 141, p. 818
J11	140.0 ± 3.0	L	Basal Kimmerid.	Odin and McDowell, Abs. 142, p. 819
J12	136.0 ± 3.0	L	Basal Kimmerid.	Odin and McDowell, Abs. 142, p. 819
J13	134.0 ± 4.0	L	Portlandian	Kennedy and Odin, Abs. 99, p. 764
J14	133.0 ± 4.2	L	Mid-Portland.	Kennedy and Odin, Abs. 76, p. 737
C16	119.0 ± 2.0	L	Latest Valang.	Kreuzer, Abs. 148, p. 830
C17	116.9 ± 2.6	L	Mid-Hauterivian	Odin and Conard, Abs. 74, p. 734
C18	113.7 ± 3.3	L	Mid-Hauterivian	Odin and Conard, Abs. 74, p. 734
C19	110.7 ± 3.6	L	Late Barremian	Conard and Odin, Abs. 73, p. 734
C20	109.3 ± 6.0	H	Late Aptian	Montigny and others, Abs. 188, p. 860
C21	108.0 ± 2.6	L	Late Aptian	Kreuzer and Thiermann, Abs. 146, p. 827
C22	107.3 ± 3.9	L	Late Aptian	Curry and Odin, Abs. 71, p. 732
C26	112.0 ± 3.3	L	Late Aptian	Kennedy and others, Abs. 98, p. 763
C27	108.6 ± 3.3	L	Early Albian	Kennedy and others, Abs. 70, p. 731
C28	100.5 ± 3.3	L	Early Albian	Elewaut and others, Abs. 78, p. 740
C29	108.3 ± 4.0	L	Early Albian	Elewaut and others, Abs. 78, p. 740
C30	100.5 ± 1.0	L	Early Albian	Kreuzer and others, Abs. 144, p. 821
C31	101.1 ± 3.7	L	Mid-Albian	Elewaut and others, Abs. 79, p. 741
C32	102.4 ± 2.3	L	Mid-Albian	Elewaut and others, Abs. 79, p. 741
C33	96.5 ± 2.7	L	Late Albian	Kreuzer and Thiermann, Abs. 145, p. 826
C34	98.1 ± 3.9	L	Late Albian	Kennedy and Odin, Abs. 65, p. 727
C35	98.6 ± 2.6	L	Late Albian	Kennedy and Odin, Abs. 65, p. 727
C36	97.6 ± 2.0	H	Late Albian	Odin and Obradovich, Abs. 111, p. 774
C37	97.5 ± 2.0	H	Late Albian	Odin and Obradovich, Abs. 111, p. 774
C38	98.4 ± 3.2	L	Late Albian	Kennedy and Odin, Abs. 63, p. 725
C39	99.5 ± 3.1	L	Latest Albian	Kennedy and Odin, Abs. 63, p. 725
C40	99.7 ± 1.2	H	Late Albian	Obradovich, Abs. 157, p. 838
C41	94.6 ± 0.8	L	Early Cenoman.	Kreuzer and others, Abs. 211, p. 887
C42	94.7 ± 1.1	L	Early Cenoman.	Kennedy and Odin, Abs. 62, p. 722
C43	94.8 ± 3.1	L	Early Cenoman.	Elewaut and others, Abs. 80, p. 742
C44	90.4 ± 2.0	L	Mid-Cenomanian	Elewaut and others, Abs. 81, p. 743
C45	92.9 ± 2.1	L	Mid-Cenomanian	Elewaut and others, Abs. 81, p. 743
C46	91.2 ± 0.5	L	Early Turonian	Kreuzer and others, Abs. 226, p. 903
C47	91.5 ± 1.8	H	Early Turonian	Lanphere, Abs. 118, p. 780
C48	90.5 ± 0.4	L	Early Turonian	Kreuzer and others, Abs. 226, p. 903
C49	88.1 ± 1.5	L	Late Turonian	Kreuzer and Seibertz, Abs. 227, p. 906
C50	85.0 ± 1.0	L	Late Turonian	Kreuzer and Rabitz, Abs. 94, p. 758
C50A	86.0 ± 1.0	L	Late Turonian	Kreuzer and Rabitz, Abs. 94, p. 758
C51	89.0 ± 1.5	H	Turonian/Coniacian boundary	Odin and Obradovich, Abs. 108, p. 772
C52	87.1 ± 2.8	L	Coniacian	Elewaut and others, Abs. 83, p. 745
C53	84.4 ± 1.6	H	Earliest Santonian	Odin and Obradovich, Abs. 107, p. 771
C54	79.3 ± 1.6	H	Earliest Campanian	Odin and Obradovich, Abs. 106, p. 771
C55	77.6 ± 2.5	L	Early Campanian	Kennedy and Odin, Abs. 140, p. 817
C56	74.9 ± 2.3	L	Late Campanian	Kennedy and Odin, Abs. 140, p. 817
C57	74.3 ± 1.4	H	Latest Campanian	Odin and Obradovich, Abs. 105, p. 769
C59	71.0 ± 2.1	L	Late Maastrichtian	Kennedy and Odin, Abs. 139, p. 815
C50	70.1 ± 1.4	H	Late Maastrichtian	Odin and Obradovich, Abs. 104, p. 768
C60	69.0 ± 1.4	H	Late Maastrichtian	Odin and Obradovich, Abs. 104, p. 768

High-temperature dates are Rb/Sr or K/Ar dates on minerals formed at high temperatures, such as those in tuffs, ashes, bentonites, lava flows, biotite, etc. Low-temperature dates are most commonly K/Ar dates on glauconites. See individual references for stratigraphic and analytical details on the dates. All dates were converted to new decay constants in Odin (1982a).

APPENDIX C: CENOZOIC SEQUENCES

Cenozoic sequences were studied in outcrops on the Isle of Wight and in southern England, Belgium, the Paris Basin and southern France, West Germany, Italy, Spain, along the Gulf Coast of the United States, in the Carolinas, New Zealand, and in Australia. Sections studied and the ages of the sequences include the following.

On the Isle of Wight, a relatively complete Upper Paleocene through Lower Oligocene succession of sequences

was studied at the White Cliff Bay and Alum Bay sections. In addition, in southern England sections at Herne Bay (type area of the Thanetian Stage), Barton (stratotype of the Barritonian Stage), and Sheppey Island (Ypresian) were studied.

In Belgium, sections in the type area of the Rupelian Stage included those at Sint Niklaas, Kruibeke, and Steendorp. Other outcrops included sections at Pellenberg (Tongrian) and Tongeren (stratotype of the Tongrian Stage); in the type area of the Ypresian Stage, the Kortemark, Egem, and Aalbeke sections; the Balegem section (type Ledian); the

Wemmel section (Wemmelian Stage stratotype); the Ciply section in the Mons Basin (Montian Stage stratotype); in the type area of the Bruxellian Stage, the Zetrud-Lumay and Braine l'Alleud sections; the Gelinden section (Thanetian); and the Vroenhoven section along the Albert Canal (K/T boundary and Danian).

In the Paris Basin, France, outcrops were studied at St. Leu d'Esserent and St. Vaast-les-Mello (Lutetian stratotype). Lutetian sections were also studied at Guitrancourt and Damery. Cuisian sections included those at Cuise-la-Motte (stratotype of the Cuisian) and Gisors. Other outcrops included sections at Auvers-sur-Oise (stratotype of the Auversian), Marine (type Marinesian), Pourcy (Sparnaciana), Cormeilles (Ludian, Sannoisian, and Stampian), and Chalons-sur-Vesle (Thanetian).

In southern France, outcrops in the type area of the Aquitanian Stage included Moulin de Bernachon, Moulin de l'Eglise, L'Ariey (stratotypes of the Aquitanian), and Relevee de Balizac sections. Other outcrops included sections at Grignols (Upper Aquitanian-Lower Burdigalian), Champ du Peloua, Ruisseau de la Coquilleyre, and Pont Pourquey, La Sime (type area of the Burdigalian Stage).

Other European outcrops included the section at Doberg bei Bünde in West Germany (Chattian stratotype); in northern Spain the type Ilerdian section at Tremp, Lerida; in Italy the stratotype of the Priabonian at Priabona. In addition, most literature sources containing measured sections and litho- and chronostratigraphic information on the stratotypes and reference sections of the Late Neogene stages in Italy, i.e., Langhian, Serravallian, Tortonian, Messinian, Zanclean, and Calabrian, were also perused extensively, and sequence-stratigraphic models were proposed on the basis of litho- and biofacies information (field work in these areas is planned for 1987).

Along the United States East Coast, outcrops in North Carolina included the Belgrade quarry near Belgrade (Lower Miocene); Trent River section (Oligocene); New Bern quarry near New Bern (Upper Eocene-Oligocene); and Ideal (Martin Marietta) quarry in New Hannover County (Middle Eocene). Outcrops in South Carolina included quarries in Georgetown and Berkeley counties (Middle Eocene) and the Santee Portland quarry (Upper Eocene).

Along the United States Gulf Coast, outcrops in Alabama included Little Stave Creek (Middle Eocene-Oligocene); St. Stephens quarry (uppermost Eocene through lowest Miocene); sections along the Alabama, Tombigbee, and Chattahoochie rivers (Paleogene); and the Braggs section (K/T boundary).

On South Island, New Zealand, coastal sections were studied from South Canterbury to North Otago (Eocene through Middle Miocene), at North Canterbury (Upper Cretaceous to Oligocene), and from Greymouth to Karamea (Eocene through Middle Miocene) along the west coast.

In Australia, outcrops were studied along the flanks of the Otway Mountains. Along the eastern flanks of the Otways, the Bells Headland, Airey's Inlet, and Soapy Rocks sections (uppermost Eocene through lowest Miocene) were examined. The Browns Creek section (Upper Eocene-lowest Oligocene) at the southwest end of the Otways, and sections along the western flanks of the Otways from Pebble

Point (Middle Paleocene through Oligocene) to Port Campbell (Lower Miocene-Pliocene) were also studied.

APPENDIX D: CRETACEOUS SEQUENCES

Cretaceous sequences were studied in the Suisse Romande, Switzerland, in southeastern and northern France, in Belgium and the Netherlands, in the Western Interior of the United States (Colorado, Utah), and in central Texas. Sections studied and their ages include the following.

In the Suisse Romande, Switzerland, the outcrops studied were the section at Châtel-St. Dennis on the right bank of the Veveyse River (Berriasian through Lower Barremian); the section at Montsalvens (Berriasian through Santonian); the section at Valangin (stratotype of the Valanginian Stage); the Cressier and Landeron sections near Hauterive (type area of the Hauterivian Stage); the Borne Valley-Plateau d'Andey sections (Valanginian through Lower Barremian); and the Val de Fier section (Berriasian-Valanginian).

In Ardèche, southern France, the outcrops were the Vileneuve de Berg section (Valanginian-Hauterivian) and the nearby Ibie Valley section (Lower Barremian); the Berrias section (Berriasian Stage stratotype); and the Les Buissieres section near Bessas (Hauterivian). In Vaucluse, southern France, the section at Apt (stratotype of the Aptian Stage) and the Gargas section (Gargasian Stage stratotype) were studied. In Alpes-de-Haute-Provence, southern France, the sections included those near Angles (Valanginian through Barremian, stratotype of Barremian Stage); the La Clue de Vergon section near Castellane (Hauterivian); and the La Rochette section (Turonian). In the Hautes-Alpes, the Bruis section (Upper Aptian-Albian), the Villefranche-le-Château section (Albian) in Drôme, and the La Roudoule section (Albian) in the Alpes Maritime. Along the coast of Bouche-du-Rhone in southern France, the section at Cassis near La Bédoule (Bedoullian Stage stratotype) was also studied.

In northern France, sequence studies included the type area of the Cenomanian Stage and other Cenomanian-Lower Turonian sections in the Le Mans (Sarthe) area: those at Le Cormier (near Cormes), La Pigalière (St. Ulphace), Les Quatre Chemins (Le Luart), La Gare (Dollon), Les Fosses Blanches (Duneau), Le Moulin Ars (St. Calais), Le Bourgneuf (Mulsanne), Les Acacias (Yvré-l'Évêque), Longueville (Savigné-l'Évêque), Le Chateau (Ballon), Le Sablon and La Goupillerie (near Mézières-sous-Ballon), and at Mercey (Bonnétable).

In the Le Havre area of northern France, sections at Dollemard, Bléville, Octeville, St. Jouin, Le Tilleul, and Fécamp (Upper Albian through Turonian) were studied. Near Touraine, the type area of the Turonian Stage, sections at Ambroise (Lower Turonian), Montrichard (mid-Turonian), and Francueil (Upper Turonian and Turonian/Coniacian boundary) were studied along with that at La Bousinière (Upper Cenomanian).

In the Boulonnais area of northern France, outcrops included sections at Wissant (Upper Aptian-Albian) and at Cap Blanc-Nez (Cenomanian-Lower Turonian).

In the Aube, northern France, Albian outcrops were stud-

ied at Perchois-Ouest and Perchois-Est in the type area of the Albian Stage, and at Montiéramey, Courcelles, Le Jard, Radonvilliers, and Montreuil-sur-Barse. Other outcrops in northern France included sections at Saintes (stratotype of the Santonian Stage); Cognac (stratotype of Coniacian Stage); and in the type area of the Campanian, sections at Aubeterre (Campanian-Maastrichtian, stratotype of Campanian), Belvès (Santonian-Campanian), and at Bigaroque (Campanian).

In Belgium outcrops included sections at Maisières (Turonian-Coniacian); Obourg (Campanian); Hallembaye (Campanian-Maastrichtian); and Ciply (Maastrichtian). In addition, the stratotype of the Maastrichtian Stage was studied at the Maastricht quarry (ENCI) in the Netherlands.

In the Western Interior of the United States, outcrops in Colorado included the Rock Canyon Anticline near Pueblo (Upper Albian-Santonian); sections near Canon City, Wcott, Glenwood Springs, New Castle, and Grand Junction (Aptian through Santonian); and sections near Coalville, Utah (Albian through Turonian). In central Texas numerous outcrop sections near the towns of Austin, Temple, Waco, and Waxahachie were studied for mid-Albian through Maastrichtian sequences.

APPENDIX E: JURASSIC SEQUENCES

Jurassic sequences were studied along the Dorset and Somerset coasts of southern England, along the Yorkshire coast of northern England, in west-central France, in southern Germany, and in Switzerland. Sections and the ages of the sequences studied include the following.

In southern England, an almost complete succession of Jurassic sequences can be seen along the Dorset coast. Sections from Pinhay Bay to Eastcliff (Hettangian through

Toarcian), at Burton Bradstock and Tidmoor Point (Aalenian through Callovian), and from the Isle of Portland to Swanage (Oxfordian through Purbeckian) were studied. In northern England along the Yorkshire coast, sections were studied between Robin Hood Bay and Staithes (Lower Jurassic), at Blea Wyke Point (Middle Jurassic), and at Cayton Bay (Oxfordian).

In France near the areas of Thouars and St. Jacques de Thouars, the stratotype of the Toarcian Stage was studied at the Rigolier-Vrines sections.

Upper Jurassic (Oxfordian-Tithonian) sequences were studied in the Montsalvens area of Switzerland. Samples were also studied for sequence analysis from the stratotype of the Pliensbachian Stage (from a section near Pliensbach, southern Germany).

APPENDIX F: TRIASSIC SEQUENCES

Triassic sequences were studied in the Dolomites in Italy; in Tyrol, Austria; in the Salt Range, Pakistan; and on the Arctic islands of Svalbard and Bjørnøya. Sections and the ages of the sequences studied include the following.

In the western Dolomites, Italy, the outcrops were the Rosengarten section (Ladinian-Carnian); San Lucano Valley sections (Anisian-Ladinian); Plattaforma del Sella sections (Ladinian-Carnian); and Alpe di Siusi section (Ladinian).

Elsewhere, the Steinplatte sections (Rhaetian) in Tyrol, Austria; the sections in Chiddru Nala, Narmia, and Nammal Gorge (Scythian) in the Salt Range, Pakistan; and the sections in the Festningen area of Isfjorden (Griesbachian through lowest Rhaetian) in Spitsbergen were studied. Triassic sections on Bjørnøya (Bear Island) are exposed on the Miseryfjellet (Scythian through Carnian).